RESEARCH ARTICLE SUMMARY

PALEONTOLOGY

Duck-billed dinosaur fleshy midline and hooves reveal terrestrial clay-template "mummification"

Paul C. Sereno*, Evan T. Saitta, Daniel Vidal, Nathan Myhrvold, María Ciudad Real, Stephanie L. Baumgart, Lauren L. Bop, Tyler M. Keillor, Marcus Eriksen, Kraig Derstler

Full article and list of author affiliations: https://doi.org/10.1126/science.adw3536

INTRODUCTION: Called dinosaur "mummies," two skeletons of the duck-billed dinosaur *Edmontosaurus* were discovered in Wyoming more than a century ago preserved like sun-dried carcasses. The snout of one is covered with a ducklike bill, and both have large areas of scaly integument described as "skin impressions." Revisiting this area uncovered a "mummy zone," with finds including two additional *Edmontosaurus* mummies and exceptional specimens of the contemporaries *Triceratops* and *Tyrannosaurus*. How soft tissues fossilize, and whether any of the original organic materials survive, remain open questions.

RATIONALE: To investigate integument fossilization, we used high-resolution imaging, thin-section microscopy, and geochemical analyses, documenting the surrounding sediment and the structure and composition of the integument layer. Based on past research, fossilized integument (or "integument rendering") is generated through one of four pathways: cast-vestige, mold, template, or impression.

Because terms for integument structures such as "crest" or "hoof" are often used informally, we provide definitions for all major keratinous, cornified structures in tetrapods, dividing those that are entirely fleshy from those underlain by bone. We also compile and organize terms for reptilian scalation under five categories: shape, form, ornamentation, topology, and pattern.

RESULTS: The new mummies provide a complete fleshy profile for a large-bodied dinosaur. A fleshy neck-to-trunk crest transitions over the hips into an interdigitating spike row that continues to the tip of the tail. The scales on the crest and trunk are very small for a 12-m reptile, with most measuring 1 to 4 mm in diameter. Wedge-shaped hooves, here preserved in a reptile, cap the toes of fore and hind feet. All soft tissue structures are preserved as a very thin (0.5 mm or less) clay layer or template. Experiments have shown that a biofilm on the surface of decaying tissue can accumulate template clay from surrounding sediment before soft tissue degradation. We found no trace of internal integument structure or original organic material.

CONCLUSION: Recently discovered duck-billed dinosaur mummies suggest that "mummification" occurred after drought-induced mortality involving four stages: carcass desiccation and initial subaerial decay, sudden burial with minimal transport, rapid carcass infilling, and templating in clay and final decay. The cyclic drought-flood monsoonal climate of the Lance Formation and its extraordinary thickness under the mummy zone provided the environmental and geologic conditions, respectively, for rapid burial of desiccated, unscavenged carcasses without sediment reworking. Unlike the underlying permineralized skeletal bone, the integument renderings of these dinosaur mummies congealed early in the process of fossilization as a thin external clay mask, a templating process documented previously only in anoxic marine settings. □

Dinosaur mummies unmasked. Mummies of the duck-billed dinosaur *Edmontosaurus annectens* (1) document with a thin external clay template a fleshy crest over neck and trunk (2), a fleshy spike row over hips and tail (3), and hooves capping the toes of the hind feet (4). Preserved as desiccated carcasses (5) and rapidly buried rapidly by floodwaters (6) on a coastline (7), the duck-billed mummies come from the very end of the dinosaur era in what today is east-central Wyoming. [Artwork by Dani Navarro.]

*Corresponding author. Email: dinosaur@uchicago.edu Cite this article as P. C. Sereno *et al.*, *Science* **391**, eadw3536 (2026). DOI: 10.1126/science.adw3536

PALEONTOLOGY

Duck-billed dinosaur fleshy midline and hooves reveal terrestrial clay-template "mummification"

Paul C. Sereno[1,2]*, Evan T. Saitta[1], Daniel Vidal[1,3], Nathan Myhrvold[4], María Ciudad Real[1,3], Stephanie L. Baumgart[5], Lauren L. Bop[1], Tyler M. Keillor[1], Marcus Eriksen[6], Kraig Derstler[7]

Two "mummies" of the end-Cretaceous duck-billed dinosaur *Edmontosaurus annectens* preserve a fleshy crest over the neck and trunk, an interdigitating spike row over the hips and tail, and hooves capping the toes of the hind feet. A battery of tests showed that all of the fossilized integument (skin, spike, and hoof) are preserved as a thin (less than 1 millimeter) clay template that formed on the surface of a buried carcass during decay before the loss of all soft tissues and organic compounds. Unlike the underlying permineralized skeletal bone, the integument renderings of these "dinosaur mummies" are preserved as a thin external clay mask, a templating process documented previously only in anoxic marine settings.

In 1908 in east-central Wyoming, noted fossil collector C. H. Sternberg discovered a skeleton of the duck-billed dinosaur *Edmontosaurus annectens* blanketed by large areas of scaly skin rendered in sediment. Described in 1912 by H. F. Osborn and nicknamed the "AMNH mummy," this specimen preserves a broad sampling of scaly skin renderings he called "skin impressions" (*1*). Two years later in the same area, Sternberg unearthed a second specimen of the same dinosaur with extensive integument traces (*2*). Dubbed the "Senckenberg mummy," this specimen also preserves a rendering of the upper bill (*3*, *4*).

We replace Osborn's and Sternberg's widely used term "skin impression" with "rendering," because creating a negative relief impression of integument in sediment, the literal interpretation of their term, is the rarest among the four modes of fossilization we recognize (cast-vestige, mold, template, and impression). We also define "fossil mummy," compile terms for fleshy and bone-supported integument structures (e.g., crest and hoof), and provide a descriptive framework for reptilian scalation (based on shape, form, ornamentation, topology, and pattern) (see the supplementary materials and tables S1 to S3).

Using historical photographs and letters, we approximated the quarry locations for Sternberg's AMNH and Senckenberg mummies in what we describe as a "mummy zone" <10 km in diameter (Fig. 1A; for site documentation, see the supplementary materials, figs. S1 to S5, and table S5). More than a century after Sternberg's discoveries, the same local area of ravine exposures of fluvial sandstone has yielded a skeleton of *Triceratops horridus* with large areas of rendered skin (*5*), an articulated skeleton of *Tyrannosaurus rex* with a sedimentological body boundary (*6*), and "late juvenile" and "early adult" mummies of *E. annectens* estimated to be 2 and 5 to 8 years old (*7*), respectively (for more details, see the supplementary materials and tables S6 and S7). The late juvenile is the first subadult dinosaur mummy on record and the first large-bodied dinosaur preserving the fleshy midline over the trunk (Figs. 2A and 3E). The early adult is the first hadrosaurid to preserve the entire spike row from hips to tail tip and the first reptile preserving wedge-shaped pedal hooves (Figs. 2B and 3).

[1]Department of Organismal Biology and Anatomy, University of Chicago, Chicago, IL, USA. [2]Committee on Evolutionary Biology, University of Chicago, Chicago, IL, USA. [3]Grupo de Biología Evolutiva, UNED, Madrid, Spain. [4]Intellectual Ventures, Bellevue, WA, USA. [5]Department of Physiological Sciences, University of Florida College of Veterinary Medicine, Gainesville, FL, USA. [6]Ventura County Science Center, Santa Paula, CA, USA. [7]Independent researcher, Divide, CO, USA. ***Corresponding author. Email: dinosaur@uchicago.edu**

Results

Midline crest and spike row

The neck and trunk midline are surmounted by a fleshy, scaled crest that gradually merges over the hips into an interdigitating spike row that continues to the tail tip (Figs. 2, A and B; 3E; and 4A). The cervical crest is best preserved in the early adult AMNH mummy (*1*), where it reaches a height of at least 7 to 8 cm (dorsal edge likely incomplete). The sides of the neck and trunk crest are divided into elevated bands covered with relatively small (1 to 4 mm) polygonal or pebble scales and separated by grooves lined with very fine scales (≤1 mm) (Fig. 2A). The bands are aligned in segmental relationship with underlying vertebrae, as reported by Osborn (*1*). They expand distally and increase in posterodorsal inclination from neck to midtrunk (Figs. 2A and 3E).

The neck crest is entirely fleshy and presumably flexible, positioned along the midline above the very low neural spines of the cervical series. It appears sheet-like in cross section, its narrow base positioned medial to the articulation between the transverse processes and tubercles of the cervical ribs (*1*). Over the anterior trunk, the crest has a subtriangular cross section, its broader base now incorporating the tubercular articulation of underlying vertebrae (Figs. 2A and 3E). The crest triples in height over middorsal vertebrae to a depth of 17 cm in the late juvenile mummy, or ~28 cm when scaled isometrically to early adult size (for mummy body size, see the supplementary materials and table S6). Both the late juvenile and AMNH mummies are preserved as inverted carcasses resting on their backs with their fleshy crests bending from the midline under the weight of the carcass (Fig. 2A).

At midtrunk, the dorsal margin of the crest has a thickness of 1.6 cm (2.6 cm scaled to early adult size). The taller neural spines of the posterior dorsal vertebrae (*8*) presumably insert into the posterior portion of the crest, which has a checkboard pattern of finely scaled grooves (Fig. 2A). Faint lineations angle posteroventrally across the trunk crest, possibly reflecting subdermal connective tissue.

Low, elongate spikes first appear over sacral neural spines (sacral vertebrae 3 and 4) directly above the hip socket. The spikes increase in height to a maximum of ~5 cm in the anterior portion of the tail (around caudal vertebra 20) before gradually decreasing in height and length toward the distal end of the tail, as preserved in situ on a block preserving the last 53 caudal vertebrae of the tail (approximately caudal vertebrae 11 to 64; Fig. 2B). The best-preserved spikes have a smooth perimeter fringe ~5 mm in width and only 1 mm in thickness (Fig. 4A). Below the fringe, the transverse thickness of the spike increases to 1.3 cm at its base, with each side covered by posterodorsally inclined, irregularly beaded striations (Fig. 4B).

The posterior end of each spike bifurcates to receive the anterior end of the next spike, their subtriangular area of interdigitation slightly raised (Figs. 3E and 4B). A basal groove separates the spike row from polygonal scales covering each side of the tail. The tip of each caudal neural spine projects into the posterior end of the base of each spike, terminating just dorsal to the basal groove.

The skin in life appears to have been very thin over the trunk and somewhat thicker over the sides of the tail, as shown by the form of the desiccation-deflation wrinkling: short and sharp-edged on the trunk and longer and rounded on the tail (Fig. 2, A and B). On the sides of the tail, polygonal scales are smallest near the spike row (~3 mm), somewhat larger in the upper one-third of the tail (~5 to 8 mm), and largest over the ventral two-thirds of the tail (~6 to 9 mm). The desiccated skin on each side of the tail is closely appressed to the contours of the underlying bones and ossified tendons.

Fleshy profile

After the 1908 discovery of a section of the neck crest in the AMNH mummy, Osborn (*1*) and later authors (*9*) depicted *E. annectens* in life

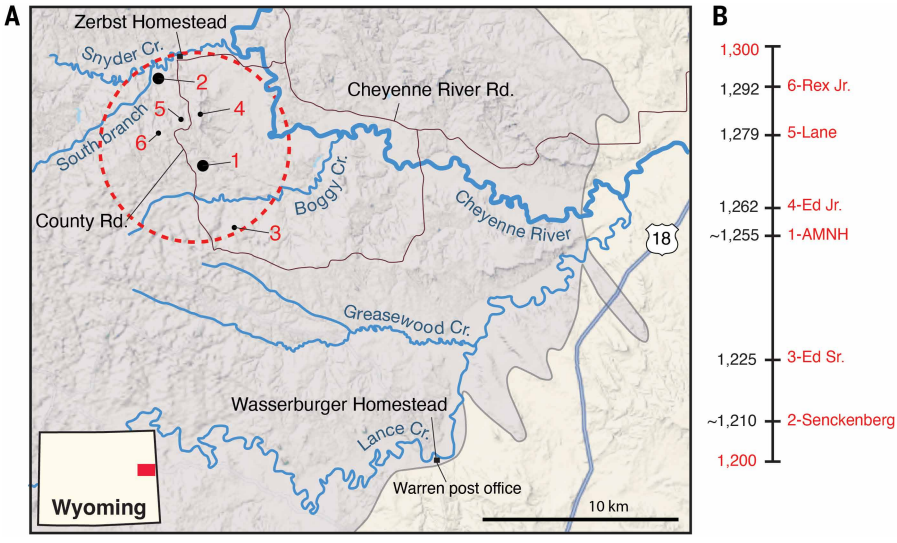

Fig. 1. Dinosaur mummy zone in the Lance Formation of east-central Wyoming. (**A**) Map of sites showing the mummy zone (red circle, 10 km diameter) with locations and approximate elevations for two *E. annectens* mummies collected more than a century ago (numbers 1 and 2) and four additional mummies collected in the past 25 years (numbers 3 to 6) that include *T. horridus* and *T. rex*. Maastrichtian (69 to 66.5 million years ago) Lance Formation (gray) and underlying Fox Hills Formation (amber) at the southern edge of the Powder River Basin (*69*) in Niobrara (formerly part of Converse) County show the location of the historical Zerbst homestead and Warren post office. (**B**) Elevation (meters) and approximate stratigraphic position for mummies 1 to 6 limited to <100 m at the top of the Lance Formation. 1, AMNH mummy (AMNH FARB 5060); 2, Senckenberg mummy (SMF R 4036); 3, new early adult mummy (UCRC PV30, "Ed Sr."); 4, new late juvenile mummy (UCRC PV31, "Ed Jr."); 5, *T. horridus* (HMNH PV.1506, "Lane"); and 6, *T. rex* (UCRC PV1, "Rex Jr.") (see the supplementary materials and table S5).

with a low midline crest extending from the neck to the middle of the tail. A pair of midline spikes were first reported in 1920 by Parks over the hips of the hadrosaurine *Gryposaurus* (*10*). Over the past 40 years, midline spikes were discovered over tail sections in *E. annectens* (*11*, *12*), a second specimen of *Gryposaurus* (*13*), and two other hadrosaurines, *Saurolophus* (*14*) and *Brachylophosaurus* (*15*). Consequently, hadrosaurid life restorations now routinely show a continuous row of separate, subrectangular spikes over the neck, trunk, and tail (*8*, *12*, *14*, *16*, *17*), usually with no alignment between spikes and underlying vertebral neural spines (for historical review, see the supplementary materials and figs. S6 to S15).

From the integument shown here, neither Osborn's nor later depictions accurately capture the fleshy profile of *E. annectens*, which has a banded, fleshy crest over the neck and trunk grading over the hips into an interdigitating spike row that extends to the tail tip, with each spike positioned over a single neural spine (Fig. 3E). The particulars of this profile may only characterize *E. annectens*, because the closely related species *E. regalis* does not have a midline crest over its neck (*18*). Thus, the generality of the midline crest among hadrosaurids remains unknown. Midline spikes over the hips and tail, by contrast, have been recorded in four hadrosaurines and may characterize this subgroup, although their interdigitating configuration may be unique to either *Edmontosaurus* or *E. annectens*. We tentatively add the fleshy midline comb over the occiput preserved in close relative *E. regalis* (*18*) (Fig. 3E).

Among living reptiles, squamates often have a fleshy crest or midline spike row, although spike number usually exceeds the underlying vertebral count (Fig. 2C). Fleshy midline spikes that interdigitate as in *E. annectens* are present only in draconine agamids (Fig. 2, D and E). Crocodylians (*19*) and other extinct archosaurs have keratin-covered osteoderms over neck, trunk, and tail that are arranged in parasagittal rows, in contrast to the fleshy midline spikes common among lepidosaurian reptiles. Segmental correspondence between spikes and the neural spines of an underlying vertebrae in *E. annectens* resembles segmental correspondence in crocodylians between armor plates to vertebrae, in some chameleons between trunk spikes and vertebrae (e.g., *Trioceros*), and between spikes and caudal vertebrae in *Sphenodon* (see the supplementary materials). Therefore, the fleshy crest and interdigitating spike row in *E. annectens* has its closest parallel among extant lepidosaurs (for more on modern analogs, see the supplementary materials and fig. S18).

Pedal skin, digital pads, and ungual sheaths

In the early adult mummy, areas of small (1 to 2 mm), polygonal, pebble-shaped scales are present over the penultimate phalanx of pedal digit III, suggesting that small scales covered the dorsal surface of the pes, unlike the larger scutate scales of birds (*20*). The underside of the pes has even smaller granular scalation, as also seen in a footprint of end-Cretaceous age that may have been made by *E. annectens* (*21*) (Fig. 3B).

Subcircular digital pads were visualized with computed tomographic (CT) scans of digit III that match a subcircular depression of the footprint (Fig. 3C). Superposition of the pes (with 15% enlargement) over the footprint positions the metatarsal-phalangeal joint of digit III over the broad central depression of the heel, with similar positioning for the same joint in digits II and IV relative to depressions near the posterolateral and posteromedial corners of the heel (Fig. 3, B and C).

A "digit-heel crease" separates the three digital pads from the heel, crossing each pedal digit ventral to the midshaft of the proximal phalanx (Fig. 3, B and C). The proximal phalanx appears to have been positioned at an angle of ~45° in midstride, articulating proximally to a near-vertical metatarsus and distally to the near-horizontal remainder of the toe (*22*, *23*). The joints at each end of this first phalanx allow considerable rotation, whereas the remaining phalanges are very short, with closely matched interphalangeal joints that limit motion (*22*), a pedal configuration called "subunguligrade" (*23*) (Fig. 3, C and D).

Hooves, here defined as wedge-shaped, flat-bottomed keratinized sheaths surrounding an ungual (see the supplementary materials and table S2), are present around the spade-shaped unguals of pedal digits II to IV (Fig. 3, A and D to F). The largest, most symmetrical hoof is on pedal digit III, measuring 15.2 cm in length, or roughly twice the length of the ungual it surrounds (7.4 cm). Previous life restorations of hadrosaurid feet show keratinized sheaths tightly fitted to the pedal unguals (*16*, *23*, *24*) rather than sheaths that extend far beyond the ungual as in extant equines (*25*, *26*). In coronal section, the dorsal surface of the hoof parallels the dorsal surface of the ungual subtending an angle of ~40° to the horizontal (Fig. 3, A, D, and F), slightly less than in equines (50° to 55°) (*25*). Also visible in cross section is a shallow ventral depression, or frog, as occurs in equine hooves (*26*). Finally, the hoof surface in *E. annectens* is marked by anteroposterior striations (Fig. 3A, left).

The forefoot of *E. annectens* has recently been found to have a single, central hoof over the ungual of digit III (*12*). This manual hoof also has a wedge shape in cross section, with a more extensive, broader dorsal than ventral surface. As in the central pedal hoof, the sheath extends far beyond the tip of the ungual phalanx. The hooved manual digit III is joined by a web of skin to a skin-covered digit II to form a

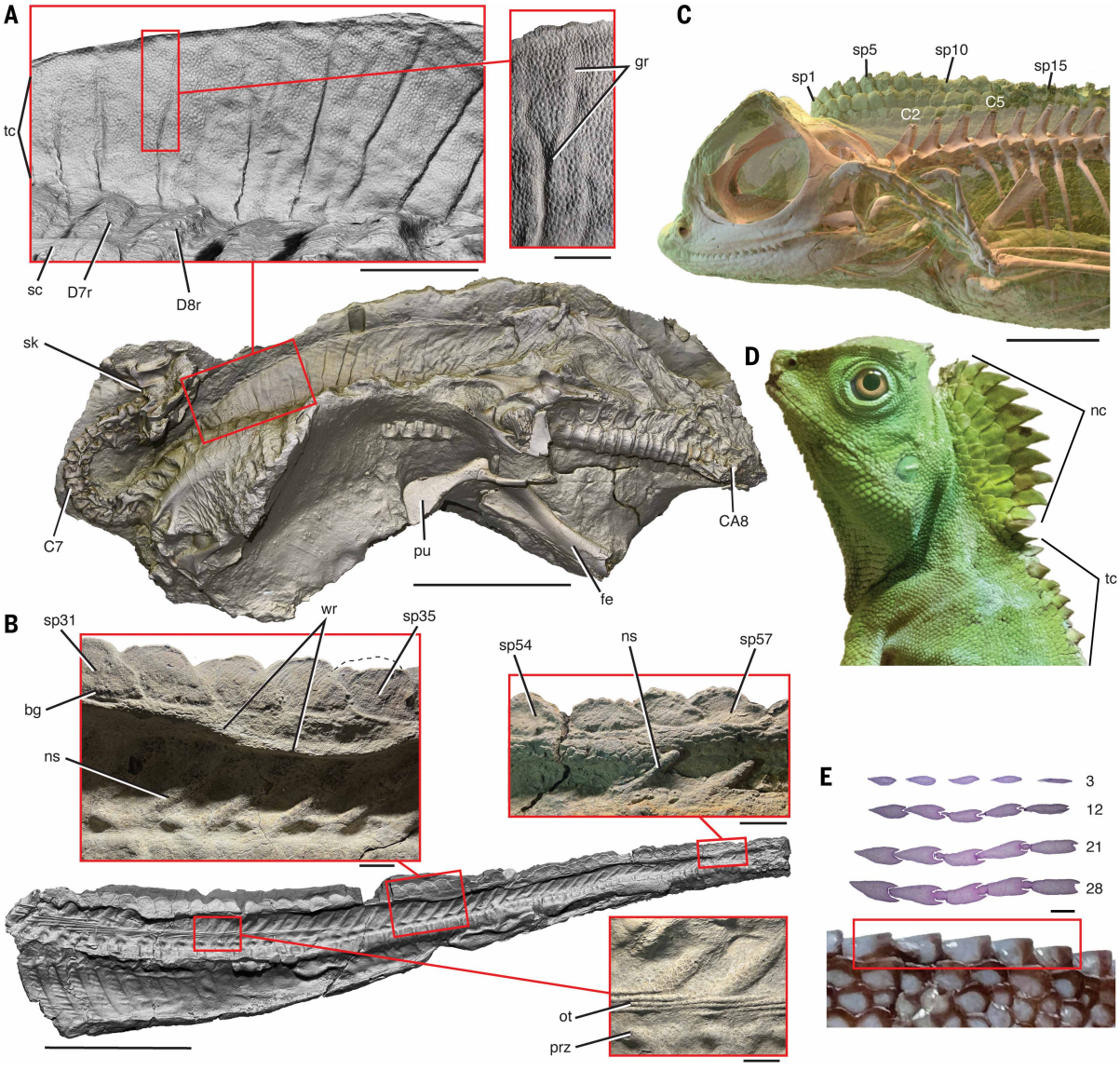

Fig. 2. Midline crest and spike row in *E. annectens* with extant squamate analog. (**A**) Midline crest over the trunk of a late juvenile mummy (UCRC PV31; maximum length 222 cm) with close-up lateral view of the anterior trunk crest and a finely scaled groove above the seventh and eighth dorsal vertebrae. (**B**) Spike row over the mid and distal tail of an early adult mummy (UCRC PV30; maximum length 279 cm) with close-up views of interdigitating spikes above the mid and distal caudal vertebrae and the desiccated scaly skin covering caudal vertebrae and ossified tendons (reversed from original). (**C**) Translucent view showing the distance, and lack of correspondence, between the spikes and neural spines of the cervical vertebrae in Doria's angle-headed lizard (*G. doriae*, FMNH H:249773) from Borneo. (**D**) Heightened neck crest of a female chameleon angle-headed lizard (*G. chamaeleontinus*) from Indonesia and Malaysia (reversed from Wikimedia Commons original). (**E**) Serial stained thin sections (top, dorsal view) of the interdigitating spikes (bottom, left lateral view) over the trunk of Doria's angle-headed lizard (*G. doriae*, FMNH H:249773) from Borneo. 3, 12, 21, 28, thin sections (10 μm) number 3, 12, 21, and 28; bg, basal groove; C2, 5, 7, cervical vertebra 2, 5, 7; CA8, caudal vertebra 8; D7r, D8r, seventh and eighth dorsal ribs; gr, groove; fe, femur; nc, neck crest; ns, neural spine; ot, ossified tendon; prz, prezygapophysis; pu, pubis; sk, skull; sp1, 5, 10, 15, spike 1, 5, 10, skin 15 over the neck of *G. doriae*; sp31, 35, 54, 57, spikes associated with the neural spines of caudal vertebrae 31, 35, 54, 57; tc, trunk crest; wr, wrinkle. Scale bars, 50 cm (bottom), 10 cm (left box), 3 cm (right box) (A), 50 cm (bottom), 3 cm (boxes) (B), 1 cm (C), and 1 mm (E).

scaled footpad at the end of a vertically held manus (Fig. 3E). During quadrupedal walking, the manus generated narrow, crescentic footprints (*1*, *12*, *21*). Thus, *E. annectens* and other hadrosaurids have mesaxonic symmetry in both fore and hind feet, but unlike any mammalian quadruped, the manus and pes assume different postures, the former unguligrade and the latter subunguligrade (Fig. 3E).

Reptilian biped with hooves

Hooves, the anatomical hallmark of living "ungulates," characterize the fore and hindfeet of two distinctive subgroups of living placental mammals, the "even-toed" Artiodactyla (suids, hippos, camels, and ruminants) with a pair of paraxonic hooves (digits III and IV) and the "odd-toed" Perissodactyla (horses, tapirs, and rhinos) with mesaxonic hooves centered on digit III. The fore and hind toes of living elephants are also hooved (*27*, *28*), as are those of several extinct subclades of placental mammals (notoungulates, litopterns, and uintatheres) (*29*, *30*) and the recently extinct marsupial pig-footed bandicoot (*Chaeropus*) (*31*). Recent fossil discoveries (*29*, *30*, *32*) and phylogenomic syntheses (*33*, *34*) have generated a new framework for mammalian phylogeny that supports the parallel origin, and subsequent loss, of hooves in

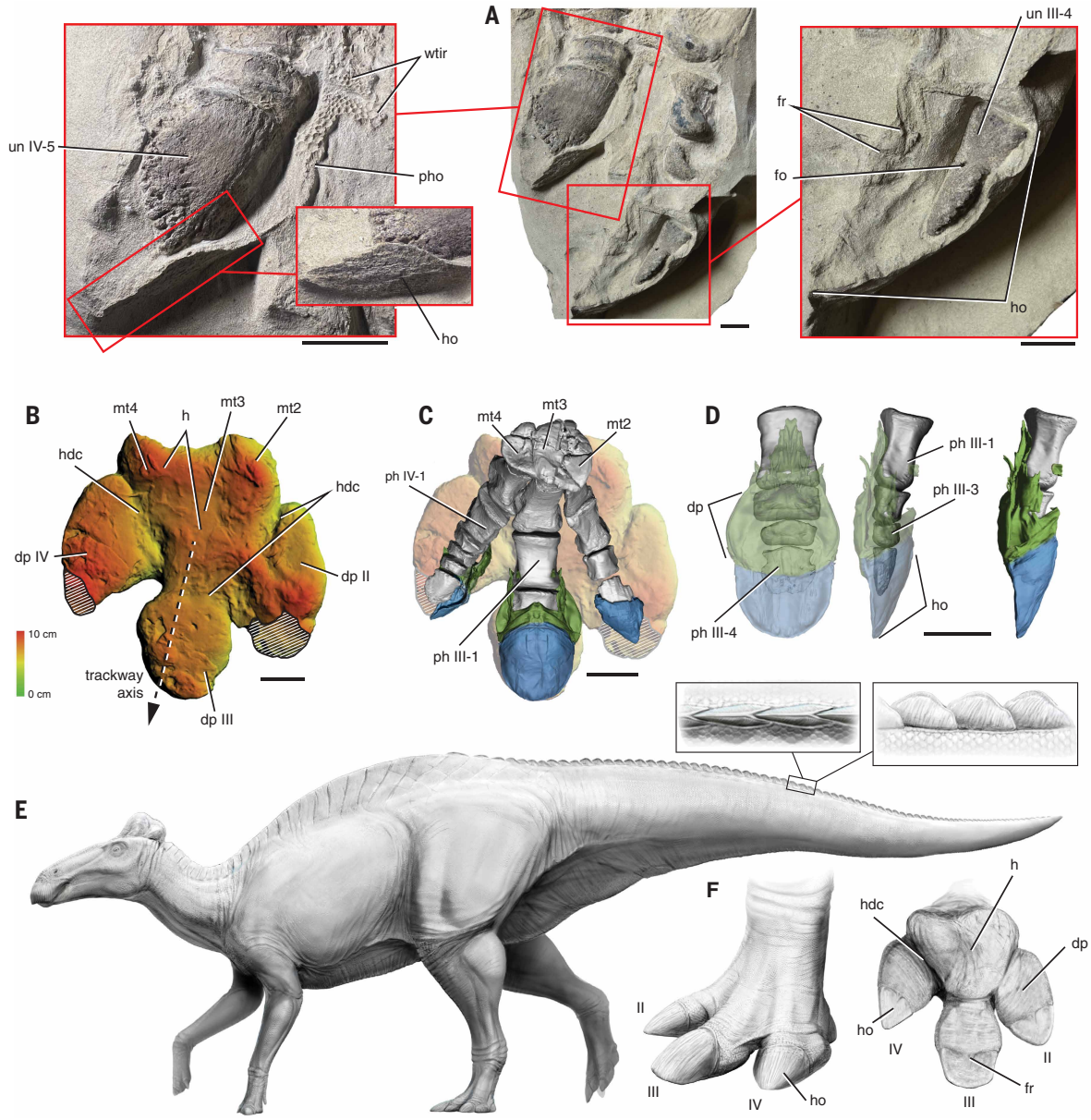

Fig. 3. Pedal hooves, digital pads, and fleshy profile in *E. annectens*. (**A**) Distal ends of right pedal digits III and IV in lateral and dorsolateral views, respectively, with enlarged views of the last phalanges, scaly skin, hoof cross section, and hoof surface texture of digit IV (left) and the last phalanx and hoof cross section of digit III (right) (UCRC PV30). (**B**) Relief map of a natural cast of a hadrosaurid right pedal footprint from the St. Mary River Formation (Maastrichtian) of Alberta (compare *E. annectens*; TMP 87.76.6; reversed to match right pes in dorsal view) (*21*). (**C**) Bones, partial hooves, and digital pads of the right pes of an early adult of *E. annectens* (UCRC PV30) in dorsal view (enlarged 15%) superposed over the natural cast of a right pedal footprint (TMP 87.76.6). Hooves are shown in blue and digital pads in green. (**D**) Hoof and digital pad of right pedal digit III in translucent ventral (left), translucent lateral (middle), and opaque lateral (right) views. Hooves are shown in blue and digital pads in green. (**E**) Life restoration of *E. annectens* in lateral view with occipital comb based on *E. regalis* (*18*) and enlargement of three caudal spikes in dorsal (left) and lateral (right) views. (**F**) Restoration of the left pes in dorsolateral (left) and ventral (right) views. II to IV, pedal digits II to IV; dp, digital pad; dhc, digit-heel crease; fo, foramen; fr, frog; h, heel; ho, hoof; mt2 to mt4, metatarsal 2 to 4; ph, phalanx; pho, perihoof; un, ungual; wtir, weathered-template integument rendering. Scale bars, 5 cm (left) and 3 cm (middle, right) (A), 10 cm for footprint [(B) and (C)], pes (C), and digit III (D).

various mammalian clades (*30*, *32*). Despite this phylogenetic complexity, all hooved mammals lived during the Cenozoic (*34*, *35*), are quadrupedal, evolved the hooved condition at small (1 to 2 kg) or moderate (< 200 kg; uintatheres and proboscideans) body size, and have fore and hindfeet with matching posture (both subunguligrade or unguligrade).

By contrast, end-Cretaceous *E. annectens* preserves the oldest hoof renderings for any tetrapod, the first record of hooves in a reptile, the first instance of a hooved tetrapod capable of bipedal locomotion, and the first hooved tetrapod with disparate fore and hindfoot posture (unguligrade versus subunguligrade, respectively). The disparity in fore and hindfoot posture seems possible only in a facultative quadruped with a posterior-centered body mass closer to the hindleg and with foreleg support limited to slow speeds. Conversely, obligate mammalian quadrupeds have an anterior-centered body mass closer to the foreleg and integrated locomotor demands that require matching fore and hindfoot posture.

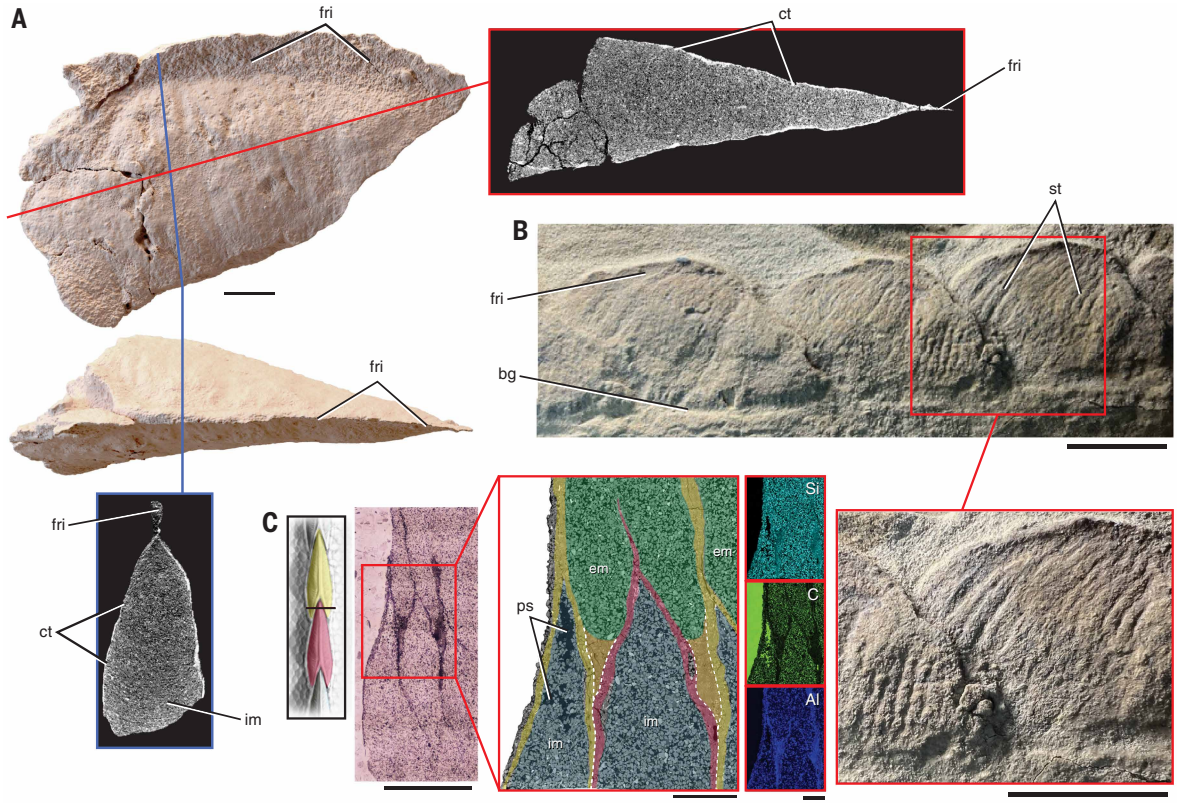

Fig. 4. Microstructure and geochemistry of spike integument renderings in *E. annectens* (UCRC PV30). (**A**) Spike of midcaudal vertebra (CA29) prepared free of external matrix in right lateral and dorsal views with CT cross sections in transverse and near horizontal planes. (**B**) Spikes of midcaudal vertebrae (CA32 to CA34) in lateral view (reversed) with an enlarged view (bottom) of interdigitation between successive spikes (over CA33 and CA34). (**C**) Backscatter electron microscopy showing two midcaudal spikes (CA30, yellow; CA31, red) in dorsal view showing position of transverse thin section (far left), transverse thin section (left), an enlarged view of transverse thin section in backscatter electron microscopy (middle), and energy-dispersive x-ray spectroscopy maps showing silicon and aluminum presence and carbon absence in the spikes (right); epoxy embedding medium external to the specimen on the slide was removed or uniform toned. CA30 spike is shown in yellow, CA31 spike is shown in red, interspike external infilling is shown in orange, external matrix is shown in green, and the internal matrix is shown in blue. Al, aluminum; bg, basal groove; C, carbon; ct, clay template; em, external matrix; fri, fringe; im, internal matrix; ps, pore space; Si, silicon; st, striations. Scale bars, 1 cm (A), 3 cm (B), and 1 cm (left) or 0.25 mm (middle, right) (C).

Judging from fossil and footprint records, the hooved unguligrade manus and subunguligrade pes first evolved among basal hadrosauriforms (e.g., *Iguanodon*) of considerable body mass (>500 kg) during the earliest Cretaceous. Late Jurassic outgroups (e.g., *Camptosaurus*) retain a spread manus and clawed, digitigrade hind feet generating bipedal digitigrade footprints with jointed digital pads (*24*). Hooves likely evolved even earlier in the Jurassic among armored ornithischians (stegosaurs and ankylosaurs), the manus and pes of which are stoutly proportioned and subunguligrade in posture, have spade-shaped unguals (*36*, *37*), and are linked to footprints with rounded toe imprints (*24*, *38*).

Clay template masks integument

We used a battery of optical, CT, electron microscopy, and x-ray spectroscopy techniques (see the supplementary materials and table S11) to investigate the structure and chemistry of the integument renderings of the new dinosaur mummies, all of which (scale, spike, and hoof) are preserved as a thin (<1 mm) clay layer bounded externally and internally by nearly identical sandstone matrix (Figs. 3A and 4).

The sand-sized, poorly sorted, weakly cemented matrix shows no evidence of internal structure or the presence of organics as visualized in thin section, CT scan, and by various spectroscopy techniques (Fig. 4C). Nor was there any evidence of original or degraded organics in either the clay layer or adjacent matrix. Indistinguishable external and internal matrices suggest that the carcass was breached before burial, permitting rapid infilling of cavities as well as integument structures (spikes, hooves) that must have been hollowed by subaerial decay (Figs. 3A and 4A). We found no evidence of "soft-tissue replacement structures" and endogenous "organic compounds" as reported in an *E. annectens* mummy from North Dakota (*12*, *39*) and from two integument patches from other hadrosaurines (*40*, *41*), all of which also were buried in terrestrial strata.

The clay layer in all of the integument renderings in the new mummies is composed predominantly of kaolinite and illite, which were present in trace amounts in the surrounding matrix. The clay layer has a relatively uniform thickness (<1 mm) across a wide variety of integument types (skin scales, spike, and hoof), suggesting that it marks a boundary rather than a replacement layer. In thin section of interdigitating spikes, the clay appears to accumulate in external crevasses between adjacent spikes (Fig. 4C), suggesting that it was deposited on the outside of the carcass. Therefore, we interpret the clay layer as a template congealing at a biofilm on the surface of the buried, decaying carcass rather than a replacement cast of an original tissue layer (*42*).

Clay templating (*43*–*45*) can preserve the external form of soft-bodied animals in Precambrian and Paleozoic Lagerstätten (*46*, *47*) when a biofilm (*48*–*50*) electrostatically draws the positive cations in clay minerals from surrounding sediment to the surface of a carcass in fine-grained lacustrine or marine depositional settings. Soft integumental structures, such as the bristles or feathers of nonavian dinosaurs, also have been preserved in Mesozoic lacustrine sediments through

carbonaceous compression fossilization (*51*, *52*). The *E. annectens* mummies from the Lance Formation, by contrast, are large, three-dimensional (3D) fossils buried in better oxygenated, coarse-grained fluvial deposits with clay as a minor component. Therefore, clay templating may generate soft tissue integument renderings in a wider range of depositional settings than previously realized.

Discussion

Epidermal renderings

Upon discovering the first dinosaur mummy in 1908, Sternberg (*53* remarked on the "impressions of its folding skin," and Osborn (*1*) described the fossilized integument as an "epidermal" or "skin impression." Osborn, however, clearly understood the fossilized integument of the AMNH mummy as an "epidermal cast" of some kind in sand with "clayey elements" that completely replaced the original surficial layer of skin. "Integument rendering" is the heuristic term we suggest here for fossilized soft tissue integument that includes four principal modes of preservation: cast-vestige, mold, template, and impression (see the supplementary materials and table S1). A diaphanous clay template, rather than cast-vestige replacement, is strongly supported for the *E. annectens* mummies from the mummy zone.

Dinosaur mummification

We corroborate closely the initial stages of Osborn's (*1*, *54*) taphonomic hypothesis for the AMNH mummy as our stages 1 and 2, both occurring within a single season. Stages 3 and 4 commence immediately after burial.

Stage 1. Carcass desiccation and initial decay: Wrinkled skin renderings closely draped over underlying skeletal bone of the new mummies and the dorsiflexed neck position of the late juvenile mummy provide indisputable evidence of postmortem subaerial desiccation (Figs. 2 and 3). Sustained aridity, or drought, has been identified as the cause of death for both the AMNH mummy (*55*) and scores of hadrosaurids in bone-bed accumulations in Late Cretaceous strata of the Western Interior (*56*). Within the first 7 to 10 days after death, carcasses of proboscideans (*57*, *58*) and humans (*59*, *60*) in arid environments are subject to integument desiccation, decay of deeper fleshy tissues through autolysis, bloating, release of gasses, and scavenging. Although Osborn (*1*) suggested that the "muscles and viscera" under the integument of the AMNH mummy shrank from dehydration, their removal by decay is shown by the immediate proximity of scaly skin to underlying bone visible over the pectoral girdles, rib cage, and sides of the tail, where considerable muscle mass was present in life. Decay also must have removed soft tissues inside the crest, spike row, and hooves of the new mummies, allowing for their rapid infilling upon burial (see stage 3 below). Scavenging is not apparent on any of the mummies from the mummy zone. The forelimbs, hind limbs, and tail of the late juvenile mummy (UCRC PV31) were present but partially removed by erosion. Drought-induced deaths of elephants often result in an overabundance of carcasses, leaving many untouched by scavengers and concentrated near or within dry riverbeds (*55*, *57*).

Stage 2. Sudden short-distance fluvial transport and burial: Seasonal monsoons characterized by cyclic drought and flooding, far from a rare pairing of antipodal environmental catastrophes [but see (*12*)], was the dominant climatic pattern for the Western Interior during the Late Cretaceous (*61*). Surrounding each mummy from the mummy zone is an uninterrupted body of sediment that suddenly engulfed each carcass, with evidence of high-energy fluvial transport in matrix associated with the specimens and at their localities (mud clasts, conglomerates, cross-bedding, broken bone, and tree trunk debris). The four mummies of *E. annectens* in the mummy zone are not only fully articulated and cloaked in unabraded integument, but they are also preserved in 3D (see the supplementary materials and table S5). Three of these preserve the anterior half of the body in a common death pose, resting upside down on one side of the trunk with forelimbs outstretched (the UCRC PV31, AMNH, and Senckenberg mummies). The fleshy crest preserved on the underside of two of these mummies (the UCRC PV31 and AMNH mummies) is deflected to one side, which must have occurred when it was still pliable at the time of death. These details support carcass burial by floodwaters at or near the site of death over a matter of hours or, at most, days (*55*). From the foregoing, we conclude that the span of time between death and sudden burial of the four *E. annectens* mummies in the mummy zone was on the order of a week or weeks within a single season.

Stage 3. Rapid infilling of a breached carcass: Sandstone matrix engulfing the carcass also infilled the body cavities and much smaller spaces generated during subaerial decay within the spikes and hooves (Figs. 3A and 4A). Because external and interior, or infilled, sediment is indistinguishable and composed principally of incompressible quartz grains, infilling would have been rapid, fully penetrating, and capable of preserving the 3D morphology of dehydrated integument.

Stage 4. Integument templating in clay and final decay: In the wet, porous sediment, a thin biofilm covered the surface of the decaying integument, electrostatically attracting residual clay from the surrounding matrix. Carpenter (*54*) nearly conceived this taphonomic scenario, citing the emergence after burial of a biofilm but omitting mention of an associated clay layer. Composed primarily of kaolinite and illite, the clay layer composing the integument rendering of the new *E. annectens* mummies appears to have been electrostatically drawn from a residual clay component of the matrix. At <1 mm in thickness, the clay layer faithfully records the 3D surface form and texture of the integument. The integument itself, including all tissue, cellular and subcellular structures, and organic biomolecules, broke down and was carried away in solution, with lithostatic compaction causing sand grains to press into inner and outer margins of the clay layer (Fig. 4C). Mummification was likely complete within weeks or months after burial, followed by the deposition of minor heavy minerals on the clay boundary (e.g., ironstone concretion around the end of the tail of the early adult) and eventually the permineralization of underlying skeletal bone.

The dinosaur mummy zone

E. annectens and hadrosaurids in general account for most dinosaur mummies (see the supplementary materials and table S4). The best-preserved mummies come from a small mummy zone <10 km in diameter in east-central Wyoming and from <100 m of the uppermost portion of the Lance Formation (Maastrichtian) (Fig. 1). Four of the six mummies in the zone came from the bottom 50 m of that section and pertain to the hadrosaurine *E. annectens*. Is there something special about hadrosaurid skin or the mummy zone that favored integument preservation?

Although thicker skin (*62*) has been suggested as the reason hadrosaurids dominate dinosaur mummies compared with contemporary ceratopsids, the integument covering the sides of the trunk in *Edmontosaurus* is extremely small-scaled (1 to 4 mm in diameter) with sharp-crested wrinkles that suggest the skin was very thin (Fig. 2A). Trunk scales in *Triceratops* (HMNS PV.1506), by contrast, are the largest ever recorded (~10 cm in diameter) and compose skin areas that appear to be too thick to wrinkle during desiccation.

Differences in preferred habitat more plausibly account for the predominance of hadrosaurid over ceratopsid mummies. *Triceratops* tends to be preserved in mudstones farther inland on the floodplain (*63*) with only two reported bone beds (*64*, *65*), whereas *Edmontosaurus* tends to be preserved in sandstone channel deposits closer to the coastline (*63*) with many large-scale bone beds [e.g., (*7*, *66*, *67*)].

The dinosaur mummy zone is located at the southern end of principal outcrops of the stratigraphically equivalent, flat-lying Hell Creek

and Lance Formations (*67*–*69*), both of which preserve hadrosaurids with integument renderings. The Hell Creek Formation is exposed in the Williston Basin from the Canadian border across Montana to the western edge of the Dakotas, and the Lance Creek Formation is exposed in the Powder River Basin and a north-south oblong trough extending from southern Montana to east-central Wyoming (*67*, *68*). The Lance Formation in southern Montana is ~200 m thick but gradually increases to >1000 m toward the southern edge of the Powder River Basin in the region of the mummy zone, which dates to the very end of the Cretaceous Period (*69*). The mummies rest atop a massive coastal sedimentary wedge that accumulated during a period of very rapid subsidence (~170 m/million years) (*69*). We infer from the foregoing that the extraordinary preservation of the mummy zone is due to rapid subsidence in a coastal setting subject to seasonal drought-flood cycles. The most extensive outcrops of the Lance Formation also occur at southern end of the Powder River Basin, a richly fossiliferous region that has attracted paleontologists for more than a century.

Materials and methods

Sediment sampling and analysis

Sediment samples were taken from both mummies of *E. annectens* (UCRC PV30 and UCRC PV31) adjacent to the clay template (internal and external) and from surrounding matrix away from the clay template. Likewise, sediment samples were taken from the early adult (UCRC PV30) adjacent to the hooves of the pes (internal and external) and far from the hoof sheath. We also sampled from the early adult (UCRC PV30) dark-staining minerals from scale renderings on the side of the tail and sediment from the ironstone concretion surrounding the tail tip. Finally, we sampled carbonized plant material from a lamina in the sediment under the middle of the tail.

We also analyzed sediment in thin section (see below). Sand grains are angular, with little cementation, visible pore spaces, and birefringence variation indicative of the presence of rare carbonate grains (dolomite or calcite). The sediment in both specimens is predominantly sand with minor silt and clay components and is indistinguishable on either side of the integument template. The integument template, composed predominantly of kaolinite and illite, preserves the external morphology of scaly skin, spikes, and hooves (see the supplementary materials and Figs. 2 to 4). In a few places, the clay template preserving the form of the scaly skin transitions from a positive rendering (convex scales) to what appears to be a negative rendering (pocked depressions bounded by scale interstices; Fig. 2A, left). The apparent negative rendering, however, we believe is due to missing template spanning the interstices, generating what we identify as "eroded template." A transition of this sort from positive to apparent negative rendering in an otherwise undisturbed area of scaly skin can give the false impression of inverted skin (*14*).

Imaging and analysis

X-ray diffraction of sediment: We analyzed the sediment in thin section from the midcaudal spike row of the early adult of *E. annectens* (UCRC PV30) (see the supplementary materials and table S11). X-ray diffraction (XRD) bulk analysis was performed in the Illinois State Geological Survey X-ray Diffraction Laboratory (UIUC) on a 150-μm thin section through the caudal spikes, centering a beam of ~2.54 cm diameter on the external matrix immediately adjacent to the clay template. The semiquantitative results are based on the reference intensity ratio method using corundum as the reference standard. All phase intensities quantified were recalculated (normalized) using the ratio of $\text{intensity}_{\text{phase}}/\text{intensity}_{\text{corundum}}$.

Thin sectioning of *E. annectens* spike series: A block containing a complete spike and portions of adjacent spikes (CA29 to CA31; Fig. 4C) was removed from the midtail of the early adult *E. annectens* (UCRC PV30), micro-CT scanned, digitally segmented, and prepared for thin sectioning at Spectrum Petrographics (Vancouver, WA) by vacuum embedding in epoxy (Epotek 301). Five 30-μm transverse thin sections were made of the central spike at regular increments (anterior end, anterior quarter, center, posterior quarter, and posterior end), with the posterior end section shown in Fig. 4C. An additional 150-μm transverse thin section was made at the anterior quarter for XRD analysis (see below).

Thin sectioning of extant squamate spike series: We serially sectioned the midline spike row above the head and neck of the extant squamate *Gonocephalus doriae* (Doria's angle-headed lizard from Borneo) using a formalin-fixed, ethanol-stored specimen (FMNH 249773). Using a microtome on the paraffin-embedded sample at the Human Tissue Resource Center (University of Chicago) (Fig. 2E), 10-μm thick horizontal (frontal) sections were placed on glass slides stained with hematoxylin and eosin for visualization under magnification (Dino-Lite digital microscope).

Light microscopy and stereophotogrammetry: We used an Edge digital microscope for light microscopy of small samples. Structure from motion photogrammetry of the integument and skeletons of late juvenile and early adult mummies (UCRC PV30 and UCRC PV31) was accomplished using a Fujifilm XT-4 camera with and without a ring flash to obtain the best image of the small-scale relief of the integument. The images (635 for UCRC PV31; 330 and 304 for UCRC PV30 tail and foot, respectively; resolution 6240 × 4160 pixels) were processed in Agisoft Metashape, creating a point, high-resolution 3D mesh from depth maps (10,500,000 polygons) with photorealistic texture (12,288 pixels). The tail model of the early adult mummy (Fig. 2B) rearticulated the two slabs that preserve the intact caudal series.

CT scanning and segmenting: We used a WayGate Phoenix V|tomex|s micro-CT scanner at the UChicago PaleoCT Core Facility (RRID: SCR_024763) to micro-CT scan both a block containing midcaudal spikes (CA30 and CA31) from the early adult UCRC PV30 and the head and neck of *G. doria* (FMNH H:249773), using Thermo Fisher Avizo software to segment and render the former and Materialise Mimics software to segment and render the latter. Open field jackets containing the partially prepared right hind foot and tail tip of the early adult mummy (UCRC PV30) were CT scanned using a Philips Brilliance iCT 256-slice multidetector CT scanner at the Human Imaging Resource Office Core Facility (RRID:SCR_018372; University of Chicago) (see the supplementary materials and table S11).

Electron microscopy, x-ray spectroscopy, and XRD analysis of spikes in matrix: Thin sections of a block containing several midcaudal spikes of the early adult of *E. annectens* (UCRC PV30) were visualized under light microscopy and subjected to backscattered electron imaging, energy-dispersive x-ray spectroscopy (EDS), and XRD clay analysis (for analytical abbreviations, see the supplementary materials and table S11). Electron microscopy and elemental mapping used a TESCAN LYRA3 field-emission scanning electron microscope to examine the thin section from the posterior end of the spike with the region of interest demarcated using strips of copper tape. No coating was applied to the surface of the sample. A scintillator-type backscattered electron detector was used to image the sample using a 15 Kv beam. Elemental maps were produced by energy-dispersive x-ray spectroscopy by raster imaging the slide with Oxford Instruments X-Max-80 silicon drift x-detectors. Resulting data were analyzed with Aztec software.

In natural light, the clay template is slightly darker than adjacent sandstone matrix, whereas in CT images, the clay layer appears denser (whiter) than the adjacent matrix (Fig. 4A). EDS showed aluminosilicate (silicon and aluminum) enrichment of the template material, which is consistent with clay mineralogy. The absence of significant carbon (Fig. 4C), sulfur, nitrogen, or phosphorous in the clay template

suggests that original biomolecules such as melanin, "keratin" (corneous beta-proteins), and collagen or their breakdown products are absent.

XRD analysis of the clay fraction (<2 μm) from a powdered sample from a spike was performed at the Illinois State Geological Survey X-ray Diffraction Laboratory at the University of Illinois Urbana-Champaign. Particles were oriented and saturated by ethylene glycol. Basal diffraction intensities (d001) of these concentrated clays obtained from the oriented and ethylene glycol–saturated films were compared with each other. The analysis was semiquantitatively calculated from major clay mineral intensities, and the main clay component was found to be kaolinite (54%).

REFERENCES AND NOTES

1. H. F. Osborn, Integument of the iguanodont dinosaur *Trachodon*. *Am. Mus. Nat. Hist. Mem.* **1**, 33–54 (1912).
2. C. H. Sternberg, Still in the Laramie Country, Converse County, Wyoming. *Trans. Kans. Acad. Sci.* **23**, 219–223 (1911). doi: 10.2307/3624588
3. J. Versluys, Der Schadel des Skelettes von *Trachodon annectens* im Senckenberg-Museum. *Abh. Senckenberg. Naturfors. Gesell.* **38**, 1–19 (1923).
4. D. Uhl, A reappraisal of the" stomach" contents of the *Edmontosaurus annectens* mummy at the Senckenberg Naturmuseum in Frankfurt/Main (Germany). *Z. Dtsch. Ges. Geowiss.* **171**, 71–85 (2020). doi: 10.1127/zdgg/2020/0224
5. P. Larson, M. Larson, C. Ott, R. Bakker, Skinning a *Triceratops*. *J. Vertebr. Paleontol.* **27**, 104A (2007).
6. C. Lipkin, P. C. Sereno, J. R. Horner, The furcula in *Suchomimus tenerensis* and *Tyrannosaurus rex* (Dinosauria: Theropoda: Tetanurae). *J. Paleontol.* **81**, 1523–1527 (2007). doi: 10.1666/06-024.1
7. M. Wosik, D. C. Evans, Osteohistological and taphonomic life-history assessment of *Edmontosaurus annectens* (Ornithischia: Hadrosauridae) from the Late Cretaceous (Maastrichtian) Ruth Mason dinosaur quarry, South Dakota, United States, with implication for ontogenetic segregation between juvenile and adult hadrosaurids. *J. Anat.* **241**, 272–296 (2022). doi: 10.1111/joa.13679; pmid: 35801524
8. N. E. Campione, "Postcranial anatomy of *Edmontosaurus regalis* (Hadrosauridae) from the Horseshoe Canyon Formation, Alberta, Canada" in *Hadrosaurs*, D. A. Eberth, D. C. Evans, Eds. (Indiana Univ. Press, 2015), pp. 208–244.
9. R. S. Lull, N. E. Wright, Hadrosaurian dinosaurs of North America. *Spec. Pap. Geol. Soc. Am.* **40**, 1–242 (1942).
10. W. A. Parks, The osteology of the trachodont dinosaur *Kritosaurus incurvimanus*. *Univ. Toronto Stud. Geol. Ser.* **11**, 1–74 (1920).
11. J. R. Horner, A "segmented" epidermal tail frill in a species of hadrosaurian dinosaur. *J. Paleontol.* **58**, 270–271 (1984).
12. S. K. Drumheller, C. A. Boyd, B. M. S. Barnes, M. L. Householder, Biostratinomic alterations of an *Edmontosaurus* "mummy" reveal a pathway for soft tissue preservation without invoking "exceptional conditions". *PLOS ONE* **17**, e0275240 (2022). doi: 10.1371/journal.pone.0275240; pmid: 36223345
13. C. E. Clayton *et al.*, "Non–osseous dermal scutes and integument impressions from an exceptionally preserved hadrosaurid dinosaur skeleton, Upper Cretaceous Kaiparowits Formation of Utah" in *A Review of Hadrosaurid Skin Impressions. Hadrosaur Symposium 2011 Abstract Volume*, D. R. Braman, D. C. Eberth, D. C. Evans, W. Taylor, Eds. (Royal Tyrrell Museum of Palaeontology, 2011), vol. 589, pp. 23–27.
14. P. R. Bell, Standardized terminology and potential taxonomic utility for hadrosaurid skin impressions: A case study for *Saurolophus* from Canada and Mongolia. *PLOS ONE* **7**, e31295 (2012). doi: 10.1371/journal.pone.0031295; pmid: 22319623
15. N. L. Murphy, D. Trexler, M. Thompson, "'Leonardo,' a mummified *Brachylophosaurus* (Ornithischia: Hadrosauridae) from the Judith River Formation of Montana" in *Horns and Beaks: Ceratopsian and Ornithopod Dinosaurs*, K. Carpenter, Ed. (Indiana Univ. Press, 2007), pp. 117–133.
16. F. Bertozzo, C. D. Sasso, M. Fabbri, F. Manucci, S. Maganuco, Redescription of a remarkably large *Gryposaurus notabilis* (Dinosauria: Hadrosauridae) from Alberta, Canada. *Mem. Soc. Ital. Sci. Nat. Mus. Civ. Storia Nat. Milano* **43**, 1–56 (2017).
17. P. R. Bell, "A review of hadrosaurid skin impressions" in *Hadrosaurs*, D. A. Eberth, D. C. Evans, Eds. (Indiana Univ. Press, 2014), pp. 572–590.
18. P. R. Bell, F. Fanti, P. J. Currie, V. M. Arbour, A mummified duck-billed dinosaur with a soft-tissue cock's comb. *Curr. Biol.* **24**, 70–75 (2014). doi: 10.1016/j.cub.2013.11.008; pmid: 24332547
19. F. D. Ross, G. C. Mayer, "On the dorsal armor of the Crocodilia" in *Advances in Herpetology and Evolutionary Biology*, K. Miyata, A. Rhodin, Eds. (Harvard Univ. Press, 1983), pp. 305–331.
20. P. Wu, Y.-C. Lai, R. Widelitz, C.-M. Chuong, Comprehensive molecular and cellular studies suggest avian scutate scales are secondarily derived from feathers, and more distant from reptilian scales. *Sci. Rep.* **8**, 16766 (2018). doi: 10.1038/s41598-018-35176-y; pmid: 30425309
21. P. J. Currie, G. C. Nadon, M. G. Lockley, Dinosaur footprints with skin impressions from the Cretaceous of Alberta and Colorado. *Can. J. Earth Sci.* **28**, 102–115 (1991). doi: 10.1139/e91-009
22. R. Zheng, A. A. Farke, G.-S. Kim, A photographic atlas of the pes from a hadrosaurine hadrosaurid dinosaur. *PalArch J. Vertebr. Palaeontol.* **8**, 1–12 (2011).
23. K. Moreno, M. T. Carrano, R. Snyder, Morphological changes in pedal phalanges through ornithopod dinosaur evolution: A biomechanical approach. *J. Morphol.* **268**, 50–63 (2007). doi: 10.1002/jmor.10498; pmid: 17146773
24. T. Thulborn, *Dinosaur Tracks* (Chapman and Hall, 1990).doi: 10.1007/978-94-009-0409-5
25. A. H. Parks, "Anatomy and function of the equine digit" in *Equine Laminitis*, J. K. Belknap, R. J. Geor, Eds. (Wiley, 2017), pp. 13–21; https://onlinelibrary.wiley.com/doi/10.1002/9781119169239.ch3.
26. C. C. Pollitt, The anatomy and physiology of the suspensory apparatus of the distal phalanx. *Vet. Clin. North Am. Equine Pract.* **26**, 29–49 (2010). doi: 10.1016/j.cveq.2010.01.005; pmid: 20381734
27. A. Benz, "The elephant's hoof: Macroscopic and microscopic morphology of defined locations under consideration of pathological changes," thesis, Vetsuisse-Fakultät Universität Zürich, Zürich, Switzerland (2005).
28. J. R. Hutchinson *et al.*, From flat foot to fat foot: Structure, ontogeny, function, and evolution of elephant "sixth toes," *Science* **334**, 1699–1703 (2011). doi: 10.1126/science.1211437; pmid: 22194576
29. D. A. Croft, J. N. Gelfo, G. M. López, Splendid innovation: The extinct South American native ungulates. *Annu. Rev. Earth Planet. Sci.* **48**, 259–290 (2020). doi: 10.1146/annurev-earth-072619-060126
30. N. R. Chimento, F. L. Agnolin, Phylogenetic tree of Litopterna and Perissodactyla indicates a complex early history of hoofed mammals. *Sci. Rep.* **10**, 13280 (2020). doi: 10.1038/s41598-020-70287-5; pmid: 32764723
31. S. Jackson, C. Groves, *Taxonomy of Australian Mammals* (Csiro Publishing, 2015). doi: 10.1071/9781486300136
32. M. Spaulding, M. A. O'Leary, J. Gatesy, Relationships of Cetacea (Artiodactyla) among mammals: Increased taxon sampling alters interpretations of key fossils and character evolution. *PLOS ONE* **4**, e7062 (2009). doi: 10.1371/journal.pone.0007062; pmid: 19774069
33. W. J. Murphy, N. M. Foley, K. R. Bredemeyer, J. Gatesy, M. S. Springer, Phylogenomics and the genetic architecture of the placental mammal radiation. *Annu. Rev. Anim. Biosci.* **9**, 29–53 (2021). doi: 10.1146/annurev-animal-061220-023149; pmid: 33228377
34. N. M. Foley *et al.*, A genomic timescale for placental mammal evolution. *Science* **380**, eabl8189 (2023). doi: 10.1126/science.abl8189; pmid: 37104581
35. P. M. Velazco *et al.*, Combined data analysis of fossil and living mammals: A Paleogene sister taxon of Placentalia and the antiquity of Marsupialia. *Cladistics* **38**, 359–373 (2022). doi: 10.1111/cla.12499; pmid: 35098586
36. P. Senter, Evidence for a sauropod-like metacarpal configuration in stegosaurian dinosaurs. *Acta Palaeontol. Pol.* **55**, 427–432 (2010). doi: 10.4202/app.2009.1105
37. P. J. Currie, D. Badamgarav, E. B. Koppelhus, R. Sissons, M. K. Vickaryous, Hands, feet, and behaviour in *Pinacosaurus* (Dinosauria: Ankylosauridae). *Acta Palaeontol. Pol.* **56**, 489–504 (2011). doi: 10.4202/app.2010.0055
38. F. M. Petti, S. D'Orazi Porchetti, E. Sacchi, U. Nicosia, A new purported ankylosaur trackway in the Lower Cretaceous (lower Aptian) shallow-marine carbonate deposits of Puglia, southern Italy. *Cretac. Res.* **31**, 546–552 (2010). doi: 10.1016/j.cretres.2010.07.004
39. P. L. Manning *et al.*, Mineralized soft-tissue structure and chemistry in a mummified hadrosaur from the Hell Creek Formation, North Dakota (USA). *Proc. Biol. Sci.* **276**, 3429–3437 (2009). doi: 10.1098/rspb.2009.0812; pmid: 19570788
40. M. Barbi *et al.*, Integumentary structure and composition in an exceptionally well-preserved hadrosaur (Dinosauria: Ornithischia). *PeerJ* **7**, e7875 (2019). doi: 10.7717/peerj.7875; pmid: 31637130
41. M. Fabbri, J. Wiemann, F. Manucci, D. E. G. Briggs, Three-dimensional soft tissue preservation revealed in the skin of a non-avian dinosaur. *Palaeontology* **63**, 185–193 (2020). doi: 10.1111/pala.12470
42. L. A. Parry *et al.*, Soft-bodied fossils are not simply rotten carcasses – Toward a holistic understanding of exceptional fossil preservation: Exceptional fossil preservation is complex and involves the interplay of numerous biological and geological processes. *BioEssays* **40**, 1700167 (2018). doi: 10.1002/bies.201700167; pmid: 29193177
43. K. M. Towe, Fossil preservation in the Burgess Shale. *Lethaia* **29**, 107–108 (1996). doi: 10.1111/j.1502-3931.1996.tb01844.x
44. A. Page, S. E. Gabbott, P. R. Wilby, J. A. Zalasiewicz, Ubiquitous Burgess Shale–style "clay templates" in low-grade metamorphic mudrocks. *Geology* **36**, 855–858 (2008). doi: 10.1130/G24991A.1
45. E. Naimark *et al.*, Decaying in different clays: Implications for soft-tissue preservation. *Palaeontology* **59**, 583–595 (2016). doi: 10.1111/pala.12246
46. B. Becker-Kerber *et al.*, Clay templates in Ediacaran vendotaeniaceans: Implications for the taphonomy of carbonaceous fossils. *Geol. Soc. Am. Bull.* **134**, 1334–1346 (2022). doi: 10.1130/B36033.1
47. R. P. Anderson, N. J. Tosca, E. E. Saupe, J. Wade, D. E. G. Briggs, Early formation and taphonomic significance of kaolinite associated with Burgess Shale fossils. *Geology* **49**, 355–359 (2021). doi: 10.1130/G48067.1

48. J. Reitner, "Biofilms and fossilization" in *Encyclopedia of Geobiology*, J. Reitner, V. Thiel, Eds. (Springer, 2011), pp. 136–137. doi: 10.1007/978-1-4020-9212-1_26
49. R. A. Raff, E. C. Raff, The role of biology in the fossilization of embryos and other soft-bodied organisms: Microbial biofilms and Lagerstätten. *Paleontol. Soc. Pap.* **20**, 83–100 (2014). doi: 10.1017/S1089332600002813
50. T. Tolker-Nielsen, Biofilm Development. *Microbiol. Spectr.* **3**, MB-0001-2014 (2015). doi: 10.1128/microbiolspec.MB-0001-2014; pmid: 26104692
51. M. A. Norell, X. Xu, Feathered dinosaurs. *Annu. Rev. Earth Planet. Sci.* **33**, 277–299 (2005). doi: 10.1146/annurev.earth.33.092203.122511
52. G. Mayr, M. Pittman, E. Saitta, T. G. Kaye, J. Vinther, Structure and homology of *Psittacosaurus* tail bristles. *Palaeontology* **59**, 793–802 (2016). doi: 10.1111/pala.12257
53. C. H. Sternberg, Expedition to the Laramie Beds of Converse County, Wyoming. *Trans. Kans. Acad. Sci.* **22**, 113–116 (1908). doi: 10.2307/3624729
54. K. Carpenter, How to make a fossil: Part 2 – Dinosaur mummies and other soft tissue. *J Paleontol. Sci.* **7**, 1–23 (2007).
55. K. Carpenter, "Paleoecological significance of droughts during the Late Cretaceous of the Western Interior" in *Fourth Symposium on Mesozoic Terrestrial Ecosystems, Short Papers*, P. M. Currie, E. H. Koster, Eds. (Tyrrell Museum of Palaeontology, 1987), pp. 42–47.
56. R. R. Rogers, Taphonomy of three dinosaur bone beds in the Upper Cretaceous Two Medicine Formation of northwestern Montana: Evidence for drought-related mortality. *Palaios* **5**, 394–413 (1990). doi: 10.2307/3514834
57. G. Haynes, *Mammoths, Mastodonts, and Elephants: Biology, Behavior and the Fossil Record* (Cambridge Univ. Press, 1991).
58. P. A. White, C. G. Diedrich, Taphonomy story of a modern African elephant *Loxodonta africana* carcass on a lakeshore in Zambia (Africa). *Quat. Int.* **276–277**, 287–296 (2012). doi: 10.1016/j.quaint.2012.07.025
59. A. Galloway, W. H. Birkby, A. M. Jones, T. E. Henry, B. O. Parks, Decay rates of human remains in an arid environment. *J. Forensic Sci.* **34**, 607–616 (1989). doi: 10.1520/JFS12680J; pmid: 2738563
60. C. L. Parks, A study of the human decomposition sequence in central Texas. *J. Forensic Sci.* **56**, 19–22 (2011). doi: 10.1111/j.1556-4029.2010.01544.x; pmid: 20840291
61. H. C. Fricke, B. Z. Foreman, J. O. Sewall, Integrated climate model-oxygen isotope evidence for a North American monsoon during the Late Cretaceous. *Earth Planet. Sci. Lett.* **289**, 11–21 (2010). doi: 10.1016/j.epsl.2009.10.018
62. M. Davis, Census of dinosaur skin reveals lithology may not be the most important factor in increased preservation of hadrosaurid skin. *Acta Palaeontol. Pol.* **59**, 601–605 (2014).
63. T. R. Lyson, N. R. Longrich, Spatial niche partitioning in dinosaurs from the latest cretaceous (Maastrichtian) of North America. *Proc. Biol. Sci.* **278**, 1158–1164 (2011). doi: 10.1098/rspb.2010.1444; pmid: 20943689
64. J. de Rooij *et al.*, Stable isotope record of *Triceratops* from a mass accumulation (Lance Formation, Wyoming, USA) provides insights into *Triceratops* behaviour and ecology. *Palaeogeogr. Palaeoclimatol. Palaeoecol.* **607**, 111274 (2022). doi: 10.1016/j.palaeo.2022.111274
65. S. W. Keenan, J. B. Scannella, "Paleobiological implications of a *Triceratops* bonebed from the Hell Creek Formation, Garfield County, northeastern Montana" in *Through the End of the Cretaceous in the Type Locality of the Hell Creek Formation in Montana and Adjacent Areas*, G. P. Wilson, W. A. Clemens, J. R. Horner, J. H. Hartman, Eds. (Geological Society of America, 2014), Special Paper 503, pp. 349–364; doi: 10.1130/2014.2503(14)
66. K. Snyder, M. McLain, J. Wood, A. Chadwick, Over 13,000 elements from a single bonebed help elucidate disarticulation and transport of an *Edmontosaurus* thanatocoenosis. *PLOS ONE* **15**, e0233182 (2020). doi: 10.1371/journal.pone.0233182; pmid: 32437394
67. K. R. Johnson, D. J. Nichols, J. H. Hartman, "Hell Creek Formation: A 2001 synthesis" in *The Hell Creek Formation and the Cretaceous-Tertiary Boundary in the Northern Great Plains: An Integrated Continental Record of the End of the Cretaceous*, J. H. Hartman, K. R. Johnson, D. J. Nichols, Eds. (US Geological Survey, 2002), vol. 361, pp. 503–510; doi: 10.1130/0-8137-2361-2.503
68. J. R. Gill, W. A. Cobban, Stratigraphy and geologic history of the Montana Group and equivalent rocks, Montana, Wyoming, and North and South Dakota. *Geol. Surv. Profess. Pap.* **776**, 1–37 (1973). doi: 10.3133/pp776
69. C. W. Connor, "The Lance Formation: Petrography and stratigraphy, Powder River Basin and nearby basins, Wyoming and Montana" in *Evolution of Sedimentary Basins—Powder River Basin*, V. F. Nuccio, P. L. Hansley, W. A. Cobban, C. G. Whitney, Eds. (US Geological Survey, Bulletin 1917-1, 1992); https://pubs.usgs.gov/bul/1917i/report.pdf.
70. P. C. Sereno *et al.*, Microscopic and chemical data for: Duck-billed dinosaur fleshy midline and hooves reveal terrestrial clay-template "mummification," Dryad (2025); https://doi.org/10.5061/dryad.q573n5tx4.

ACKNOWLEDGMENTS

We thank D. Navarro for gray-tone flesh reconstructions and color scene renderings; E. Fitzgerald and R. Masek for fossil preparation; D. Henderson (Royal Tyrrell Museum of Palaeontology) for footprint photography; M. Whitney (Loyola University) for assistance with light microscopy; R. Kamei and J. Mata (Field Museum of Natural History) for access to extant preserved reptile specimens; J. Mallon (Canadian Museum of Nature) for data on *E. regalis*; N. Gruszauskas (HIRO facility, University of Chicago) for CT scans; G. Olack (FIB-SEM facility, University of Chicago) for assistance with electron and x-ray spectroscopy; M. Pentrak for XRD analysis (XRD/XRF Materials Characterization Laboratory, University of Illinois Urbana-Champaign); T. Li, X. Jiang, and E. Markiewicz (University of Chicago) for assistance with dissection, embedding, and thin sectioning of *Gonocephalus*; L. Alibardi (University of Bologna) for discussion about reptile histology; L. Parry (Oxford University) and S. Darroch (Senckenberg Museum of Natural History) for discussion on clay templating; K. Stauffer (Zerbst Ranch) for historical information on Wyoming homesteads; D. Levering (Sternberg Museum of Natural History) and C. Mehling (American Museum of Natural History) for access to archival letters and images; C. Boyd (North Dakota Geological Survey) and S. Drumheller (University of Tennessee-Knoxville) for discussion on dinosaur mummies; S. Kidwell (University of Chicago), J. Vinther (Bristol University), K. Carpenter (University of Colorado Museum), T. Green (New York Institute of Technology), and Filippo Bertozzo for comments on taphonomic interpretations and tables; and MorphoSource for archiving CT scans. **Funding:** This research was supported by an anonymous gift to P.C.S. of the Fossil Lab (University of Chicago) and a Marie Sklodowska Curie Actions grant (EvoSaurAF 101068861) to D.V. **Author contributions:** P.C.S. wrote the initial draft. E.T.S. contributed to the initial draft and led all microstructural and chemical analyses and spectroscopy visualizations. D.V., N.M., and S.L.B. contributed to the final draft. D.V. conducted stereophotogrammetric imaging of both mummies. L.L.B. and P.C.S. prepared Figs. 1 to 4. L.L.B. generated micro-CT scans. L.L.B. and M.C.R. segmented the CT and MRI scans. L.L.B., M.C.R., and D.V. assisted in reconstructions. S.L.B. managed digital data curation. T.M.K. prepared specimens and contributed to the final draft and supplementary information. P.C.S., E.T.S., D.V., and L.L.B. created all finished figures. S.L.B. created figure parts and visualizations. E.T.S. and T.M.K. guided fossil and recent specimen sectioning and sampling. P.C.S., E.T.S., M.E., and K.D. provided field data and observations. **Competing interests:** The authors declare no competing interests. **Data, code, and materials availability:** All reconstructions and data supporting our findings are available within the main text or the supplementary materials. CT scans and 3D models (extended data table S7) are available on MorphoSource (https://www.morphosource.org/projects/000664781?locale=en). Microscopic and chemical data are available on Dryad (*70*).

SUPPLEMENTARY MATERIALS

science.org/doi/10.1126/science.adw3536
Supplementary Text; Figs. S1 to S22; Tables S1 to S11; References (*71*–*117*);
MDAR Reproducibility Checklist

Submitted 29 January 2025; accepted 9 September 2025; published online 23 October 2025
10.1126/science.adw3536

Duck-billed dinosaur fleshy midline and hooves reveal terrestrial clay-template "mummification"

Paul C. Sereno, Evan T. Saitta, Daniel Vidal, Nathan Myhrvold, María Ciudad Real, Stephanie L. Baumgart, Lauren L. Bop, Tyler M. Keillor, Marcus Eriksen, and Kraig Derstler

Science **391** (6780), eadw3536. DOI: 10.1126/science.adw3536

Editor's summary

A hundred years ago at a site in Wyoming, a seemingly mummified dinosaur was discovered. Since that time, other sites have revealed extraordinarily preserved features of early organisms, such as integument and feathers. The majority of these sites occur in regions where conditions were anoxic and wet, but the Wyoming site was entirely different, being decay prone, oxygenated, and influenced by both drought and floods. Sereno *et al*. describe two additional duck-billed dinosaur "mummies" from this site for which incredible detail was preserved, including a crest, a row of spikes, and hooves. The authors were also able to identify the taphonomic process that preserved these features in this unexpected climate. —Sacha Vignieri

RESEARCH ARTICLE SUMMARY

PALEONTOLOGY

Duck-billed dinosaur fleshy midline and hooves reveal terrestrial clay-template "mummification"

Paul C. Sereno*, Evan T. Saitta, Daniel Vidal, Nathan Myhrvold, María Ciudad Real, Stephanie L. Baumgart, Lauren L. Bop, Tyler M. Keillor, Marcus Eriksen, Kraig Derstler

Full article and list of author affiliations: https://doi.org/10.1126/science.adw3536

INTRODUCTION: Called dinosaur "mummies," two skeletons of the duck-billed dinosaur *Edmontosaurus* were discovered in Wyoming more than a century ago preserved like sun-dried carcasses. The snout of one is covered with a ducklike bill, and both have large areas of scaly integument described as "skin impressions." Revisiting this area uncovered a "mummy zone," with finds including two additional *Edmontosaurus* mummies and exceptional specimens of the contemporaries *Triceratops* and *Tyrannosaurus*. How soft tissues fossilize, and whether any of the original organic materials survive, remain open questions.

RATIONALE: To investigate integument fossilization, we used high-resolution imaging, thin-section microscopy, and geochemical analyses, documenting the surrounding sediment and the structure and composition of the integument layer. Based on past research, fossilized integument (or "integument rendering") is generated through one of four pathways: cast-vestige, mold, template, or impression.

Because terms for integument structures such as "crest" or "hoof" are often used informally, we provide definitions for all major keratinous, cornified structures in tetrapods, dividing those that are entirely fleshy from those underlain by bone. We also compile and organize terms for reptilian scalation under five categories: shape, form, ornamentation, topology, and pattern.

RESULTS: The new mummies provide a complete fleshy profile for a large-bodied dinosaur. A fleshy neck-to-trunk crest transitions over the hips into an interdigitating spike row that continues to the tip of the tail. The scales on the crest and trunk are very small for a 12-m reptile, with most measuring 1 to 4 mm in diameter. Wedge-shaped hooves, here preserved in a reptile, cap the toes of fore and hind feet. All soft tissue structures are preserved as a very thin (0.5 mm or less) clay layer or template. Experiments have shown that a biofilm on the surface of decaying tissue can accumulate template clay from surrounding sediment before soft tissue degradation. We found no trace of internal integument structure or original organic material.

CONCLUSION: Recently discovered duck-billed dinosaur mummies suggest that "mummification" occurred after drought-induced mortality involving four stages: carcass desiccation and initial subaerial decay, sudden burial with minimal transport, rapid carcass infilling, and templating in clay and final decay. The cyclic drought-flood monsoonal climate of the Lance Formation and its extraordinary thickness under the mummy zone provided the environmental and geologic conditions, respectively, for rapid burial of desiccated, unscavenged carcasses without sediment reworking. Unlike the underlying permineralized skeletal bone, the integument renderings of these dinosaur mummies congealed early in the process of fossilization as a thin external clay mask, a templating process documented previously only in anoxic marine settings. □

Dinosaur mummies unmasked. Mummies of the duck-billed dinosaur *Edmontosaurus annectens* (1) document with a thin external clay template a fleshy crest over neck and trunk (2), a fleshy spike row over hips and tail (3), and hooves capping the toes of the hind feet (4). Preserved as desiccated carcasses (5) and rapidly buried rapidly by floodwaters (6) on a coastline (7), the duck-billed mummies come from the very end of the dinosaur era in what today is east-central Wyoming. [Artwork by Dani Navarro.]

*Corresponding author. Email: dinosaur@uchicago.edu Cite this article as P. C. Sereno *et al.*, *Science* **391**, eadw3536 (2026). DOI: 10.1126/science.adw3536

PALEONTOLOGY

Duck-billed dinosaur fleshy midline and hooves reveal terrestrial clay-template "mummification"

Paul C. Sereno[1,2]*, Evan T. Saitta[1], Daniel Vidal[1,3], Nathan Myhrvold[4], María Ciudad Real[1,3], Stephanie L. Baumgart[5], Lauren L. Bop[1], Tyler M. Keillor[1], Marcus Eriksen[6], Kraig Derstler[7]

Two "mummies" of the end-Cretaceous duck-billed dinosaur *Edmontosaurus annectens* preserve a fleshy crest over the neck and trunk, an interdigitating spike row over the hips and tail, and hooves capping the toes of the hind feet. A battery of tests showed that all of the fossilized integument (skin, spike, and hoof) are preserved as a thin (less than 1 millimeter) clay template that formed on the surface of a buried carcass during decay before the loss of all soft tissues and organic compounds. Unlike the underlying permineralized skeletal bone, the integument renderings of these "dinosaur mummies" are preserved as a thin external clay mask, a templating process documented previously only in anoxic marine settings.

In 1908 in east-central Wyoming, noted fossil collector C. H. Sternberg discovered a skeleton of the duck-billed dinosaur *Edmontosaurus annectens* blanketed by large areas of scaly skin rendered in sediment. Described in 1912 by H. F. Osborn and nicknamed the "AMNH mummy," this specimen preserves a broad sampling of scaly skin renderings he called "skin impressions" (*1*). Two years later in the same area, Sternberg unearthed a second specimen of the same dinosaur with extensive integument traces (*2*). Dubbed the "Senckenberg mummy," this specimen also preserves a rendering of the upper bill (*3*, *4*).

We replace Osborn's and Sternberg's widely used term "skin impression" with "rendering," because creating a negative relief impression of integument in sediment, the literal interpretation of their term, is the rarest among the four modes of fossilization we recognize (cast-vestige, mold, template, and impression). We also define "fossil mummy," compile terms for fleshy and bone-supported integument structures (e.g., crest and hoof), and provide a descriptive framework for reptilian scalation (based on shape, form, ornamentation, topology, and pattern) (see the supplementary materials and tables S1 to S3).

Using historical photographs and letters, we approximated the quarry locations for Sternberg's AMNH and Senckenberg mummies in what we describe as a "mummy zone" <10 km in diameter (Fig. 1A; for site documentation, see the supplementary materials, figs. S1 to S5, and table S5). More than a century after Sternberg's discoveries, the same local area of ravine exposures of fluvial sandstone has yielded a skeleton of *Triceratops horridus* with large areas of rendered skin (*5*), an articulated skeleton of *Tyrannosaurus rex* with a sedimentological body boundary (*6*), and "late juvenile" and "early adult" mummies of *E. annectens* estimated to be 2 and 5 to 8 years old (*7*), respectively (for more details, see the supplementary materials and tables S6 and S7). The late juvenile is the first subadult dinosaur mummy on record and the first large-bodied dinosaur preserving the fleshy midline over the trunk (Figs. 2A and 3E). The early adult is the first hadrosaurid to preserve the entire spike row from hips to tail tip and the first reptile preserving wedge-shaped pedal hooves (Figs. 2B and 3).

[1]Department of Organismal Biology and Anatomy, University of Chicago, Chicago, IL, USA. [2]Committee on Evolutionary Biology, University of Chicago, Chicago, IL, USA. [3]Grupo de Biología Evolutiva, UNED, Madrid, Spain. [4]Intellectual Ventures, Bellevue, WA, USA. [5]Department of Physiological Sciences, University of Florida College of Veterinary Medicine, Gainesville, FL, USA. [6]Ventura County Science Center, Santa Paula, CA, USA. [7]Independent researcher, Divide, CO, USA. ***Corresponding author. Email: dinosaur@uchicago.edu**

Results

Midline crest and spike row

The neck and trunk midline are surmounted by a fleshy, scaled crest that gradually merges over the hips into an interdigitating spike row that continues to the tail tip (Figs. 2, A and B; 3E; and 4A). The cervical crest is best preserved in the early adult AMNH mummy (*1*), where it reaches a height of at least 7 to 8 cm (dorsal edge likely incomplete). The sides of the neck and trunk crest are divided into elevated bands covered with relatively small (1 to 4 mm) polygonal or pebble scales and separated by grooves lined with very fine scales (≤1 mm) (Fig. 2A). The bands are aligned in segmental relationship with underlying vertebrae, as reported by Osborn (*1*). They expand distally and increase in posterodorsal inclination from neck to midtrunk (Figs. 2A and 3E).

The neck crest is entirely fleshy and presumably flexible, positioned along the midline above the very low neural spines of the cervical series. It appears sheet-like in cross section, its narrow base positioned medial to the articulation between the transverse processes and tubercles of the cervical ribs (*1*). Over the anterior trunk, the crest has a subtriangular cross section, its broader base now incorporating the tubercular articulation of underlying vertebrae (Figs. 2A and 3E). The crest triples in height over middorsal vertebrae to a depth of 17 cm in the late juvenile mummy, or ~28 cm when scaled isometrically to early adult size (for mummy body size, see the supplementary materials and table S6). Both the late juvenile and AMNH mummies are preserved as inverted carcasses resting on their backs with their fleshy crests bending from the midline under the weight of the carcass (Fig. 2A).

At midtrunk, the dorsal margin of the crest has a thickness of 1.6 cm (2.6 cm scaled to early adult size). The taller neural spines of the posterior dorsal vertebrae (*8*) presumably insert into the posterior portion of the crest, which has a checkboard pattern of finely scaled grooves (Fig. 2A). Faint lineations angle posteroventrally across the trunk crest, possibly reflecting subdermal connective tissue.

Low, elongate spikes first appear over sacral neural spines (sacral vertebrae 3 and 4) directly above the hip socket. The spikes increase in height to a maximum of ~5 cm in the anterior portion of the tail (around caudal vertebra 20) before gradually decreasing in height and length toward the distal end of the tail, as preserved in situ on a block preserving the last 53 caudal vertebrae of the tail (approximately caudal vertebrae 11 to 64; Fig. 2B). The best-preserved spikes have a smooth perimeter fringe ~5 mm in width and only 1 mm in thickness (Fig. 4A). Below the fringe, the transverse thickness of the spike increases to 1.3 cm at its base, with each side covered by posterodorsally inclined, irregularly beaded striations (Fig. 4B).

The posterior end of each spike bifurcates to receive the anterior end of the next spike, their subtriangular area of interdigitation slightly raised (Figs. 3E and 4B). A basal groove separates the spike row from polygonal scales covering each side of the tail. The tip of each caudal neural spine projects into the posterior end of the base of each spike, terminating just dorsal to the basal groove.

The skin in life appears to have been very thin over the trunk and somewhat thicker over the sides of the tail, as shown by the form of the desiccation-deflation wrinkling: short and sharp-edged on the trunk and longer and rounded on the tail (Fig. 2, A and B). On the sides of the tail, polygonal scales are smallest near the spike row (~3 mm), somewhat larger in the upper one-third of the tail (~5 to 8 mm), and largest over the ventral two-thirds of the tail (~6 to 9 mm). The desiccated skin on each side of the tail is closely appressed to the contours of the underlying bones and ossified tendons.

Fleshy profile

After the 1908 discovery of a section of the neck crest in the AMNH mummy, Osborn (*1*) and later authors (*9*) depicted *E. annectens* in life

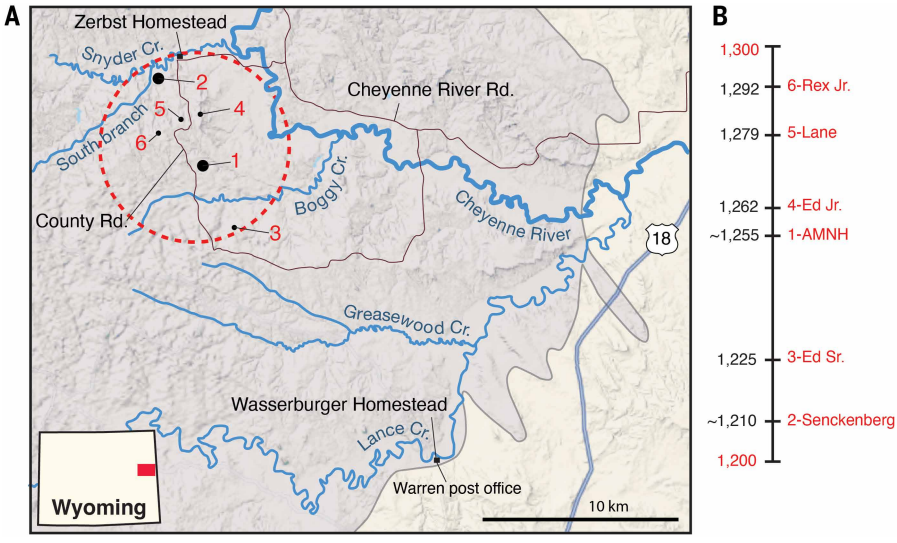

Fig. 1. Dinosaur mummy zone in the Lance Formation of east-central Wyoming. (**A**) Map of sites showing the mummy zone (red circle, 10 km diameter) with locations and approximate elevations for two *E. annectens* mummies collected more than a century ago (numbers 1 and 2) and four additional mummies collected in the past 25 years (numbers 3 to 6) that include *T. horridus* and *T. rex*. Maastrichtian (69 to 66.5 million years ago) Lance Formation (gray) and underlying Fox Hills Formation (amber) at the southern edge of the Powder River Basin (*69*) in Niobrara (formerly part of Converse) County show the location of the historical Zerbst homestead and Warren post office. (**B**) Elevation (meters) and approximate stratigraphic position for mummies 1 to 6 limited to <100 m at the top of the Lance Formation. 1, AMNH mummy (AMNH FARB 5060); 2, Senckenberg mummy (SMF R 4036); 3, new early adult mummy (UCRC PV30, "Ed Sr."); 4, new late juvenile mummy (UCRC PV31, "Ed Jr."); 5, *T. horridus* (HMNH PV.1506, "Lane"); and 6, *T. rex* (UCRC PV1, "Rex Jr.") (see the supplementary materials and table S5).

with a low midline crest extending from the neck to the middle of the tail. A pair of midline spikes were first reported in 1920 by Parks over the hips of the hadrosaurine *Gryposaurus* (*10*). Over the past 40 years, midline spikes were discovered over tail sections in *E. annectens* (*11*, *12*), a second specimen of *Gryposaurus* (*13*), and two other hadrosaurines, *Saurolophus* (*14*) and *Brachylophosaurus* (*15*). Consequently, hadrosaurid life restorations now routinely show a continuous row of separate, subrectangular spikes over the neck, trunk, and tail (*8*, *12*, *14*, *16*, *17*), usually with no alignment between spikes and underlying vertebral neural spines (for historical review, see the supplementary materials and figs. S6 to S15).

From the integument shown here, neither Osborn's nor later depictions accurately capture the fleshy profile of *E. annectens*, which has a banded, fleshy crest over the neck and trunk grading over the hips into an interdigitating spike row that extends to the tail tip, with each spike positioned over a single neural spine (Fig. 3E). The particulars of this profile may only characterize *E. annectens*, because the closely related species *E. regalis* does not have a midline crest over its neck (*18*). Thus, the generality of the midline crest among hadrosaurids remains unknown. Midline spikes over the hips and tail, by contrast, have been recorded in four hadrosaurines and may characterize this subgroup, although their interdigitating configuration may be unique to either *Edmontosaurus* or *E. annectens*. We tentatively add the fleshy midline comb over the occiput preserved in close relative *E. regalis* (*18*) (Fig. 3E).

Among living reptiles, squamates often have a fleshy crest or midline spike row, although spike number usually exceeds the underlying vertebral count (Fig. 2C). Fleshy midline spikes that interdigitate as in *E. annectens* are present only in draconine agamids (Fig. 2, D and E). Crocodylians (*19*) and other extinct archosaurs have keratin-covered osteoderms over neck, trunk, and tail that are arranged in parasagittal rows, in contrast to the fleshy midline spikes common among lepidosaurian reptiles. Segmental correspondence between spikes and the neural spines of an underlying vertebrae in *E. annectens* resembles segmental correspondence in crocodylians between armor plates to vertebrae, in some chameleons between trunk spikes and vertebrae (e.g., *Trioceros*), and between spikes and caudal vertebrae in *Sphenodon* (see the supplementary materials). Therefore, the fleshy crest and interdigitating spike row in *E. annectens* has its closest parallel among extant lepidosaurs (for more on modern analogs, see the supplementary materials and fig. S18).

Pedal skin, digital pads, and ungual sheaths

In the early adult mummy, areas of small (1 to 2 mm), polygonal, pebble-shaped scales are present over the penultimate phalanx of pedal digit III, suggesting that small scales covered the dorsal surface of the pes, unlike the larger scutate scales of birds (*20*). The underside of the pes has even smaller granular scalation, as also seen in a footprint of end-Cretaceous age that may have been made by *E. annectens* (*21*) (Fig. 3B).

Subcircular digital pads were visualized with computed tomographic (CT) scans of digit III that match a subcircular depression of the footprint (Fig. 3C). Superposition of the pes (with 15% enlargement) over the footprint positions the metatarsal-phalangeal joint of digit III over the broad central depression of the heel, with similar positioning for the same joint in digits II and IV relative to depressions near the posterolateral and posteromedial corners of the heel (Fig. 3, B and C).

A "digit-heel crease" separates the three digital pads from the heel, crossing each pedal digit ventral to the midshaft of the proximal phalanx (Fig. 3, B and C). The proximal phalanx appears to have been positioned at an angle of ~45° in midstride, articulating proximally to a near-vertical metatarsus and distally to the near-horizontal remainder of the toe (*22*, *23*). The joints at each end of this first phalanx allow considerable rotation, whereas the remaining phalanges are very short, with closely matched interphalangeal joints that limit motion (*22*), a pedal configuration called "subunguligrade" (*23*) (Fig. 3, C and D).

Hooves, here defined as wedge-shaped, flat-bottomed keratinized sheaths surrounding an ungual (see the supplementary materials and table S2), are present around the spade-shaped unguals of pedal digits II to IV (Fig. 3, A and D to F). The largest, most symmetrical hoof is on pedal digit III, measuring 15.2 cm in length, or roughly twice the length of the ungual it surrounds (7.4 cm). Previous life restorations of hadrosaurid feet show keratinized sheaths tightly fitted to the pedal unguals (*16*, *23*, *24*) rather than sheaths that extend far beyond the ungual as in extant equines (*25*, *26*). In coronal section, the dorsal surface of the hoof parallels the dorsal surface of the ungual subtending an angle of ~40° to the horizontal (Fig. 3, A, D, and F), slightly less than in equines (50° to 55°) (*25*). Also visible in cross section is a shallow ventral depression, or frog, as occurs in equine hooves (*26*). Finally, the hoof surface in *E. annectens* is marked by anteroposterior striations (Fig. 3A, left).

The forefoot of *E. annectens* has recently been found to have a single, central hoof over the ungual of digit III (*12*). This manual hoof also has a wedge shape in cross section, with a more extensive, broader dorsal than ventral surface. As in the central pedal hoof, the sheath extends far beyond the tip of the ungual phalanx. The hooved manual digit III is joined by a web of skin to a skin-covered digit II to form a

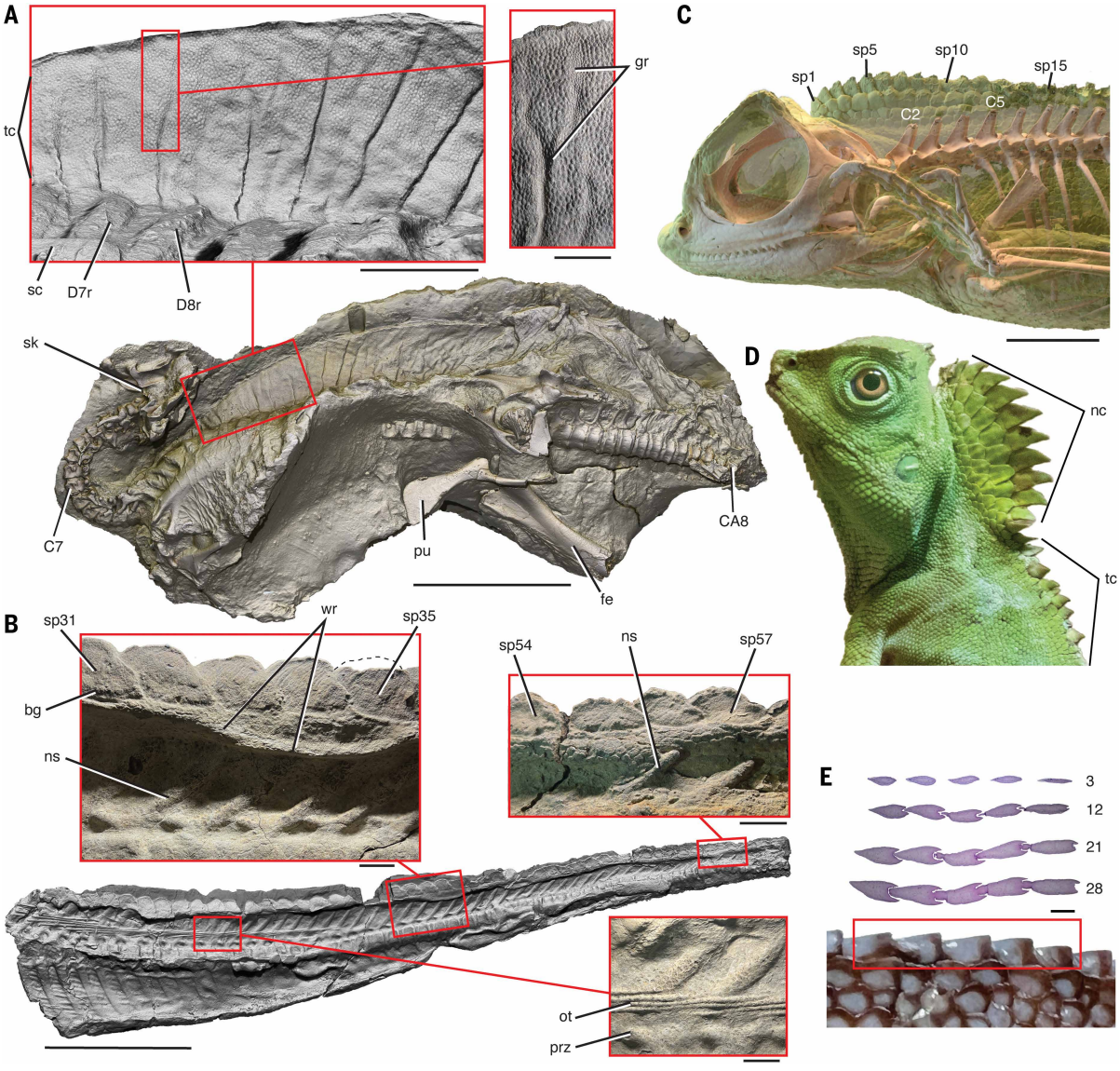

Fig. 2. Midline crest and spike row in *E. annectens* with extant squamate analog. (**A**) Midline crest over the trunk of a late juvenile mummy (UCRC PV31; maximum length 222 cm) with close-up lateral view of the anterior trunk crest and a finely scaled groove above the seventh and eighth dorsal vertebrae. (**B**) Spike row over the mid and distal tail of an early adult mummy (UCRC PV30; maximum length 279 cm) with close-up views of interdigitating spikes above the mid and distal caudal vertebrae and the desiccated scaly skin covering caudal vertebrae and ossified tendons (reversed from original). (**C**) Translucent view showing the distance, and lack of correspondence, between the spikes and neural spines of the cervical vertebrae in Doria's angle-headed lizard (*G. doriae*, FMNH H:249773) from Borneo. (**D**) Heightened neck crest of a female chameleon angle-headed lizard (*G. chamaeleontinus*) from Indonesia and Malaysia (reversed from Wikimedia Commons original). (**E**) Serial stained thin sections (top, dorsal view) of the interdigitating spikes (bottom, left lateral view) over the trunk of Doria's angle-headed lizard (*G. doriae*, FMNH H:249773) from Borneo. 3, 12, 21, 28, thin sections (10 μm) number 3, 12, 21, and 28; bg, basal groove; C2, 5, 7, cervical vertebra 2, 5, 7; CA8, caudal vertebra 8; D7r, D8r, seventh and eighth dorsal ribs; gr, groove; fe, femur; nc, neck crest; ns, neural spine; ot, ossified tendon; prz, prezygapophysis; pu, pubis; sk, skull; sp1, 5, 10, 15, spike 1, 5, 10, skin 15 over the neck of *G. doriae*; sp31, 35, 54, 57, spikes associated with the neural spines of caudal vertebrae 31, 35, 54, 57; tc, trunk crest; wr, wrinkle. Scale bars, 50 cm (bottom), 10 cm (left box), 3 cm (right box) (A), 50 cm (bottom), 3 cm (boxes) (B), 1 cm (C), and 1 mm (E).

scaled footpad at the end of a vertically held manus (Fig. 3E). During quadrupedal walking, the manus generated narrow, crescentic footprints (*1*, *12*, *21*). Thus, *E. annectens* and other hadrosaurids have mesaxonic symmetry in both fore and hind feet, but unlike any mammalian quadruped, the manus and pes assume different postures, the former unguligrade and the latter subunguligrade (Fig. 3E).

Reptilian biped with hooves

Hooves, the anatomical hallmark of living "ungulates," characterize the fore and hindfeet of two distinctive subgroups of living placental mammals, the "even-toed" Artiodactyla (suids, hippos, camels, and ruminants) with a pair of paraxonic hooves (digits III and IV) and the "odd-toed" Perissodactyla (horses, tapirs, and rhinos) with mesaxonic hooves centered on digit III. The fore and hind toes of living elephants are also hooved (*27*, *28*), as are those of several extinct subclades of placental mammals (notoungulates, litopterns, and uintatheres) (*29*, *30*) and the recently extinct marsupial pig-footed bandicoot (*Chaeropus*) (*31*). Recent fossil discoveries (*29*, *30*, *32*) and phylogenomic syntheses (*33*, *34*) have generated a new framework for mammalian phylogeny that supports the parallel origin, and subsequent loss, of hooves in

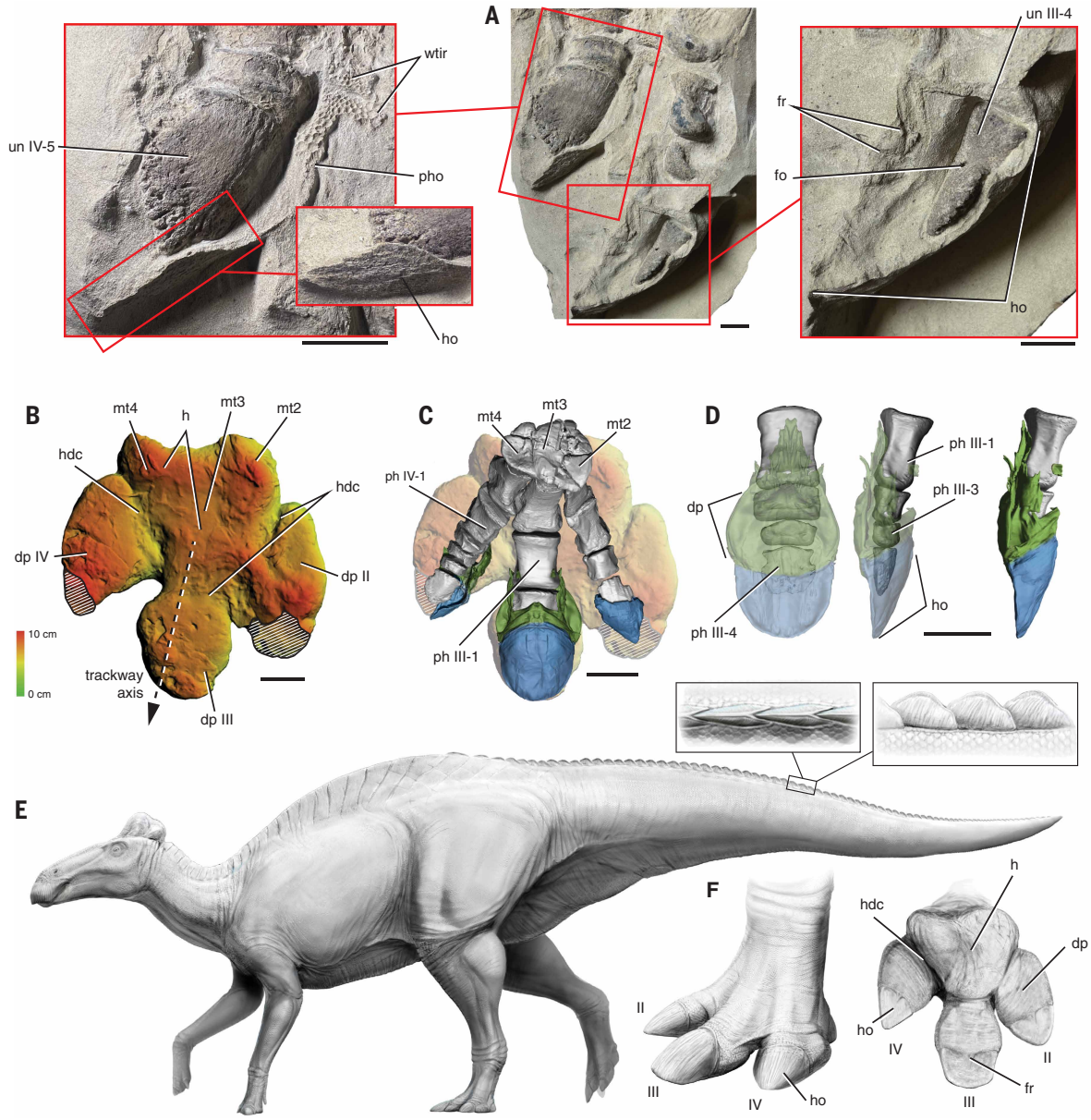

Fig. 3. Pedal hooves, digital pads, and fleshy profile in *E. annectens*. (**A**) Distal ends of right pedal digits III and IV in lateral and dorsolateral views, respectively, with enlarged views of the last phalanges, scaly skin, hoof cross section, and hoof surface texture of digit IV (left) and the last phalanx and hoof cross section of digit III (right) (UCRC PV30). (**B**) Relief map of a natural cast of a hadrosaurid right pedal footprint from the St. Mary River Formation (Maastrichtian) of Alberta (compare *E. annectens*; TMP 87.76.6; reversed to match right pes in dorsal view) (*21*). (**C**) Bones, partial hooves, and digital pads of the right pes of an early adult of *E. annectens* (UCRC PV30) in dorsal view (enlarged 15%) superposed over the natural cast of a right pedal footprint (TMP 87.76.6). Hooves are shown in blue and digital pads in green. (**D**) Hoof and digital pad of right pedal digit III in translucent ventral (left), translucent lateral (middle), and opaque lateral (right) views. Hooves are shown in blue and digital pads in green. (**E**) Life restoration of *E. annectens* in lateral view with occipital comb based on *E. regalis* (*18*) and enlargement of three caudal spikes in dorsal (left) and lateral (right) views. (**F**) Restoration of the left pes in dorsolateral (left) and ventral (right) views. II to IV, pedal digits II to IV; dp, digital pad; dhc, digit-heel crease; fo, foramen; fr, frog; h, heel; ho, hoof; mt2 to mt4, metatarsal 2 to 4; ph, phalanx; pho, perihoof; un, ungual; wtir, weathered-template integument rendering. Scale bars, 5 cm (left) and 3 cm (middle, right) (A), 10 cm for footprint [(B) and (C)], pes (C), and digit III (D).

various mammalian clades (*30*, *32*). Despite this phylogenetic complexity, all hooved mammals lived during the Cenozoic (*34*, *35*), are quadrupedal, evolved the hooved condition at small (1 to 2 kg) or moderate (< 200 kg; uintatheres and proboscideans) body size, and have fore and hindfeet with matching posture (both subunguligrade or unguligrade).

By contrast, end-Cretaceous *E. annectens* preserves the oldest hoof renderings for any tetrapod, the first record of hooves in a reptile, the first instance of a hooved tetrapod capable of bipedal locomotion, and the first hooved tetrapod with disparate fore and hindfoot posture (unguligrade versus subunguligrade, respectively). The disparity in fore and hindfoot posture seems possible only in a facultative quadruped with a posterior-centered body mass closer to the hindleg and with foreleg support limited to slow speeds. Conversely, obligate mammalian quadrupeds have an anterior-centered body mass closer to the foreleg and integrated locomotor demands that require matching fore and hindfoot posture.

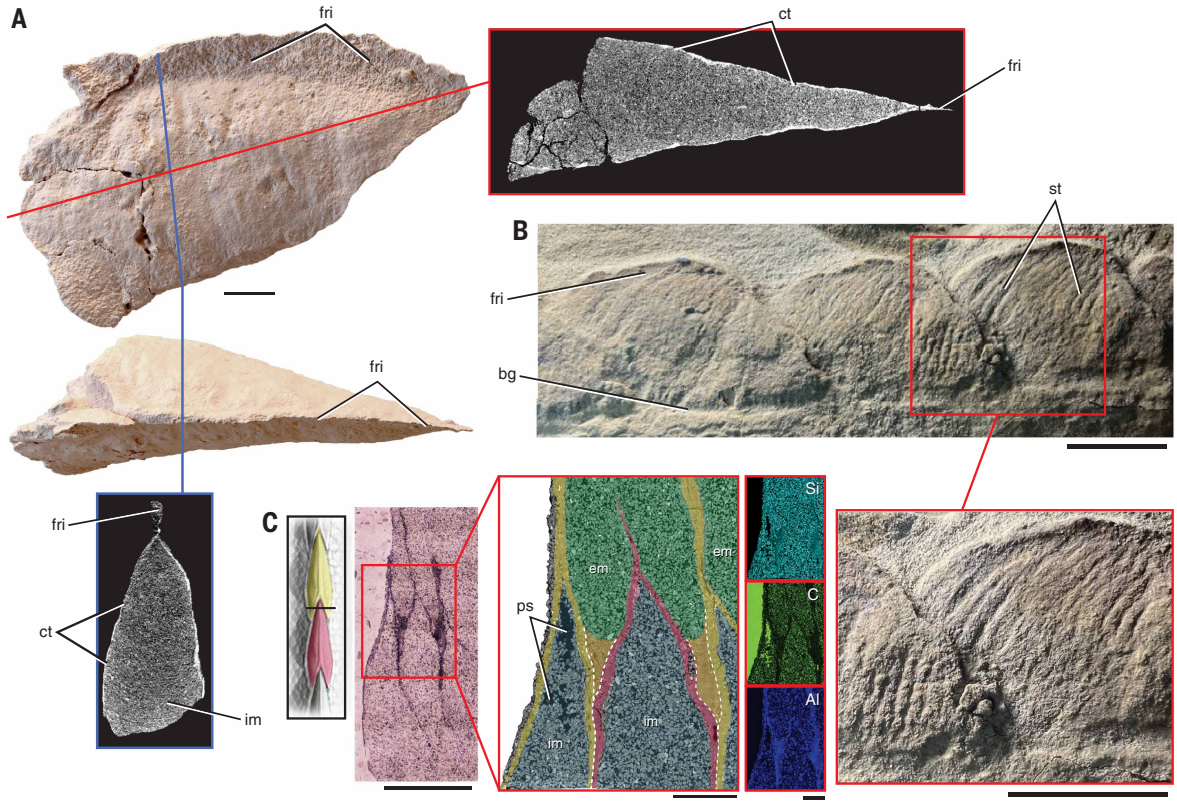

Fig. 4. Microstructure and geochemistry of spike integument renderings in *E. annectens* (UCRC PV30). (**A**) Spike of midcaudal vertebra (CA29) prepared free of external matrix in right lateral and dorsal views with CT cross sections in transverse and near horizontal planes. (**B**) Spikes of midcaudal vertebrae (CA32 to CA34) in lateral view (reversed) with an enlarged view (bottom) of interdigitation between successive spikes (over CA33 and CA34). (**C**) Backscatter electron microscopy showing two midcaudal spikes (CA30, yellow; CA31, red) in dorsal view showing position of transverse thin section (far left), transverse thin section (left), an enlarged view of transverse thin section in backscatter electron microscopy (middle), and energy-dispersive x-ray spectroscopy maps showing silicon and aluminum presence and carbon absence in the spikes (right); epoxy embedding medium external to the specimen on the slide was removed or uniform toned. CA30 spike is shown in yellow, CA31 spike is shown in red, interspike external infilling is shown in orange, external matrix is shown in green, and the internal matrix is shown in blue. Al, aluminum; bg, basal groove; C, carbon; ct, clay template; em, external matrix; fri, fringe; im, internal matrix; ps, pore space; Si, silicon; st, striations. Scale bars, 1 cm (A), 3 cm (B), and 1 cm (left) or 0.25 mm (middle, right) (C).

Judging from fossil and footprint records, the hooved unguligrade manus and subunguligrade pes first evolved among basal hadrosauriforms (e.g., *Iguanodon*) of considerable body mass (>500 kg) during the earliest Cretaceous. Late Jurassic outgroups (e.g., *Camptosaurus*) retain a spread manus and clawed, digitigrade hind feet generating bipedal digitigrade footprints with jointed digital pads (*24*). Hooves likely evolved even earlier in the Jurassic among armored ornithischians (stegosaurs and ankylosaurs), the manus and pes of which are stoutly proportioned and subunguligrade in posture, have spade-shaped unguals (*36*, *37*), and are linked to footprints with rounded toe imprints (*24*, *38*).

Clay template masks integument

We used a battery of optical, CT, electron microscopy, and x-ray spectroscopy techniques (see the supplementary materials and table S11) to investigate the structure and chemistry of the integument renderings of the new dinosaur mummies, all of which (scale, spike, and hoof) are preserved as a thin (<1 mm) clay layer bounded externally and internally by nearly identical sandstone matrix (Figs. 3A and 4).

The sand-sized, poorly sorted, weakly cemented matrix shows no evidence of internal structure or the presence of organics as visualized in thin section, CT scan, and by various spectroscopy techniques (Fig. 4C). Nor was there any evidence of original or degraded organics in either the clay layer or adjacent matrix. Indistinguishable external and internal matrices suggest that the carcass was breached before burial, permitting rapid infilling of cavities as well as integument structures (spikes, hooves) that must have been hollowed by subaerial decay (Figs. 3A and 4A). We found no evidence of "soft-tissue replacement structures" and endogenous "organic compounds" as reported in an *E. annectens* mummy from North Dakota (*12*, *39*) and from two integument patches from other hadrosaurines (*40*, *41*), all of which also were buried in terrestrial strata.

The clay layer in all of the integument renderings in the new mummies is composed predominantly of kaolinite and illite, which were present in trace amounts in the surrounding matrix. The clay layer has a relatively uniform thickness (<1 mm) across a wide variety of integument types (skin scales, spike, and hoof), suggesting that it marks a boundary rather than a replacement layer. In thin section of interdigitating spikes, the clay appears to accumulate in external crevasses between adjacent spikes (Fig. 4C), suggesting that it was deposited on the outside of the carcass. Therefore, we interpret the clay layer as a template congealing at a biofilm on the surface of the buried, decaying carcass rather than a replacement cast of an original tissue layer (*42*).

Clay templating (*43*–*45*) can preserve the external form of soft-bodied animals in Precambrian and Paleozoic Lagerstätten (*46*, *47*) when a biofilm (*48*–*50*) electrostatically draws the positive cations in clay minerals from surrounding sediment to the surface of a carcass in fine-grained lacustrine or marine depositional settings. Soft integumental structures, such as the bristles or feathers of nonavian dinosaurs, also have been preserved in Mesozoic lacustrine sediments through

carbonaceous compression fossilization (*51*, *52*). The *E. annectens* mummies from the Lance Formation, by contrast, are large, three-dimensional (3D) fossils buried in better oxygenated, coarse-grained fluvial deposits with clay as a minor component. Therefore, clay templating may generate soft tissue integument renderings in a wider range of depositional settings than previously realized.

Discussion

Epidermal renderings

Upon discovering the first dinosaur mummy in 1908, Sternberg (*53* remarked on the "impressions of its folding skin," and Osborn (*1*) described the fossilized integument as an "epidermal" or "skin impression." Osborn, however, clearly understood the fossilized integument of the AMNH mummy as an "epidermal cast" of some kind in sand with "clayey elements" that completely replaced the original surficial layer of skin. "Integument rendering" is the heuristic term we suggest here for fossilized soft tissue integument that includes four principal modes of preservation: cast-vestige, mold, template, and impression (see the supplementary materials and table S1). A diaphanous clay template, rather than cast-vestige replacement, is strongly supported for the *E. annectens* mummies from the mummy zone.

Dinosaur mummification

We corroborate closely the initial stages of Osborn's (*1*, *54*) taphonomic hypothesis for the AMNH mummy as our stages 1 and 2, both occurring within a single season. Stages 3 and 4 commence immediately after burial.

Stage 1. Carcass desiccation and initial decay: Wrinkled skin renderings closely draped over underlying skeletal bone of the new mummies and the dorsiflexed neck position of the late juvenile mummy provide indisputable evidence of postmortem subaerial desiccation (Figs. 2 and 3). Sustained aridity, or drought, has been identified as the cause of death for both the AMNH mummy (*55*) and scores of hadrosaurids in bone-bed accumulations in Late Cretaceous strata of the Western Interior (*56*). Within the first 7 to 10 days after death, carcasses of proboscideans (*57*, *58*) and humans (*59*, *60*) in arid environments are subject to integument desiccation, decay of deeper fleshy tissues through autolysis, bloating, release of gasses, and scavenging. Although Osborn (*1*) suggested that the "muscles and viscera" under the integument of the AMNH mummy shrank from dehydration, their removal by decay is shown by the immediate proximity of scaly skin to underlying bone visible over the pectoral girdles, rib cage, and sides of the tail, where considerable muscle mass was present in life. Decay also must have removed soft tissues inside the crest, spike row, and hooves of the new mummies, allowing for their rapid infilling upon burial (see stage 3 below). Scavenging is not apparent on any of the mummies from the mummy zone. The forelimbs, hind limbs, and tail of the late juvenile mummy (UCRC PV31) were present but partially removed by erosion. Drought-induced deaths of elephants often result in an overabundance of carcasses, leaving many untouched by scavengers and concentrated near or within dry riverbeds (*55*, *57*).

Stage 2. Sudden short-distance fluvial transport and burial: Seasonal monsoons characterized by cyclic drought and flooding, far from a rare pairing of antipodal environmental catastrophes [but see (*12*)], was the dominant climatic pattern for the Western Interior during the Late Cretaceous (*61*). Surrounding each mummy from the mummy zone is an uninterrupted body of sediment that suddenly engulfed each carcass, with evidence of high-energy fluvial transport in matrix associated with the specimens and at their localities (mud clasts, conglomerates, cross-bedding, broken bone, and tree trunk debris). The four mummies of *E. annectens* in the mummy zone are not only fully articulated and cloaked in unabraded integument, but they are also preserved in 3D (see the supplementary materials and table S5). Three of these preserve the anterior half of the body in a common death pose, resting upside down on one side of the trunk with forelimbs outstretched (the UCRC PV31, AMNH, and Senckenberg mummies). The fleshy crest preserved on the underside of two of these mummies (the UCRC PV31 and AMNH mummies) is deflected to one side, which must have occurred when it was still pliable at the time of death. These details support carcass burial by floodwaters at or near the site of death over a matter of hours or, at most, days (*55*). From the foregoing, we conclude that the span of time between death and sudden burial of the four *E. annectens* mummies in the mummy zone was on the order of a week or weeks within a single season.

Stage 3. Rapid infilling of a breached carcass: Sandstone matrix engulfing the carcass also infilled the body cavities and much smaller spaces generated during subaerial decay within the spikes and hooves (Figs. 3A and 4A). Because external and interior, or infilled, sediment is indistinguishable and composed principally of incompressible quartz grains, infilling would have been rapid, fully penetrating, and capable of preserving the 3D morphology of dehydrated integument.

Stage 4. Integument templating in clay and final decay: In the wet, porous sediment, a thin biofilm covered the surface of the decaying integument, electrostatically attracting residual clay from the surrounding matrix. Carpenter (*54*) nearly conceived this taphonomic scenario, citing the emergence after burial of a biofilm but omitting mention of an associated clay layer. Composed primarily of kaolinite and illite, the clay layer composing the integument rendering of the new *E. annectens* mummies appears to have been electrostatically drawn from a residual clay component of the matrix. At <1 mm in thickness, the clay layer faithfully records the 3D surface form and texture of the integument. The integument itself, including all tissue, cellular and subcellular structures, and organic biomolecules, broke down and was carried away in solution, with lithostatic compaction causing sand grains to press into inner and outer margins of the clay layer (Fig. 4C). Mummification was likely complete within weeks or months after burial, followed by the deposition of minor heavy minerals on the clay boundary (e.g., ironstone concretion around the end of the tail of the early adult) and eventually the permineralization of underlying skeletal bone.

The dinosaur mummy zone

E. annectens and hadrosaurids in general account for most dinosaur mummies (see the supplementary materials and table S4). The best-preserved mummies come from a small mummy zone <10 km in diameter in east-central Wyoming and from <100 m of the uppermost portion of the Lance Formation (Maastrichtian) (Fig. 1). Four of the six mummies in the zone came from the bottom 50 m of that section and pertain to the hadrosaurine *E. annectens*. Is there something special about hadrosaurid skin or the mummy zone that favored integument preservation?

Although thicker skin (*62*) has been suggested as the reason hadrosaurids dominate dinosaur mummies compared with contemporary ceratopsids, the integument covering the sides of the trunk in *Edmontosaurus* is extremely small-scaled (1 to 4 mm in diameter) with sharp-crested wrinkles that suggest the skin was very thin (Fig. 2A). Trunk scales in *Triceratops* (HMNS PV.1506), by contrast, are the largest ever recorded (~10 cm in diameter) and compose skin areas that appear to be too thick to wrinkle during desiccation.

Differences in preferred habitat more plausibly account for the predominance of hadrosaurid over ceratopsid mummies. *Triceratops* tends to be preserved in mudstones farther inland on the floodplain (*63*) with only two reported bone beds (*64*, *65*), whereas *Edmontosaurus* tends to be preserved in sandstone channel deposits closer to the coastline (*63*) with many large-scale bone beds [e.g., (*7*, *66*, *67*)].

The dinosaur mummy zone is located at the southern end of principal outcrops of the stratigraphically equivalent, flat-lying Hell Creek

and Lance Formations (*67*–*69*), both of which preserve hadrosaurids with integument renderings. The Hell Creek Formation is exposed in the Williston Basin from the Canadian border across Montana to the western edge of the Dakotas, and the Lance Creek Formation is exposed in the Powder River Basin and a north-south oblong trough extending from southern Montana to east-central Wyoming (*67*, *68*). The Lance Formation in southern Montana is ~200 m thick but gradually increases to >1000 m toward the southern edge of the Powder River Basin in the region of the mummy zone, which dates to the very end of the Cretaceous Period (*69*). The mummies rest atop a massive coastal sedimentary wedge that accumulated during a period of very rapid subsidence (~170 m/million years) (*69*). We infer from the foregoing that the extraordinary preservation of the mummy zone is due to rapid subsidence in a coastal setting subject to seasonal drought-flood cycles. The most extensive outcrops of the Lance Formation also occur at southern end of the Powder River Basin, a richly fossiliferous region that has attracted paleontologists for more than a century.

Materials and methods

Sediment sampling and analysis

Sediment samples were taken from both mummies of *E. annectens* (UCRC PV30 and UCRC PV31) adjacent to the clay template (internal and external) and from surrounding matrix away from the clay template. Likewise, sediment samples were taken from the early adult (UCRC PV30) adjacent to the hooves of the pes (internal and external) and far from the hoof sheath. We also sampled from the early adult (UCRC PV30) dark-staining minerals from scale renderings on the side of the tail and sediment from the ironstone concretion surrounding the tail tip. Finally, we sampled carbonized plant material from a lamina in the sediment under the middle of the tail.

We also analyzed sediment in thin section (see below). Sand grains are angular, with little cementation, visible pore spaces, and birefringence variation indicative of the presence of rare carbonate grains (dolomite or calcite). The sediment in both specimens is predominantly sand with minor silt and clay components and is indistinguishable on either side of the integument template. The integument template, composed predominantly of kaolinite and illite, preserves the external morphology of scaly skin, spikes, and hooves (see the supplementary materials and Figs. 2 to 4). In a few places, the clay template preserving the form of the scaly skin transitions from a positive rendering (convex scales) to what appears to be a negative rendering (pocked depressions bounded by scale interstices; Fig. 2A, left). The apparent negative rendering, however, we believe is due to missing template spanning the interstices, generating what we identify as "eroded template." A transition of this sort from positive to apparent negative rendering in an otherwise undisturbed area of scaly skin can give the false impression of inverted skin (*14*).

Imaging and analysis

X-ray diffraction of sediment: We analyzed the sediment in thin section from the midcaudal spike row of the early adult of *E. annectens* (UCRC PV30) (see the supplementary materials and table S11). X-ray diffraction (XRD) bulk analysis was performed in the Illinois State Geological Survey X-ray Diffraction Laboratory (UIUC) on a 150-μm thin section through the caudal spikes, centering a beam of ~2.54 cm diameter on the external matrix immediately adjacent to the clay template. The semiquantitative results are based on the reference intensity ratio method using corundum as the reference standard. All phase intensities quantified were recalculated (normalized) using the ratio of $\text{intensity}_{\text{phase}}/\text{intensity}_{\text{corundum}}$.

Thin sectioning of *E. annectens* spike series: A block containing a complete spike and portions of adjacent spikes (CA29 to CA31; Fig. 4C) was removed from the midtail of the early adult *E. annectens* (UCRC PV30), micro-CT scanned, digitally segmented, and prepared for thin sectioning at Spectrum Petrographics (Vancouver, WA) by vacuum embedding in epoxy (Epotek 301). Five 30-μm transverse thin sections were made of the central spike at regular increments (anterior end, anterior quarter, center, posterior quarter, and posterior end), with the posterior end section shown in Fig. 4C. An additional 150-μm transverse thin section was made at the anterior quarter for XRD analysis (see below).

Thin sectioning of extant squamate spike series: We serially sectioned the midline spike row above the head and neck of the extant squamate *Gonocephalus doriae* (Doria's angle-headed lizard from Borneo) using a formalin-fixed, ethanol-stored specimen (FMNH 249773). Using a microtome on the paraffin-embedded sample at the Human Tissue Resource Center (University of Chicago) (Fig. 2E), 10-μm thick horizontal (frontal) sections were placed on glass slides stained with hematoxylin and eosin for visualization under magnification (Dino-Lite digital microscope).

Light microscopy and stereophotogrammetry: We used an Edge digital microscope for light microscopy of small samples. Structure from motion photogrammetry of the integument and skeletons of late juvenile and early adult mummies (UCRC PV30 and UCRC PV31) was accomplished using a Fujifilm XT-4 camera with and without a ring flash to obtain the best image of the small-scale relief of the integument. The images (635 for UCRC PV31; 330 and 304 for UCRC PV30 tail and foot, respectively; resolution 6240 × 4160 pixels) were processed in Agisoft Metashape, creating a point, high-resolution 3D mesh from depth maps (10,500,000 polygons) with photorealistic texture (12,288 pixels). The tail model of the early adult mummy (Fig. 2B) rearticulated the two slabs that preserve the intact caudal series.

CT scanning and segmenting: We used a WayGate Phoenix V|tomex|s micro-CT scanner at the UChicago PaleoCT Core Facility (RRID: SCR_024763) to micro-CT scan both a block containing midcaudal spikes (CA30 and CA31) from the early adult UCRC PV30 and the head and neck of *G. doria* (FMNH H:249773), using Thermo Fisher Avizo software to segment and render the former and Materialise Mimics software to segment and render the latter. Open field jackets containing the partially prepared right hind foot and tail tip of the early adult mummy (UCRC PV30) were CT scanned using a Philips Brilliance iCT 256-slice multidetector CT scanner at the Human Imaging Resource Office Core Facility (RRID:SCR_018372; University of Chicago) (see the supplementary materials and table S11).

Electron microscopy, x-ray spectroscopy, and XRD analysis of spikes in matrix: Thin sections of a block containing several midcaudal spikes of the early adult of *E. annectens* (UCRC PV30) were visualized under light microscopy and subjected to backscattered electron imaging, energy-dispersive x-ray spectroscopy (EDS), and XRD clay analysis (for analytical abbreviations, see the supplementary materials and table S11). Electron microscopy and elemental mapping used a TESCAN LYRA3 field-emission scanning electron microscope to examine the thin section from the posterior end of the spike with the region of interest demarcated using strips of copper tape. No coating was applied to the surface of the sample. A scintillator-type backscattered electron detector was used to image the sample using a 15 Kv beam. Elemental maps were produced by energy-dispersive x-ray spectroscopy by raster imaging the slide with Oxford Instruments X-Max-80 silicon drift x-detectors. Resulting data were analyzed with Aztec software.

In natural light, the clay template is slightly darker than adjacent sandstone matrix, whereas in CT images, the clay layer appears denser (whiter) than the adjacent matrix (Fig. 4A). EDS showed aluminosilicate (silicon and aluminum) enrichment of the template material, which is consistent with clay mineralogy. The absence of significant carbon (Fig. 4C), sulfur, nitrogen, or phosphorous in the clay template

suggests that original biomolecules such as melanin, "keratin" (corneous beta-proteins), and collagen or their breakdown products are absent.

XRD analysis of the clay fraction (<2 μm) from a powdered sample from a spike was performed at the Illinois State Geological Survey X-ray Diffraction Laboratory at the University of Illinois Urbana-Champaign. Particles were oriented and saturated by ethylene glycol. Basal diffraction intensities (d001) of these concentrated clays obtained from the oriented and ethylene glycol–saturated films were compared with each other. The analysis was semiquantitatively calculated from major clay mineral intensities, and the main clay component was found to be kaolinite (54%).

REFERENCES AND NOTES

1. H. F. Osborn, Integument of the iguanodont dinosaur *Trachodon*. *Am. Mus. Nat. Hist. Mem.* **1**, 33–54 (1912).
2. C. H. Sternberg, Still in the Laramie Country, Converse County, Wyoming. *Trans. Kans. Acad. Sci.* **23**, 219–223 (1911). doi: 10.2307/3624588
3. J. Versluys, Der Schadel des Skelettes von *Trachodon annectens* im Senckenberg-Museum. *Abh. Senckenberg. Naturfors. Gesell.* **38**, 1–19 (1923).
4. D. Uhl, A reappraisal of the" stomach" contents of the *Edmontosaurus annectens* mummy at the Senckenberg Naturmuseum in Frankfurt/Main (Germany). *Z. Dtsch. Ges. Geowiss.* **171**, 71–85 (2020). doi: 10.1127/zdgg/2020/0224
5. P. Larson, M. Larson, C. Ott, R. Bakker, Skinning a *Triceratops*. *J. Vertebr. Paleontol.* **27**, 104A (2007).
6. C. Lipkin, P. C. Sereno, J. R. Horner, The furcula in *Suchomimus tenerensis* and *Tyrannosaurus rex* (Dinosauria: Theropoda: Tetanurae). *J. Paleontol.* **81**, 1523–1527 (2007). doi: 10.1666/06-024.1
7. M. Wosik, D. C. Evans, Osteohistological and taphonomic life-history assessment of *Edmontosaurus annectens* (Ornithischia: Hadrosauridae) from the Late Cretaceous (Maastrichtian) Ruth Mason dinosaur quarry, South Dakota, United States, with implication for ontogenetic segregation between juvenile and adult hadrosaurids. *J. Anat.* **241**, 272–296 (2022). doi: 10.1111/joa.13679; pmid: 35801524
8. N. E. Campione, "Postcranial anatomy of *Edmontosaurus regalis* (Hadrosauridae) from the Horseshoe Canyon Formation, Alberta, Canada" in *Hadrosaurs*, D. A. Eberth, D. C. Evans, Eds. (Indiana Univ. Press, 2015), pp. 208–244.
9. R. S. Lull, N. E. Wright, Hadrosaurian dinosaurs of North America. *Spec. Pap. Geol. Soc. Am.* **40**, 1–242 (1942).
10. W. A. Parks, The osteology of the trachodont dinosaur *Kritosaurus incurvimanus*. *Univ. Toronto Stud. Geol. Ser.* **11**, 1–74 (1920).
11. J. R. Horner, A "segmented" epidermal tail frill in a species of hadrosaurian dinosaur. *J. Paleontol.* **58**, 270–271 (1984).
12. S. K. Drumheller, C. A. Boyd, B. M. S. Barnes, M. L. Householder, Biostratinomic alterations of an *Edmontosaurus* "mummy" reveal a pathway for soft tissue preservation without invoking "exceptional conditions". *PLOS ONE* **17**, e0275240 (2022). doi: 10.1371/journal.pone.0275240; pmid: 36223345
13. C. E. Clayton *et al.*, "Non–osseous dermal scutes and integument impressions from an exceptionally preserved hadrosaurid dinosaur skeleton, Upper Cretaceous Kaiparowits Formation of Utah" in *A Review of Hadrosaurid Skin Impressions. Hadrosaur Symposium 2011 Abstract Volume*, D. R. Braman, D. C. Eberth, D. C. Evans, W. Taylor, Eds. (Royal Tyrrell Museum of Palaeontology, 2011), vol. 589, pp. 23–27.
14. P. R. Bell, Standardized terminology and potential taxonomic utility for hadrosaurid skin impressions: A case study for *Saurolophus* from Canada and Mongolia. *PLOS ONE* **7**, e31295 (2012). doi: 10.1371/journal.pone.0031295; pmid: 22319623
15. N. L. Murphy, D. Trexler, M. Thompson, "'Leonardo,' a mummified *Brachylophosaurus* (Ornithischia: Hadrosauridae) from the Judith River Formation of Montana" in *Horns and Beaks: Ceratopsian and Ornithopod Dinosaurs*, K. Carpenter, Ed. (Indiana Univ. Press, 2007), pp. 117–133.
16. F. Bertozzo, C. D. Sasso, M. Fabbri, F. Manucci, S. Maganuco, Redescription of a remarkably large *Gryposaurus notabilis* (Dinosauria: Hadrosauridae) from Alberta, Canada. *Mem. Soc. Ital. Sci. Nat. Mus. Civ. Storia Nat. Milano* **43**, 1–56 (2017).
17. P. R. Bell, "A review of hadrosaurid skin impressions" in *Hadrosaurs*, D. A. Eberth, D. C. Evans, Eds. (Indiana Univ. Press, 2014), pp. 572–590.
18. P. R. Bell, F. Fanti, P. J. Currie, V. M. Arbour, A mummified duck-billed dinosaur with a soft-tissue cock's comb. *Curr. Biol.* **24**, 70–75 (2014). doi: 10.1016/j.cub.2013.11.008; pmid: 24332547
19. F. D. Ross, G. C. Mayer, "On the dorsal armor of the Crocodilia" in *Advances in Herpetology and Evolutionary Biology*, K. Miyata, A. Rhodin, Eds. (Harvard Univ. Press, 1983), pp. 305–331.
20. P. Wu, Y.-C. Lai, R. Widelitz, C.-M. Chuong, Comprehensive molecular and cellular studies suggest avian scutate scales are secondarily derived from feathers, and more distant from reptilian scales. *Sci. Rep.* **8**, 16766 (2018). doi: 10.1038/s41598-018-35176-y; pmid: 30425309
21. P. J. Currie, G. C. Nadon, M. G. Lockley, Dinosaur footprints with skin impressions from the Cretaceous of Alberta and Colorado. *Can. J. Earth Sci.* **28**, 102–115 (1991). doi: 10.1139/e91-009
22. R. Zheng, A. A. Farke, G.-S. Kim, A photographic atlas of the pes from a hadrosaurine hadrosaurid dinosaur. *PalArch J. Vertebr. Palaeontol.* **8**, 1–12 (2011).
23. K. Moreno, M. T. Carrano, R. Snyder, Morphological changes in pedal phalanges through ornithopod dinosaur evolution: A biomechanical approach. *J. Morphol.* **268**, 50–63 (2007). doi: 10.1002/jmor.10498; pmid: 17146773
24. T. Thulborn, *Dinosaur Tracks* (Chapman and Hall, 1990).doi: 10.1007/978-94-009-0409-5
25. A. H. Parks, "Anatomy and function of the equine digit" in *Equine Laminitis*, J. K. Belknap, R. J. Geor, Eds. (Wiley, 2017), pp. 13–21; https://onlinelibrary.wiley.com/doi/10.1002/9781119169239.ch3.
26. C. C. Pollitt, The anatomy and physiology of the suspensory apparatus of the distal phalanx. *Vet. Clin. North Am. Equine Pract.* **26**, 29–49 (2010). doi: 10.1016/j.cveq.2010.01.005; pmid: 20381734
27. A. Benz, "The elephant's hoof: Macroscopic and microscopic morphology of defined locations under consideration of pathological changes," thesis, Vetsuisse-Fakultät Universität Zürich, Zürich, Switzerland (2005).
28. J. R. Hutchinson *et al.*, From flat foot to fat foot: Structure, ontogeny, function, and evolution of elephant "sixth toes," *Science* **334**, 1699–1703 (2011). doi: 10.1126/science.1211437; pmid: 22194576
29. D. A. Croft, J. N. Gelfo, G. M. López, Splendid innovation: The extinct South American native ungulates. *Annu. Rev. Earth Planet. Sci.* **48**, 259–290 (2020). doi: 10.1146/annurev-earth-072619-060126
30. N. R. Chimento, F. L. Agnolin, Phylogenetic tree of Litopterna and Perissodactyla indicates a complex early history of hoofed mammals. *Sci. Rep.* **10**, 13280 (2020). doi: 10.1038/s41598-020-70287-5; pmid: 32764723
31. S. Jackson, C. Groves, *Taxonomy of Australian Mammals* (Csiro Publishing, 2015). doi: 10.1071/9781486300136
32. M. Spaulding, M. A. O'Leary, J. Gatesy, Relationships of Cetacea (Artiodactyla) among mammals: Increased taxon sampling alters interpretations of key fossils and character evolution. *PLOS ONE* **4**, e7062 (2009). doi: 10.1371/journal.pone.0007062; pmid: 19774069
33. W. J. Murphy, N. M. Foley, K. R. Bredemeyer, J. Gatesy, M. S. Springer, Phylogenomics and the genetic architecture of the placental mammal radiation. *Annu. Rev. Anim. Biosci.* **9**, 29–53 (2021). doi: 10.1146/annurev-animal-061220-023149; pmid: 33228377
34. N. M. Foley *et al.*, A genomic timescale for placental mammal evolution. *Science* **380**, eabl8189 (2023). doi: 10.1126/science.abl8189; pmid: 37104581
35. P. M. Velazco *et al.*, Combined data analysis of fossil and living mammals: A Paleogene sister taxon of Placentalia and the antiquity of Marsupialia. *Cladistics* **38**, 359–373 (2022). doi: 10.1111/cla.12499; pmid: 35098586
36. P. Senter, Evidence for a sauropod-like metacarpal configuration in stegosaurian dinosaurs. *Acta Palaeontol. Pol.* **55**, 427–432 (2010). doi: 10.4202/app.2009.1105
37. P. J. Currie, D. Badamgarav, E. B. Koppelhus, R. Sissons, M. K. Vickaryous, Hands, feet, and behaviour in *Pinacosaurus* (Dinosauria: Ankylosauridae). *Acta Palaeontol. Pol.* **56**, 489–504 (2011). doi: 10.4202/app.2010.0055
38. F. M. Petti, S. D'Orazi Porchetti, E. Sacchi, U. Nicosia, A new purported ankylosaur trackway in the Lower Cretaceous (lower Aptian) shallow-marine carbonate deposits of Puglia, southern Italy. *Cretac. Res.* **31**, 546–552 (2010). doi: 10.1016/j.cretres.2010.07.004
39. P. L. Manning *et al.*, Mineralized soft-tissue structure and chemistry in a mummified hadrosaur from the Hell Creek Formation, North Dakota (USA). *Proc. Biol. Sci.* **276**, 3429–3437 (2009). doi: 10.1098/rspb.2009.0812; pmid: 19570788
40. M. Barbi *et al.*, Integumentary structure and composition in an exceptionally well-preserved hadrosaur (Dinosauria: Ornithischia). *PeerJ* **7**, e7875 (2019). doi: 10.7717/peerj.7875; pmid: 31637130
41. M. Fabbri, J. Wiemann, F. Manucci, D. E. G. Briggs, Three-dimensional soft tissue preservation revealed in the skin of a non-avian dinosaur. *Palaeontology* **63**, 185–193 (2020). doi: 10.1111/pala.12470
42. L. A. Parry *et al.*, Soft-bodied fossils are not simply rotten carcasses – Toward a holistic understanding of exceptional fossil preservation: Exceptional fossil preservation is complex and involves the interplay of numerous biological and geological processes. *BioEssays* **40**, 1700167 (2018). doi: 10.1002/bies.201700167; pmid: 29193177
43. K. M. Towe, Fossil preservation in the Burgess Shale. *Lethaia* **29**, 107–108 (1996). doi: 10.1111/j.1502-3931.1996.tb01844.x
44. A. Page, S. E. Gabbott, P. R. Wilby, J. A. Zalasiewicz, Ubiquitous Burgess Shale–style "clay templates" in low-grade metamorphic mudrocks. *Geology* **36**, 855–858 (2008). doi: 10.1130/G24991A.1
45. E. Naimark *et al.*, Decaying in different clays: Implications for soft-tissue preservation. *Palaeontology* **59**, 583–595 (2016). doi: 10.1111/pala.12246
46. B. Becker-Kerber *et al.*, Clay templates in Ediacaran vendotaeniaceans: Implications for the taphonomy of carbonaceous fossils. *Geol. Soc. Am. Bull.* **134**, 1334–1346 (2022). doi: 10.1130/B36033.1
47. R. P. Anderson, N. J. Tosca, E. E. Saupe, J. Wade, D. E. G. Briggs, Early formation and taphonomic significance of kaolinite associated with Burgess Shale fossils. *Geology* **49**, 355–359 (2021). doi: 10.1130/G48067.1

48. J. Reitner, "Biofilms and fossilization" in *Encyclopedia of Geobiology*, J. Reitner, V. Thiel, Eds. (Springer, 2011), pp. 136–137. doi: 10.1007/978-1-4020-9212-1_26
49. R. A. Raff, E. C. Raff, The role of biology in the fossilization of embryos and other soft-bodied organisms: Microbial biofilms and Lagerstätten. *Paleontol. Soc. Pap.* **20**, 83–100 (2014). doi: 10.1017/S1089332600002813
50. T. Tolker-Nielsen, Biofilm Development. *Microbiol. Spectr.* **3**, MB-0001-2014 (2015). doi: 10.1128/microbiolspec.MB-0001-2014; pmid: 26104692
51. M. A. Norell, X. Xu, Feathered dinosaurs. *Annu. Rev. Earth Planet. Sci.* **33**, 277–299 (2005). doi: 10.1146/annurev.earth.33.092203.122511
52. G. Mayr, M. Pittman, E. Saitta, T. G. Kaye, J. Vinther, Structure and homology of *Psittacosaurus* tail bristles. *Palaeontology* **59**, 793–802 (2016). doi: 10.1111/pala.12257
53. C. H. Sternberg, Expedition to the Laramie Beds of Converse County, Wyoming. *Trans. Kans. Acad. Sci.* **22**, 113–116 (1908). doi: 10.2307/3624729
54. K. Carpenter, How to make a fossil: Part 2 – Dinosaur mummies and other soft tissue. *J Paleontol. Sci.* **7**, 1–23 (2007).
55. K. Carpenter, "Paleoecological significance of droughts during the Late Cretaceous of the Western Interior" in *Fourth Symposium on Mesozoic Terrestrial Ecosystems, Short Papers*, P. M. Currie, E. H. Koster, Eds. (Tyrrell Museum of Palaeontology, 1987), pp. 42–47.
56. R. R. Rogers, Taphonomy of three dinosaur bone beds in the Upper Cretaceous Two Medicine Formation of northwestern Montana: Evidence for drought-related mortality. *Palaios* **5**, 394–413 (1990). doi: 10.2307/3514834
57. G. Haynes, *Mammoths, Mastodonts, and Elephants: Biology, Behavior and the Fossil Record* (Cambridge Univ. Press, 1991).
58. P. A. White, C. G. Diedrich, Taphonomy story of a modern African elephant *Loxodonta africana* carcass on a lakeshore in Zambia (Africa). *Quat. Int.* **276–277**, 287–296 (2012). doi: 10.1016/j.quaint.2012.07.025
59. A. Galloway, W. H. Birkby, A. M. Jones, T. E. Henry, B. O. Parks, Decay rates of human remains in an arid environment. *J. Forensic Sci.* **34**, 607–616 (1989). doi: 10.1520/JFS12680J; pmid: 2738563
60. C. L. Parks, A study of the human decomposition sequence in central Texas. *J. Forensic Sci.* **56**, 19–22 (2011). doi: 10.1111/j.1556-4029.2010.01544.x; pmid: 20840291
61. H. C. Fricke, B. Z. Foreman, J. O. Sewall, Integrated climate model-oxygen isotope evidence for a North American monsoon during the Late Cretaceous. *Earth Planet. Sci. Lett.* **289**, 11–21 (2010). doi: 10.1016/j.epsl.2009.10.018
62. M. Davis, Census of dinosaur skin reveals lithology may not be the most important factor in increased preservation of hadrosaurid skin. *Acta Palaeontol. Pol.* **59**, 601–605 (2014).
63. T. R. Lyson, N. R. Longrich, Spatial niche partitioning in dinosaurs from the latest cretaceous (Maastrichtian) of North America. *Proc. Biol. Sci.* **278**, 1158–1164 (2011). doi: 10.1098/rspb.2010.1444; pmid: 20943689
64. J. de Rooij *et al.*, Stable isotope record of *Triceratops* from a mass accumulation (Lance Formation, Wyoming, USA) provides insights into *Triceratops* behaviour and ecology. *Palaeogeogr. Palaeoclimatol. Palaeoecol.* **607**, 111274 (2022). doi: 10.1016/j.palaeo.2022.111274
65. S. W. Keenan, J. B. Scannella, "Paleobiological implications of a *Triceratops* bonebed from the Hell Creek Formation, Garfield County, northeastern Montana" in *Through the End of the Cretaceous in the Type Locality of the Hell Creek Formation in Montana and Adjacent Areas*, G. P. Wilson, W. A. Clemens, J. R. Horner, J. H. Hartman, Eds. (Geological Society of America, 2014), Special Paper 503, pp. 349–364; doi: 10.1130/2014.2503(14)
66. K. Snyder, M. McLain, J. Wood, A. Chadwick, Over 13,000 elements from a single bonebed help elucidate disarticulation and transport of an *Edmontosaurus* thanatocoenosis. *PLOS ONE* **15**, e0233182 (2020). doi: 10.1371/journal.pone.0233182; pmid: 32437394
67. K. R. Johnson, D. J. Nichols, J. H. Hartman, "Hell Creek Formation: A 2001 synthesis" in *The Hell Creek Formation and the Cretaceous-Tertiary Boundary in the Northern Great Plains: An Integrated Continental Record of the End of the Cretaceous*, J. H. Hartman, K. R. Johnson, D. J. Nichols, Eds. (US Geological Survey, 2002), vol. 361, pp. 503–510; doi: 10.1130/0-8137-2361-2.503
68. J. R. Gill, W. A. Cobban, Stratigraphy and geologic history of the Montana Group and equivalent rocks, Montana, Wyoming, and North and South Dakota. *Geol. Surv. Profess. Pap.* **776**, 1–37 (1973). doi: 10.3133/pp776
69. C. W. Connor, "The Lance Formation: Petrography and stratigraphy, Powder River Basin and nearby basins, Wyoming and Montana" in *Evolution of Sedimentary Basins—Powder River Basin*, V. F. Nuccio, P. L. Hansley, W. A. Cobban, C. G. Whitney, Eds. (US Geological Survey, Bulletin 1917-1, 1992); https://pubs.usgs.gov/bul/1917i/report.pdf.
70. P. C. Sereno *et al.*, Microscopic and chemical data for: Duck-billed dinosaur fleshy midline and hooves reveal terrestrial clay-template "mummification," Dryad (2025); https://doi.org/10.5061/dryad.q573n5tx4.

ACKNOWLEDGMENTS

We thank D. Navarro for gray-tone flesh reconstructions and color scene renderings; E. Fitzgerald and R. Masek for fossil preparation; D. Henderson (Royal Tyrrell Museum of Palaeontology) for footprint photography; M. Whitney (Loyola University) for assistance with light microscopy; R. Kamei and J. Mata (Field Museum of Natural History) for access to extant preserved reptile specimens; J. Mallon (Canadian Museum of Nature) for data on *E. regalis*; N. Gruszauskas (HIRO facility, University of Chicago) for CT scans; G. Olack (FIB-SEM facility, University of Chicago) for assistance with electron and x-ray spectroscopy; M. Pentrak for XRD analysis (XRD/XRF Materials Characterization Laboratory, University of Illinois Urbana-Champaign); T. Li, X. Jiang, and E. Markiewicz (University of Chicago) for assistance with dissection, embedding, and thin sectioning of *Gonocephalus*; L. Alibardi (University of Bologna) for discussion about reptile histology; L. Parry (Oxford University) and S. Darroch (Senckenberg Museum of Natural History) for discussion on clay templating; K. Stauffer (Zerbst Ranch) for historical information on Wyoming homesteads; D. Levering (Sternberg Museum of Natural History) and C. Mehling (American Museum of Natural History) for access to archival letters and images; C. Boyd (North Dakota Geological Survey) and S. Drumheller (University of Tennessee-Knoxville) for discussion on dinosaur mummies; S. Kidwell (University of Chicago), J. Vinther (Bristol University), K. Carpenter (University of Colorado Museum), T. Green (New York Institute of Technology), and Filippo Bertozzo for comments on taphonomic interpretations and tables; and MorphoSource for archiving CT scans. **Funding:** This research was supported by an anonymous gift to P.C.S. of the Fossil Lab (University of Chicago) and a Marie Sklodowska Curie Actions grant (EvoSaurAF 101068861) to D.V. **Author contributions:** P.C.S. wrote the initial draft. E.T.S. contributed to the initial draft and led all microstructural and chemical analyses and spectroscopy visualizations. D.V., N.M., and S.L.B. contributed to the final draft. D.V. conducted stereophotogrammetric imaging of both mummies. L.L.B. and P.C.S. prepared Figs. 1 to 4. L.L.B. generated micro-CT scans. L.L.B. and M.C.R. segmented the CT and MRI scans. L.L.B., M.C.R., and D.V. assisted in reconstructions. S.L.B. managed digital data curation. T.M.K. prepared specimens and contributed to the final draft and supplementary information. P.C.S., E.T.S., D.V., and L.L.B. created all finished figures. S.L.B. created figure parts and visualizations. E.T.S. and T.M.K. guided fossil and recent specimen sectioning and sampling. P.C.S., E.T.S., M.E., and K.D. provided field data and observations. **Competing interests:** The authors declare no competing interests. **Data, code, and materials availability:** All reconstructions and data supporting our findings are available within the main text or the supplementary materials. CT scans and 3D models (extended data table S7) are available on MorphoSource (https://www.morphosource.org/projects/000664781?locale=en). Microscopic and chemical data are available on Dryad (*70*).

SUPPLEMENTARY MATERIALS

science.org/doi/10.1126/science.adw3536
Supplementary Text; Figs. S1 to S22; Tables S1 to S11; References (*71*–*117*);
MDAR Reproducibility Checklist

Submitted 29 January 2025; accepted 9 September 2025; published online 23 October 2025
10.1126/science.adw3536

CORRECTED 11 NOVEMBER 2025; SEE BELOW

Science
AAAS

Supplementary Materials for

Duck-billed dinosaur fleshy midline and hooves reveal terrestrial clay–template "mummification"

Paul C. Sereno *et al.*

Email: dinosaur@uchicago.edu

DOI: 10.1126/science.adw3536

The PDF file includes:

Other Supplementary Material for this manuscript includes the following:

MDAR Reproducibility Checklist (.pdf)

Correction (11 November 2025): Some minor clarifying language and an update to increase accuracy in the location description have been added.

Contents

1. Provenance of the new *Edmontosaurus* mummies

Provenance: Lance Formation, Niobrara County, east central Wyoming.

UCRC VP30 (Ed Sr.), 43° 21′ 14.0″ N, 104° 30′ 47.1″ E, altitude 1,225 m, distal half of an adult skeleton with extensive integument renderings including the tail spikes and hooves on the hind feet.

UCRC PV31 (Ed Jr.), 43° 24′ 16.3″ N, 104° 32′ 6.2″ E, altitude 1,262 m, most of a juvenile skeleton lacking portions of fore- and hind limbs with extensive integument renderings including the trunk and its overlying crest.

Age: ~66 Mya. The Lance Formation is widely recognized as latest Cretaceous in age (~69–66 Mya), bounded above and below by the Fort Union and Fox Hills Sandstone Formations (*69*). The location of the two new mummies at the top of a very thick section of the formation suggests they come from the very end of the Cretaceous close to the K-Pg boundary (66 Mya).

Taxon: cf. *Edmontosaurus annectens* based on the shape of the occiput of the juvenile skeleton, the presence of scale clusters on rendered integument, and the consistent form of the skeleton compared to abundant remains from this formation (see 5.2 Taxonomic identification and maturity).

Authentication: *Edmontosaurus annectens* is known from many articulated skeletons and bonebeds in the Lance Formation. The four new "mummy zone" sites were visited (by PCS) during excavation and collection.

Collectors: UCRC PV30, Marcus Eriksen, collected in 2001-2003. UCRC PV31, Kraig Derstler, collected in 1998.

Collection: Housed and accessioned in the University of Chicago Research Collection (UCRC PV 30, early adult; UCRC PV31, early juvenile) at the Fossil Lab (5437 S. Wabash Avenue, Chicago, IL 60615). For examination, contact Tyler Keillor (Lab Manager, tkeillor@uchicago.edu).

2. Terms for fossilized integument, integument structures and reptilian scalation

2.1 Institutional abbreviations

AMNH	American Museum of Natural History, New York, USA
ELDM	Erlianhaote Dinosaur Museum, Erlian, Inner Mongolia, China
HMNS	Houston Museum of Natural Science, Houston, USA
IVPP	Institute of Vertebrate Paleontology and Paleoanthropology, Beijing, China
JRF	Judith River Foundation, Malta, USA
NDGS	North Dakota Geologic Survey, Bismarck, USA
NMC	Canadian Museum of Nature, Ottawa, Canada
NMSG	Naturmuseum St. Gallen, St. Gallen, Switzerland
MCCM	Museo de las Ciencias de Castilla-La Mancha, Cuenca, Spain
MOR	Museum of the Rockies, Bozeman, USA
PIN	Paleontological Institute, Moscow, Russia
RAM	Raymond M. Alf Museum of Paleontology, Claremont, USA
ROM	Royal Ontario Museum, Toronto, Canada
SMF	Senckenberg Nature Museum, Frankfurt, Germany
SMNH	Sternberg Museum of Natural History, Hays, Kansas, USA
TMP	Royal Tyrrell Museum of Palaeontology, Drumheller, Alberta
UALVP	University of Alberta, Laboratory for Vertebrate Paleontology, Edmonton,

	Canada
UCRC	University of Chicago Research Collection, Chicago, USA
UMNH	Utah Museum of Natural History, University of Utah, Salt Lake City, UT, USA
ZCDM	Zucheng Dinosaur Museum, Zucheng, Shandong, China
ZPAL	Institute of Paleobiology, Polish Academy of Sciences, Warsaw, Poland

2.2 Terms for fossilized integument

Soft integument fossils, collectively referred to here as "integument renderings," are generated by distinctive taphonomic processes that yield four modes of preservation (cast-vestige, mold, template, impression). *Cast-vestige* integument renderings are preserved in positive relief via processes of permineralization or replacement (e.g., phosphatization) that preserve the external form and, more rarely, traces of organic material (e.g., melanin) (*70–72*). Cast-vestige renderings may be composed entirely, or almost entirely, of replacing exogenous materials and preserved in three-dimensions or compressed in sediment or enveloped in concretion (*73*, 74).

Other renderings are natural (negative) *molds* of an integument surface generated by surrounding sediment. A *mold*, unlike the other three modes, may occur synchronously or after any other of the modes of preservation. The *Triceratops* mummy (*5*) from the mummy zone, for example, preserves natural molds of scaly skin that, in some cases, match (positive) counterpart renderings.

Table S1. Modes of preservation of soft integument in terrestrial sediment.

No.	Rendering Mode	Definition
1	Cast-vestige	Positive relief replication of integument in compressed or three-dimensional form by permineralization or replacement (e.g., phosphatization) that may preserve external form or traces of internal form (e.g., melanosome) or original organic materials (e.g., melanin) (*72*, *108–113*)
2	Mold	Negative relief mold that preserves the external form of an integument surface (*114*)
3	Template	Positive relief, thin (<1 mm) enveloping clay mask that preserves the external form of an integument surface (*43–47*)
4	Impression	Negative relief impression of external integument form produced by pressing integument into soft, fine-grained sediment (*21*, *115*, *116*)

A *template*, or mask, may preserve the external form of integument in positive relief as a thin (< 1 mm) clay layer that preserves the external form of an integument surface (*45–47*).

Finally, integument may also be rendered in negative relief as an *impression* in soft sediment via physical contact and transfer of external morphology. In this study we used a high-fidelity hadrosaurid footprint preserving digital pad and scale morphology (*21*). Although initially generated as an impression in soft sediment, the surviving footprint is a positive relief natural cast made by sediment infilling of the original footprint (Fig. 3B). Footprints preserving scalation are extremely rare and require very particular sediment conditions, given the range of discordance possible between the footprint and sole of the trackmaker (*75–77*).

2.3 Integument structures in tetrapods

We compile and define the integument structures of recent and fossil tetrapods (*78*) to clarify the terms we use for integument renderings in *E. annectens* (table S2). We start with the meaning of "fossil mummy" and then divide tetrapod integument structures based on whether they are entirely fleshy or supported by underlying bone. Following anatomical practice in squamates, for example, a fleshy midline structure is identified as a "crest" as opposed to a "sail," which is supported internally by neural spines. For that reason, we describe the fleshy midline structure over the neck and trunk of *E. annectens* as a "crest" rather than as a "sail" and differentiate it from a "frill," as it was sometimes described by Osborn (*1*). We also heuristically define the terms "hoof," "claw" and "nail" for the principal forms taken by distal digital sheaths as commonly understood (*79*, *80*). By these definitions, the wedge-shaped, flat-bottomed sheath capping the pedal digits in *E. annectens* are clearly identified as hooves. Intermediates to the proposed hoof-claw-nail partitioning are relatively rare.

Table S2. Terminology for integument structures in tetrapods. The term "mummy" is used for specimens of extant or extinct tetrapods with exceptional and extensive preservation of integument. Most tetrapod fossilized integument falls into two categories, fleshy structures with and without bony support (*78–80*). The term "crest" has been commonly applied to both flesh-only and hybrid flesh-bone structures.

Integument Category	Structural Term(s)	Definition
Significant integument renderings enveloping a fossilized skeleton	Fossil mummy	An articulated, or mostly intact, partial or complete fossilized skeleton overlain by large areas of integument renderings (crests, scaly skin, feathers, claws, hooves, etc.) that usually shows evidence of pre-burial desiccation in skeletal positioning (e.g., neck retraction) and/or in rendered soft tissues (e.g., wrinkles, draping over skeletal bone) (e.g., *Edmontosaurus annectens*, Ed Sr., UCRC PV30)
	Intact mummy	Mummy buried as an intact body or carcass with few external openings slowing infilling by sediment that tends to be finer-grained than sediment immediately external to the mummy (e.g., *Tyrannosaurus rex*, Rex Jr., UCRC PV1)
	Breached mummy	Mummy buried as a carcass with external openings allowing rapid infilling by sediment that tends to be indistinguishable from sediment immediately external to the mummy (e.g., *Edmontosaurus annectens*, Ed Sr., UCRC PV30)
Skin or keratinous, cornified structures without bony support	Wattle Caruncle Eye Ring Snood Lappet Gular sac	Fleshy cranial appendage in various forms (e.g., midline, V-shaped, pendant) with variable surface ornamentation, color, presence of scales or feathers, and capacity for erection (e.g., *Cephalopterus*, *Sarcoramphus*, *Bucorvus*, *Meleagris*, *Centrocercus*, *Torgos*)
	Crest (soft tissue) Comb	Fleshy or feathered, transversely compressed, cranial or postcranial, midline projection (e.g., *Vultur*, *Upupa*, †*Edmontosaurus*)
	Spike	Prominent keratinous scale formed within the epidermis most commonly in the dorsal midline over the axial skeleton (e.g., *Iguana*, *Moloch*)
Skin or keratinous, cornified structures supported by underlying bone of similar shape	Rhamphotheca (beak)	Keratinous covering and extension of the anterior ends of upper and lower jaws (e.g., *Chelydra*, *Alca*, †*Parasaurolophus*)
	Horn	Keratinous covering and extension of dermal bone horn cores on the cranium and more rarely on the postcranium (e.g., *Phrynosoma*, *Diceros*, *Bison,* †*Carnotaurus*)
	Frill	Bilateral, often arcuate, keratin-sheathed or fleshy appendage supported at least in part by bone and located on the head or neck (e.g., *Chlamydosaurus*, †*Triceratops*)
	Crest (bony core)	Cornified or keratin-sheathed, laterally compressed, sagittal or parasagittal cranial ornament underlain by bone with little or no pneumatization (e.g., *Pelecanus*, †*Pteranodon*, †*Corythosaurus*, †*Dilophosaurus,* †*Spinosaurus*)
	Casque	Keratin-sheathed, rarely feathered, cranial ornament underlain by highly pneumatized bone in birds and nonavian theropods (e.g., *Casuarius*, *Buceros*, *Anseranas*)

	Protuberance Hump Dome Callosity Rugosity	Integument-covered, bony outgrowths, often part of expansive cranial ornamentation (e.g., *Anser*, *Balearica*, *Heloderma*, *Cuniculus,* †*Pachycephalosaurus*)
	Scute	Keratin-covered structure over the skull or skeleton supported by an underlying dermal osteoderm (e.g., *Alligator*, †*Deinosuchus*, †*Borealopelta*)
	Sail	Neural spine-supported, keratin-sheathed or scale-covered, slab-shaped midline structure (e.g., *Hydrosaurus*, *Basciliscus*, †*Dimetrodon,* †*Spinosaurus*)
	Spur	Keratin-enveloped dermal cone-shaped projection on the medial aspect of the tarsometatarsus or proximal aspect of the carpometacarpus in some birds (e.g., *Lophura*, *Vanellus*)
	Claw	Transversely compressed, distally tapering and pointed, dorsoventrally curved, keratinous sheath surrounding a terminal ungual (e.g., *Parabuteo*, *Puma*, †*Archaeopteryx*)
	Hoof	Wedge-shaped, flat-bottomed, keratinous sheath surrounding the terminal ungual of a terrestrial non-carnivore (herbivore, omnivore, insectivore). The sheath and underlying ungual have a blunt or arcuate distal margin (half-arc if paraxonic) and the foot has a subunguligrade or unguligrade posture that enhances ungual ground support (e.g., *Rangifer*, *Ovis*, †*Edmontosaurus,* †*Paraceratherium*)
	Nail	Dorsoventrally compressed, keratinous sheath overlying a terminal ungual (e.g., *Carlito*, *Homo*)

2.4 Terms for reptilian scalation

We compile and define terms for reptilian scales to clarify those we use to describe scalation in *E. annectens* (table S3). These are generally applicable scalation terms irrespective of anatomical location (i.e., excluding scale terms associated with anatomical location, such as a "lip" or "orbital" scale). We organize reptilian scale types into five categories based on shape, form, ornamentation, topology and pattern. A "feature" scale (*14*, *17, 81*), for example, is a useful topological term for scales that are relatively larger and/or of unusual shape compared to nearby scales. Smaller scales that form a numerically predominant mosaic pattern have been variously referred to in herpetological literature as "background," "ground," "reticulate," "mosaic," and, most recently, as "basement" (*14, 81*) scales. We use the older term "background" as the most intuitive for this general scalation pattern (logging alternative terms as synonyms). The five descriptive categories provide a framework for capturing in a more thorough manner the diversity of scale conditions in extant and extinct reptiles.

Table S3. Descriptive terminology for reptilian scales. Descriptive scale conditions and definitions are listed under five major descriptive categories with synonyms in parentheses [paleontological considerations include (*14*, *17*, *81*)]. Terms may be used in combination, such as a "smooth feature scale." The many scale adjectives that refer to anatomical or underlying skeletal topology (lip, cheek, orbital scales etc.) or that are associated with a stereotypical location (scutate

guard scales on the anterior aspect of the metatarsus and digits of avian and some nonavian theropods) are not included.

Descriptive Category	Categorical Definition	Scale Condition	Description
Shape	Two-dimensional contour of scale surface	Round	Circular, symmetrical
		Oval	Elongate with rounded perimeter
		Polygonal	Three or more sides
Form	Three-dimensional form of scale surface	Flat (pavement)	Flat main surface of scale
		Pebble (pebbly, rounded)	Rounded or arched scale surface
		Keeled	Longitudinal ridge
Ornamentation	Form of principal surface or edge	Smooth	Surface ornamentation absent
		Striated	Alternating linear grooves and ridges
		Ridged (fluted, grooved)	Ridged scale margin
Topology	Size or position relative to immediately adjacent scales or bone	Central	Central to peripheral scales
		Peripheral	Peripheral to a central scale
		Marginal	Along the edge of a structure
		Imbricate (overlapping)	Scale edge extending over the surface of an adjacent scale or scales
		Interdigitating	Scale inserts into or receives another scale
		Feature (shield)	Larger and often differing in shape from adjacent background scales
		Scute (bone-anchored)	Scale adhered to underlying dermal bone(s) (cranial bone, osteoderm, or carapace-plastron bone)
Pattern	Collective pattern for groups of scales	Background (ground, basement, mosaic, reticulate)	General, numerically predominant mosaic scalation pattern
		Cluster	Scales of similar size, shape or form grouped together in an irregularly shaped area
		Band	Scales of similar size, shape or form grouped together in a linear or rectilinear area

3. Large-bodied dinosaurs with significant integument renderings

3.1 Most significant dinosaur mummies

Large-bodied nonavian dinosaurs with substantial integument renderings are rare. Our compilation includes 20 specimens, 13 of which (~65%) are hadrosaurids (table S4). Four are theropods, including three that are feathered. We list together the three associated skeletons of the tyrannosaurid *Yutyrannus huali.* Only a single specimen is known among armored ornithischians,

the nodosaurid *Borealopelta markmitchelli*, and only one ceratopsid, the chasmosaurine *Triceratops horridus*, preserves enough skin renderings to be included among mummies. Sauropods are not represented, despite their body size range, longevity in the fossil record, global distribution, extraordinary diversity, and occasional integumental osteoderms.

The "mummy zone" is unique in preserving multiple mummies from more than a single dinosaur clade. Most of the mummies, in addition, are preserved as three-dimensional carcasses buried in a considerable thickness (> 1 m) of sandstone matrix.

Table S4. Large-bodied dinosaurs with exceptional integument renderings. Compilation of 20 specimens that includes 14 hadrosaurids, individual skeletons of the ceratopsid *Triceratops horrid*us and nodosaurid *Borealopelta markmitchelli*, and several theropods (*Beipiaosaurus inexpectus, Concavenator corcovatus*, *Yutyrannus huali* and *Tyrannosaurus rex*). An age of approximately 66 Mya is probable for specimens 1–4 and 6 of *Edmontosaurus annectens*, which were a found near the top of coeval Lance and Hell Creek Formations (duration 66-69 Mya). For acronyms of museum collections, see 2.1.

No.	Taxon	Specimen no., "Nickname"	Formation, site	Integument preservation
1	*Edmontosaurus annectens*	UCRC PV30 "Ed Sr."	Lance Fm., Swanson Ranch, Wyoming (Maastrichtian ~66 Mya)	Posterior half of an early adult skeleton complete to the tail tip, preserving large areas of scaly skin renderings on the tail including the midline spike row and hooves capping the pedal digits of both hind feet
2	" "	UCRC PV31 "Ed Jr."	Lance Fm., Stewart Ranch, Wyoming (Maastrichtian ~66 Mya)	Late juvenile skeleton with the ends of the fore and hind limbs and distal tail weathered away preserving large areas of scaly skin renderings over the ribcage including the midline crest
3	" "	AMNH FARB 5060 "AMNH mummy" (*1*)	Lance Fm., near Boggy Creek, Wyoming (Maastrichtian ~66 Mya)	Most of an early adult skeleton lacking the distal half of the hind limbs preserving extensive areas of scaly skin renderings including a short section of crest over the neck and the hooves capping two of the manual digits
4	" "	SMF R 4036 "Senckenberg mummy" (*3*, *4*)	Lance Fm., S. Snyder Creek, Wyoming	Partial adult skeleton lacking most of the hind limbs and distal half of the tail with an upper bill rendering and skin

			(Maastrichtian ~66 Mya)	and hoof renderings on right and left manus
5	" "	NMSG P 0001, formerly MOR V 007 (*11*)	Hell Creek Fm., Montana (Maastrichtian 69–66 Mya)	Most of an adult skeleton with an upper bill, midline tail spike section, and patches of scaly skin renderings
6	*Edmontosaurus cf. annectens*	NDGS 2000 "Dakota" (*12*, *39*)	Hell Creek Fm., southwestern North Dakota (Maastrichtian ~66 Mya)	Partial skeleton lacking the skull, right forelimb and distal end of the tail with large areas of scaly skin renderings, midline spikes above portions of the tail, and hooves capping two digits of the manus
7	*Edmontosaurus regalis*	UALVP 53290 (*18*)	Wapiti Fm., Alberta (Late Campanian ~70 Mya)	Partial skull and cervical column with cock's comb-like cranial crest and ovate neck scale renderings
8	*Saurolophus angustirostis*	PIN 4216/49 (*12*, *14*)	Nemegt Fm. ,Dragon's Tomb, Mongolia (Late Camp.-Maastr. ~75–68 Mya)	Late juvenile preserving a series of separate midline spikes in the mid tail.
9	" "	PIN 3747/2 (*12*, *14*)	Nemegt Fm., Mongolia (~Campanian ~80–70 Mya)	Mid tail with skin renderings including subtle vertical banding and large polygonal feature scales
10	" "	UALVP 52824 (*12*, *14*)	Nemegt Fm., Mongolia (~Campanian ~80–70 Mya)	Mid tail with skin renderings including tabular midline spikes
11	" "	ZPAL-MgD-1/159 (*12*, *14*)	Nemegt Fm., Dragon's Tomb, Mongolia, (~Campanian ~80–70 Mya)	Patch of basement scale renderings over intact trunk ribs
12	*Gyrposaurus notabilis*	ROM 764 (*10*)	Dinosaur Park Fm., Alberta (Late Santonian-Late Camp. 80–75 Mya)	Renderings of trapezoidal midline spikes with vertical striae over posterior dorsal and anterior sacral vertebrae
13	*Brachylophosaurus canadensis*	JRF 115H "Leonardo" (*15*)	Judith R. Fm., Malta, Montana (Early Camp. ~81–77 Mya)	Articulated late juvenile skeleton lacking the tail and any midline integument renderings but preserving an

				upper bill and areas of scaly skin renderings
14	*Corythosaurus casuarius*	AMNH 5240 (*91*)	Judith R. Fm., Malta, Montana (Early Camp. ~81–77 Mya)	Large sections of scaly skin renderings over the trunk, base of the tail and feet
15	*Triceratops horridus*	HMNS PV.1506 "Lane" (*5*)	Lance Fm., Zerbst Ranch, Wyoming (Maastrichtian ~66 Mya)	Partial skeleton with large rosette scale renderings over the trunk and pelvic girdle
16	*Borealopelta markmitchelli*	TMP 2011.033.0001	McMurray Fm., Alberta (Albian 113-100 Mya)	Anterior portion of the skeleton discovered in marine sediments with *in situ* scutes covered by integument renderings
17	*Tyrannosaurus rex*	UCRC PV1 "Rex Jr." (*6*)	Lance Fm., Zerbst Ranch, Wyoming (Maastrichtian 69–66 Mya)	Trunk with right forelimb and partial hind limb preserving body outline ventrally along the gastralia
18	*Yutyrannus huali*	ZCDM V5000, V5001, ELDM V1001	Yixian Fm., Beipiao, China (Aptian 126–124 Mya)	Skeletons with areas covered by carbonized compression preservation of simple feather renderings
19	*Concavenator corcovatus*	MCCM-LH 6666	Calizas de La Huérguina Fm., Las Hoyas, Spain (Barremian 130–125Mya)	Nearly complete skeleton with some scale, toepad and claw sheath renderings
20	*Beipiaosaurus inexpectus*	IVPP V11559	Yixian Fm., Sihetun, China (Aptian 126–124 Mya)	Skeleton with a body cover of simple feather renderings

4. Wyoming dinosaur "mummy zone"

4.1 Dinosaur mummies in the Lance Formation of east-central Wyoming

The greatest concentration of dinosaur mummies comes from the Lance Formation in a small area in east-central Wyoming we call the "mummy zone" (Fig. 1A). Four mummies of the hadrosaurid *Edmontosaurus annectens* come from a restricted zone within the uppermost section of the Lance Formation.

Table S5. "Mummy zone" specimens in the Lance Formation of east-central Wyoming. Specimens in the "mummy zone" of the Lance Formation in Niobrara County in east-central Wyoming. See section 2.1 for museum collection acronyms.

No.	Taxon (Nickname) Specimen	North	West	Altitude (m, ft)	Bones preserved, year collected, renderings
1	*Edmontosaurus annectens* (Ed Sr.) UCRC VP30	43° 21′ 14.0″ (43.3538889°)	104° 30′ 47.1″ (-104.5130833°)	1,225 m 4,019 ft	Distal half of skeleton collected in 2002 with extensive skin renderings
2	*Edmontosaurus annectens* (Ed Jr.) UCRC VP31	43° 24′ 16.3″ (43.404525°)	104° 32′ 6.2″ (-104.535043°)	1,262 m 4,140 ft	Most of the skeleton lacking the distal portions of the limbs and tail collected in 1998 with extensive skin renderings
3	*Edmontosaurus annectens* (AMNH mummy) AMNH FARB 5060	~43° 23′ 8.8″ (43.38578°)	~104° 31′ 39.1″ (-104.52754°)	~1,255 m ~4,120 ft	Skeleton without tail collected in 1908 with extensive skin renderings
4	*Edmontosaurus annectens* (Senckenberg mummy) SMF R 4036	~43° 24′ 56.6″ (43.41569°)	~104° 35′ 23.8″ (-104.58993°)	~1,210 m ~3,970 ft	Partial skeleton collected in 1910 preserving upper bill rendering and skin and hooves on both manus
5	*Triceratops horridus* (Lane) HMNS PV.1506	43° 24′ 5.1″ (43.4015833°)	104° 33′ 33.0″ (-104.5454722°)	1,279 m 4,196 ft	Partial skeleton collected in 2002 with large areas of skin renderings over the torso and pelvis
6	*Tyrannosaurus rex* (Rex Jr.) UCRC PV1	43° 23′ 42.8″ (43.3952222°)	104° 33′ 33.0″ (-104.5591667°)	1,292 m 4,239 ft	Skeleton from shoulders to hips with forelimbs and partial hindlimb collected in 2001 with a partial belly outline

4.2 AMNH mummy locality photo documentation

In August of 1908, a small field team led by C.H. Sternberg discovered the "AMNH mummy" in east-central Wyoming in what was then the eastern part of Converse County (later separated as Niobrara County). The only known photograph of the quarry (fig. S1) was set for publication in 1908 along with a short description of the discovery (*61*), but it was accidentally attached to Sternberg's next publication, which was on fossils from the Kansas Chalk (*82*) in the same volume of the *Transactions of the Kansas Academy of Science*, albeit some 140 pages later. Consequently, paleontologists believed Sternberg never took any photographs of the quarry of the AMNH mummy, historically the first and one of the greatest dinosaur mummies ever discovered.

Fig. S1. Quarry of the AMNH mummy. Photograph of the quarry of the AMNH mummy (AMNH FARB 5060) in east-central Wyoming taken by C.H. Sternberg in 1908. Photograph courtesy of the Research Library and Museum Archives, American Museum of Natural History.

In 2007 paleontologist K. Carpenter discovered Sternberg's quarry photograph. In a paper on dinosaur "mummification" (*54*), he republished the best version he could make from a copy of the 1909 publication. Carpenter's paper, nonetheless, was published in a journal not widely circulated, and so few learned that a quarry photograph existed. Using Carpenter's version of the photograph, one of us (P.C.S.) contacted the archives at the American Museum of Natural History to determine if they had any record of the photograph. They provided a high-resolution digital image of the quarry photograph (fig. S1) along with other photographs taken by Sternberg and sent to Osborn in 1909. In addition, a letter came to light written by C.H. Sternberg to H.F. Osborn on December 26, 1908, following sale of the specimen to the American Museum of Natural History. The letter, reproduced here for the first time (fig. S2), includes distances and details of rock formations that may eventually reveal the exact location of the AMNH mummy quarry and perhaps even Sternberg's route to the site.

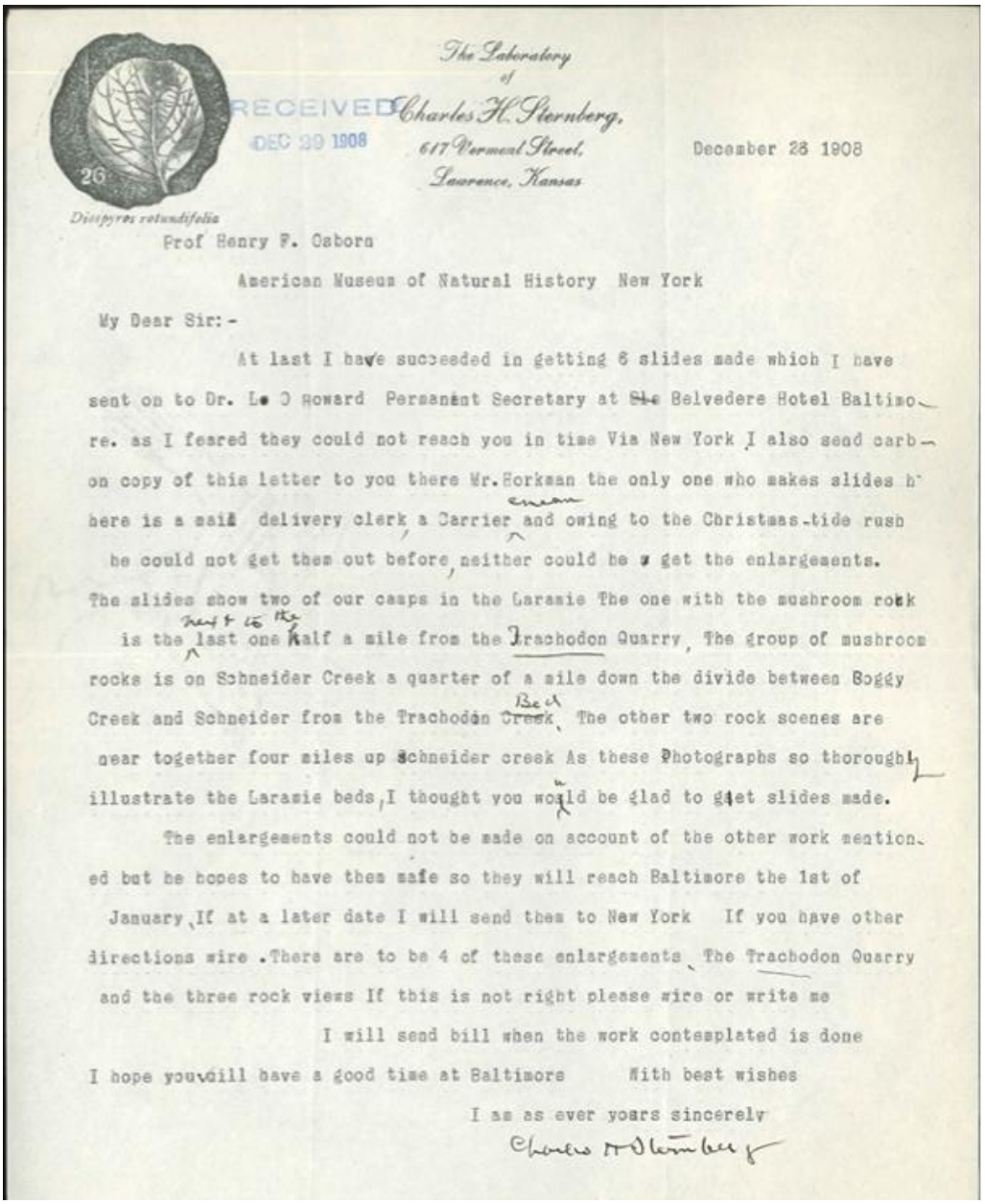

The Laboratory
of
Charles H. Sternberg,
617 Vermont Street,
Lawrence, Kansas

RECEIVED DEC 29 1908

December 28 1908

26

Dimpyros rotundifolia

Prof Henry F. Osborn

American Museum of Natural History New York

My Dear Sir:-

At last I have succeeded in getting 6 slides made which I have sent on to Dr. L. O Howard Permanent Secretary at the Belvedere Hotel Baltimore. as I feared they could not reach you in time Via New York I also send carbon copy of this letter to you there Mr. Horkman the only one who makes slides h' here is a mail delivery clerk a Carrier and owing to the Christmas-tide rush he could not get them out before, neither could he get the enlargements. The slides show two of our camps in the Laramie The one with the mushroom rock is the last one half a mile from the Trachodon Quarry, The group of mushroom rocks is on Schneider Creek a quarter of a mile down the divide between Boggy Creek and Schneider from the Trachodon Creek, The other two rock scenes are near together four miles up Schneider creek As these Photographs so thoroughly illustrate the Laramie beds, I thought you would be glad to get slides made.

The enlargements could not be made on account of the other work mentioned but he hopes to have them safe so they will reach Baltimore the 1st of January, If at a later date I will send them to New York If you have other directions wire .There are to be 4 of these enlargements, The Trachodon Quarry and the three rock views If this is not right please wire or write me

I will send bill when the work contemplated is done

I hope you will have a good time at Baltimore With best wishes

I am as ever yours sincerely

Charles H Sternberg

Fig. S2. C.H. Sternberg's letter to H.F. Osborn in 1908. Photograph courtesy of the Research Library and Museum Archives, American Museum of Natural History.

A few clues to the field location of the quarry come from Sternberg's 1908 description (*61*), and more are given in his popular account of the discovery shortly thereafter (1909b: 272-275) (*83*). He described using a "one-horse buggy" to make his way toward a field camp "near the cedar hills on Schneider Creek," which today is spelled "Snyder Creek." He likely utilized a westbound trail developed in homestead times at the end of the nineteenth century that followed the banks of the Cheyenne River. Passing upstream (west), he would have arrived at the mouth of Snyder Creek (Fig. 1A). An improved gravel road today follows the same general route on the north bank of the Cheyenne River. Sometime after Sternberg's day, a river crossing was established that continues west to the headquarters of the Zerbst Ranch near the mouth of Snyder Creek (Fig. 1A). Where

Sternberg's team would have crossed to the south side of the Cheyenne River to access Snyder Creek remains unknown.

In Sternberg's account (*83*), his sons George and Levi alerted him to their discovery of a well-preserved duck-billed skeleton on a "high escarpment of sandstone" located "over the divide. . . between Boggy and the breaks of Schneider" (1909b: 272–275) (*83*). Today's county road leads directly south from the Zerbst Ranch and passes over a divide before descending toward Boggy Creek. Thus the location and altitude of the site of the AMNH mummy is well circumscribed (Fig. 1, number 1). The quarry was described as a "mass of sandstone 12 feet wide, 15 feet deep, and 10 feet high" (fig. S1).

Fig. S3. AMNH mummy. Ventral (left) and dorsal (right) views of the prepared mummy (AMNH FARB 5060) in 1910 prior to its public display. Photographs courtesy of the Research Library and Museum Archives, American Museum of Natural History.

Sternberg's description of the mummy in the field (*83*) includes enough detail on the positioning of the limbs and rendered integument to suggest much of the specimen was fully exposed before jacketing (1909b: 274–275). The point when the excavators first noticed the skin renderings remains unknown. When excavating an articulated skeleton in an immense block of sandstone, leaving any extra margin of rock can add enormous mass to the block. Surely under this usual excavating constraint, many areas of integument renderings were lost. Sediment removed immediately adjacent to the skull and midline over the trunk and hips probably destroyed additional midline crest (fig. S3, right). The crest over the mid cervical vertebrae is protected in the notch of the backwardly arched neck and is the only portion of crest remaining. Even in this case, the finished edge of the crest appears to have been broken away during collection.

> Osborn (*1*) noted:
> "There is reason to believe that when first discovered the fossilized skeleton, including the skull, was completely encased in impressions of its integument, but many portions of the impression area were destroyed because, as above noted, of the quite natural failure of the discoverer to recognize the extremely thin "impression layer" before certain of the bones had been cleaned up." (Osborn, 1912: 35)

Osborn (*1*) also remarked that the mounted skeleton of *Edmontosaurus annectens* (AMNH FARB 5730) discovered by J.L. Wortman in 1884 was "surrounded by a natural cast of its epidermal impressions", all of which were lost during excavation and preparation (Osborn, 1912: 34).

4.3 Senckenberg mummy locality photo documentation

In September of 1910 in the same area of east-central Wyoming, the Sternberg crew found a second skeleton *Edmontosaurus* (*Trachodon*) *annectens* with significant epidermal renderings that would become known as the "Senckenberg mummy." C.H. Sternberg (*2*) recounted finding it "on the South Branch of Schneider Creek, 20 miles northwest of Warren" (Sternberg, 1911: 221) There, in a "little patch of ground on the head of South Schneider we had not explored", his crew found "the last sacral vertebra and one hind limb . . . sticking out of a high ledge of grey sandstone." Photographs from the site show considerable relief (*4*, *84*), confirming its location near the mouth of the South Branch (Fig. 1A, number 2; fig. S4). Sternberg's "Schneider Creek" today is spelled "Snyder Creek," and the search that led to discovering the location of Warren is detailed below.

The Senckenberg mummy was found on the northern end of the Zerbst Ranch, its headquarters located there as well on the south bank of Snyder Creek, which courses about 3 kms east before joining the Cheyenne River. The present-day crossing of the Cheyenne River near the junction with Snyder Creek provides access from the Cheyenne River Road, which follows the east side of the river, to the Zerbst Ranch and "mummy" zone. According to the current managers of the Zerbst Ranch (*fide* Kristen [Zerbst] Stauffer), establishment of the crossing of the Cheyenne River near Snyder Creek occurred only in more recent times and was not available in Sternberg's day. He would have to have crossed the Cheyenne River much farther south and then worked his way north to approach the headquarters of the Zerbst Ranch and his Snyder Creek locality. In Sternberg's day, the Zerbst Ranch and surrounding Cheyenne River country was included in a larger Converse County, which was subsequently subdivided, the eastern half recognized as Niobrara County. This explains why Sternberg referenced Converse, rather than Niobrara, County for his localities and photographic images.

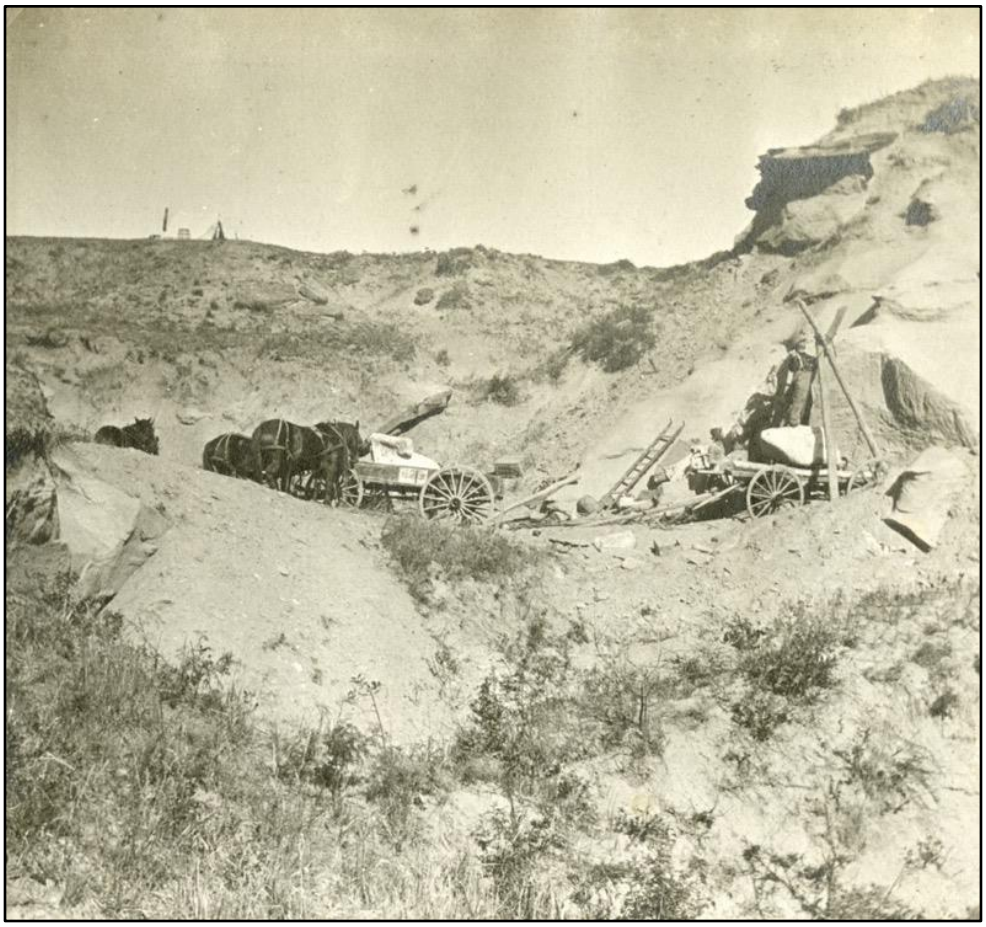

Fig. S4. Unpublished photograph of the Senckenberg mummy site. Quarry at the head of the South Branch of Snyder Creek in 1910. Photograph courtesy of the Forsyth Library, Sternberg Museum of Natural History, Fort Hays State University, Hays, Kansas.

Kristen (Zerbst) Stauffer's grandfather, William (Bill) Zerbst, was born in 1910, the same year that Sternberg found the Senckenberg mummy a short distance from the headquarters of the Zerbst Ranch (Fig. 1A, number 2; fig. S4). Kristen's great grandfather, Charles Zerbst, would have been running the ranch when Sternberg collected both of his mummies. German-born Charles and Helen Zerbst (born in 1870 and 1888, respectively) homesteaded the ranch after the turn of the century, marrying in 1909. Kristen (Zerbst) Stauffer, the great granddaughter of Charles and Helen Zerbst, currently manages the Zerbst Ranch, maintaining the family's longstanding interest in its paleontological resources. Reports in local newspapers about dinosaur fossils on the Zerbst Ranch occur periodically over the last century, with two of the four recent mummy finds (Rex Jr., Lane) initially drawing the notice of ranch personnel.

The headquarters of the Wasserburger Ranch is located approximately 23 kms south and slightly east of the Zerbst Ranch headquarters on the south bank of Lance Creek, approximately 8 kms east of Redbird and U.S. Route 85. Managed currently by Ben Wasserburger, a cousin of Kristen (Zerbst) Stauffer (her father's sister's son), the Wasserburger Ranch was established in 1918 by Ben's grandfather, John Wasserburger. At that time, the ranch headquarters included the Bright post office, which was later renamed the Warren post office after Francis E. Warren, the first governor or Wyoming Territory in 1885 and later a U.S. Senator. Rather than a named

Wyoming town, Warren was a small free-standing post office on the Wasserburger Ranch (photograph sa1-p070-01, G. Sternberg, 1910, University Archives, Fort Hays State University). Ben's grandmother, Katherine Wasserburger, served as Postmaster. The post office building has been maintained ever since as part of the ranch headquarters, although it closed as a functioning post office long ago. "Warren," thus, became a place name remembered by local ranchers steeped in family history but absent on any current Wyoming map.

Fig. S5. Location of Warren and Senckenberg mummy site. The Warren post office is located on the Wasserberger Ranch on the south bank of Lance Creek (left), with a straight-line distance of 15.2 miles to the likely site of the Senckenberg mummy.

The straight-line distance between the old Warren post office and head of the South Branch of Snyder Creek is 15.2 miles (24.5 km) in a direction N35W, which not far from Sternberg's reported distance of 20 miles northwest (fig. S5, right), which may record the distance travelled across the terrain. Steep cutbank exposures to the west of the Zerbst Ranch near the head of the South Branch of Snyder Creek are generally consistent with images Sternberg took of the locality (*4*, *83*), which would be about 1,210 m (3,970 ft.) in altitude (Fig. 1B). The Senckenberg specimen (SMF R 4036) is the northernmost mummy discovered in the "mummy zone" and likely the lowest in altitude and section (Fig. 1B). Sternberg found it two years after, and approximately 6 km northeast of, the AMNH mummy.

It is not possible to log a geologic section from one site to another in the "mummy zone," because the outcrops are mostly in ravines separated by significant areas of grassland. Nevertheless, because the beds are flat lying, we use altitude as a reasonable proxy for stratigraphic level. The "mummy zone," from the lowest point along Snyder Creek to the greatest elevation within the zone, has a maximum relief of 120 m (~400 ft.) of relief. Well logs in the area record thicknesses of the Lance Formation exceeding 1,000 m (*69*), suggesting that surface-exposed

dinosaur mummies are likely approximately 66 My old and close in time to the end-Cretaceous extinction.

5. New *Edmontosaurus annectens* "mummies"

5.1 Recent fieldwork in the "mummy zone"

During the 1990s and early 2000s, the Lance Formation south of the Cheyenne River had attracted several fossil collectors on both private public (BLM) land. The Zerbst Ranch hosted one of the authors (P.C.S.) during field work from 2000–2003, when 230 fossil localities were mapped and collected in outcrops of the Lance Formation including a skeleton of *Tyrannosaurus rex* (Rex Jr.) that preserves portions of a body outline (*6*). The ranch contracted the Black Hills Institute to collect nearby a mummy of a *Triceratops horridus* (*5*).

Two authors (M.E., K.D.) working in the area collected, respectively, the early adult (Ed. Sr.) and late juvenile (Ed. Jr.) mummies of *Edmontosaurus annectens* described in this report. Thus over a short interval of four years (1998-2002), four dinosaur "mummies" representing three of the iconic genera at the end of the dinosaur era in western North America (*Tyrannosaurus*, *Triceratops*, *Edmontosaurus*) were collected from the same area that had yielded Sternberg's first two *Edmontosaurus* mummies more than a century prior (table S5).

5.2 Taxonomic identification and maturity

The North American hadrosaurid genus *Edmontosaurus* (= *Claosaurus*, *Trachodon*, *Thespesius*, *Anatosaurus*) has two recognized species in successive time periods and strata during the Late Cretaceous of western North America: *E. regalis* of Campanian age (~83–72 Mya) and *E. annectens* of Maastrichtian age (72–65 Mya) and best known from the coeval Lance and Hell Creek Formations (*8*, *85*, *86*). The genus *Edmontosaurus* and the two species are diagnosed almost exclusively on cranial features, some of which are apparent only with maturity. The posterior half of the cranium is preserved in the late juvenile mummy (UCRC PV31) and has the lower occipital proportions characteristic of *E. annectens* (*85*, *86*). Other than their stratigraphic age and origin (Maastrichtian, Lance Creek Fm.), that morphology is diagnostic and valuable in assigning the two new mummies to *E. annectens*.

Table S6. Growth in *Edmontosaurus annectens*. Estimated femur length, body length, body mass, age, and maturity category for the well-known dinosaur *Edmontosaurus annectens* with exemplar bones or skeletons. The four discussed in this paper are in red. See section 2.1 for museum collection acronyms.

Stage no.	Femur length (cm)	Body length (m)	Body mass (kg)	Estimated age (yrs)	Maturity stage	Associated specimen
1	15	0.7	15	months	Late nestling	UCMP 128181
2	50–65	5-7	700–1000	2	Early juvenile	LACM 23504, UCRC PV31
3	65-80	8	1,000–2,000	3–4	Late juvenile	ROM 67798
4	80–90	9	2,000–2,300	4–5	Early subadult	ROM 67799
5	90–100	10	2,300–2,500	5–6	Late subadult	ROM 73850

6	100–110	10-11	2,500–5,000	7–8	Early adult	AMNH FARB 5060, UCRC PV30
7	110–130	11-12	5,000–7,100	≥9	Late adult	AMNH FARB 5730, SMF R 4036

Edmontosaurus species grow to an adult body length of approximately 12 m (40 feet) (table S6). The late adult *Edmontosaurus regalis* paratype skeleton (CMN 2289) has reached maximum body size with femoral length of 128 cm, an estimated body length of 12 m, and an estimated body mass of 7,963 kg (table S1, number 8), which matches the largest *E. annectens* (*8*) (tables S6 and S7, number 6). Long bone growth in *Edmontosaurus* and other hadrosaurs is isometric, from nestling to adult body size (*87*, *88*).

Table S7. Maturity and relative size of the most complete *Edmontosaurus* specimens. Femur length and percent body size for specimens of *E. annectens* and *E. regalis* ordered from smallest to largest individuals. The new early adult *E. annectens* (UCRC PV30) and the AMNH mummy are nearly identical size and are set at 100% with corresponding cranial, femoral and skeletal lengths of approximately 86 cm, 93 cm, and 10-11 m, respectively. For the AMNH mummy, we estimated cranial, manual digit III and femoral length from Osborn's detailed figures (*1*). For the Senckenberg mummy, percentage size was based on reported cranial length (*3*), which was used to estimate its femur length (only the proximal end preserved). For Dakota, percentage size and an estimate for femur length were based on the length of manual digit III observed in a CT scan (*12*) compared to the same measure in the well preserved right manus of the AMNH mummy (*1*). See section 2.1 for museum collection acronyms.

No.	Maturity	Relative size, Femur length	Specimen, "Nickname"	Formation, site, year collected, age	Bones preserved, renderings
Edmontosaurus annectens					
1	Late juvenile	61% Femur 56 cm (estimated from skeletal overlay)	UCRC PV31 "Ed Jr."	Lance Fm., Stewart Ranch Wyoming, collected 2001 (Maastrichtian ~66 Mya)	Subadult skeleton with the posterior portion of the skull and torso, lacking forelimbs; most of the hindlimbs and mid and distal tail lost to erosion; no integument renderings
2	Late juvenile	62% Femur 57 cm	LACM 23504 (*123*)	Hell Creek Fm., Binion Ranch, Montana, collected 1965 (Maastrichtian 69-66 Mya)	Very complete subadult skeleton without integument renderings
3	Early adult	91% Femur ~84 cm	NDGS 2000 "Dakota" (*12*)	Hell Creek Fm., southwestern	Partial skeleton lacking the skull, left forelimb

		(est. from CT scan of rt. manual digit III 34.0 cm)		North Dakota, collected 2006 (Maastrichtian ~66 Mya)	and sections of the distal tail preserving extensive skin renderings including one well preserved manus (right side)
4	Early adult	100% Femur ~92 cm (est. from figures; cranium ~86 cm, rt. manual digit III 37.5 cm)	AMNH FARB 5060 "AMNH mummy" (*1*)	Lance Fm., near Swanson's Ranch, Wyoming collected 1908 (Maastrichtian ~66 Mya)	Skull and most of the postcranial skeleton lacking the distal half of the hind limbs, preserving extensive skin renderings on the trunk and forelimbs
5	Early adult	100% Femur 93 cm (based on field photograph of exposed femur)	UCRC PV30 "Ed Sr."	Lance Fm., Swanson Ranch Wyoming, collected 2002 (Maastrichtian ~66 Mya)	Posterior 60% of the skeleton complete to the tail tip, preserving the tail scalation, the midline spike row, and hooves on both hind feet
6	Early adult	103% Femur 95 cm	NMSG P 0001, formerly MOR V 007 (*11*)	Hell Creek Fm., 25 km north of Jordan, Montana, collected 1983 (Maastrichtian 69–66 Mya)	Nearly complete skeleton with upper bill, patches of scaly skin renderings, and a section of tail spike renderings
7	Late adult	111% Femur 102 cm	USNM V2414	Lance Fm., Wyoming, collected 1891, holotype (Maastrichtian 69–66 Mya)	Partial skeleton without integument renderings
8	Late adult	122% Femur ~112 cm (est. from cranium 105 cm) (*3*)	SMF R 4036 "Senckenberg mummy" (*3*, *4*)	Lance Fm., S. Schneider Cr., Wyoming collected 1910 (Maastrichtian ~66 Mya)	Skull with upper bill and partial postcranial skeleton lacking hind limbs and distal tail, some skin renderings on manus; femur length based on cranial length compared to AMNH mummy
9	Late adult	122% Femur 112 cm	AMNH 5730	Hell Creek Fm., Montana, collected 1884	Well preserved skeleton with skin renderings lost to preparation;

				(Maastrichtian 69–66 Mya)	formerly identified as "*Anatosaurus copei*"
Edmontosaurus regalis					
10	Late adult	139% Femur 128 cm	CMN 2289 paratype (*89*)	Horseshoe Canyon Fm. (Horsethief Mbr.), Alberta, collected 1916, (Late Campanian ~70 Mya)	Excellent skull and skeleton without integument renderings

5.3 Late juvenile *E. annectens* mummy

Specimen: UCRC PV31.

Locality: Uppermost section of the Lance Fm., Stewart Ranch, Niobrara County, Wyoming (Maastrichtian, ~66 Mya).

Discovery and preparation: Found in 1998 in a ravine with portions of the limbs and tail exposed (Fig. 1A, number 4). The skeleton was excavated in a single field jacket by one of us (K.D.). Preparation of the block and most integument surfaces including the trunk crest was completed by R. Masek, T. Keillor and E. Fitzgerald in the Fossil Lab at the University of Chicago. No adhesives or hardener were applied to the integument renderings so as not to add any extraneous chemicals.

General features: The specimen is a fully articulated, partial subadult skeleton, measuring 224 cm in length with the ribcage measuring a maximum of 65 cm in depth and 55 cm in width. It was buried following postmortem desiccation, as shown by the opisthotonic position of the skull (*89*, *90*) and wrinkled and tightly bound skin renderings. The matrix infilling of the ribcage is horizontally laminated, and there is no indication of skin renderings draped from the ribcage across the center of the torso as is present in AMNH FARB 5060 (*1*).

Portions of the skeleton lost to erosion at the site of discovery include the right scapular blade and the distal portions of fore and hind limbs, ventral portion of the pelvic girdle and left prepubic process, some anterior chevrons, and the mid and distal portions of the tail. Although the premaxillae and much of the remainder of the cranium were preserved in place, the maxillae and a few other anterior cranial bones and the lower jaws were missing. The snout end of the cranium shows signs of disarticulation, which is not surprising given the immaturity of the specimen. The left lacrimal and one of the quadrates were slightly displaced from natural articulation.

The postcranial skeleton is preserved in natural articulation. All cervical ribs, for example, are preserved articulated to the neck vertebrae and compose a virtually complete rib transition from neck to trunk. The axial skeleton is articulated, centrum to centrum, to the last preserved caudal vertebra (CA10). Paired sternals and coracoids are preserved very close to their natural position, all four bones converging. The sternal region of AMNH FARB 5060, by comparison, is displaced into the chest cavity, as noted by Osborn (p. 35) (*1*). left and right coracoids are separated by a narrow space three centimeters in width. The association of the distal ends of the sternal ventrolateral processes and the ribcage are preserved better than in any other hadrosauroid specimen, as the rib shafts are exposed from the cervical to the dorsal series.

The pelvic girdle and proximal ends of the hind limbs and the tail also are all preserved in natural position, demonstrating that the ends of the prepubic process of the pubis extend farther anteriorly and laterally than the preacetabular process of the ilium.

The torso came to rest on its right side with the neck and cranium displaced slightly to the left side above the ribcage. The fleshy midline crest is also be deflected to the left of the midline of the skeleton, which can be estimated from the exposed ventral margin of trunk centra. The fleshy trunk crest, thus, appears to have been deflected by the mass of the overturned carcass prior to desiccation. The crest over the trunk appears has a wedge-shaped base, thickening substantially toward the ribcage, obscuring the transverse processes and tuberculum of the ribs. Looking posteriorly from the anterior end of the specimen, the sagittal plane of the ribcage is tipped only about 25° from the vertical toward the right side. The mid and posterior dorsal vertebrae are gently rotated counterclockwise, such that the sagittal plane through the pelvic girdle and base of the tail is vertical. This portion of the skeleton is positioned upside down. The hind legs are not positioned symmetrically to each side but rather both are tipped toward the right side like the anterior portion of the torso.

Integument renderings: Skin renderings are preserved in many places along the length of the preserved portion of the skeleton. Some renderings are overlain close to underlying bones and other renderings are on layers of matrix as patches or as midline structures far from any bone surface. All the scales are small (< 3 mm) to very small (< 1 mm), and the skin over the body appears to be very thin. Desiccation wrinkles, well preserved over the left scapular blade, are sharp, edged and linear, as if the skin composed only a thin layer overlying the bone. Similar features and a similar interpretation of a small-scaled, very thin integument were made from the same region of the body in AMNH FARB 5060 (Osborn, 1912: 46) (*1*). This general skin rendering over the ribcage and shoulder girdle differs from the appearance of the larger scaled skin on the sides of the tail of the adult mummy (UCRC PV30). The larger-scaled tail skin appears to be thicker and lacks sharp-edged wrinkles.

Patches of scaly skin composed of low relief, flat to slightly convex scales surrounded by very small pebble scales document the cluster pattern of larger scales described by Osborn (*1*), which thus far have been found only in *Edmontosaurus annectens* (Osborn, 1912: 48). Traces of the midline crest are present above C7–9 although not as completely preserved as in AMNH FARB 5060. Starting at C12 several bands of pebble scales 3 cm in width are separate by narrow grooves composed of very fine pebble scales less than 1 mm in diameter. The depth of the preserved crest is approximately 3 cm, although the dorsal edge is unnaturally sharp and thus appears to have been truncated during initial preparation. A well-preserved edge is not present until at least 10 cm more posteriorly over the anteriormost dorsal vertebrae of the trunk. The cervical frill appears to be transversely narrow and close to the midline, as exposed in left lateral view. The prominent articulation between the costal tuberculum and transverse processes of the left posterior cervical ribs is visible lateral to the frill, which would be located over the midline as a narrow, banded sheet.

The dorsal crest is well preserved and exposed and increases in width to subsume the articulation between the costal tuberculum and transverse processes of the anterior dorsal ribs. The crest over the anterior trunk, thus, is quite fleshy and would have a subtriangular cross-section. The proximal two-thirds of the trunk crest has the same pattern of bands of small pebble scales separated by finely scaled grooves. The bands expand in anteroposterior width distally and therefore are increasingly canted posteriorly over the middle of the trunk.

Scaly skin renderings are preserved over the left side of the ribcage and scapulocoracoid and appear to be very thin. Patches that have broken away show the integument template to be very thin, exposing the surface of scapular blade beneath. Sharp-edged wrinkles in places over the scapula and torso suggest that the skin over this portion of the body was very thin in life.

Table S8. Scans and digital models. CT scans and digital models of integument renderings of the late juvenile and early adult mummies of *E. annectens* and two species of the angle-headed lizard *Gonocephalus*. See section 2.1 for museum collection acronyms.

Taxon/Specimen	Description	Data Type
Edmontosaurus annectens UCRC PV31	Left side of trunk	Photogrammetry (Fig. 2A)
Edmontosaurus annectens UCRC PV30	Mid and distal tail	Photogrammetry (Fig. 2B)
	Final 10–12 caudal vertebrae in concretion	CT scan (UC Hospital)
	Mid caudal spike rendering	micro-CT scan (UC PaleoCT)
	Trunk skin rendering on block	CT scan (UC Hospital)
	Right hind foot, digital pads and hooves	CT scan (UC Hospital)
Gonocephalus doriae FMNH H:249773	Head and neck	micro-CT scan (UC PaleoCT) (Fig. 2C)
	Whole body	micro-CT scan (UC PaleoCT)

There is no indication of spike-like eminences or projections along the rounded top margin of the crest. Given the substantial body size of the late juvenile, it is unlikely that the absence of spikes over the trunk is due to immaturity. The most anterior spikes have a low profile and first appear over the hips of the early adult specimen (UCRC PV30).

5.4 Early adult *E. annectens* mummy

Specimen: UCRC PV30.

Locality: Lance Fm., Swanson Ranch, Niobrara County, Wyoming (Maastrichtian, 69–66 Mya).

Discovery and preparation: Only a single dorsal vertebra and some ossified tendons were initially exposed, projecting from the vertical cutbank wall of a seasonally dry creek that drains north into Boggy Creek (Fig. 1, number 3). Those bones were positioned beneath more than two meters of sandstone extending to the top of the cutbank. Found in 2000 by S. Nesbitt and J.P. Cavigell, two of us (M.E., P.C.S) visited to examine the exposed bones. Excavation led by one of us (M.E) began in 2001 and was finished in 2003. During the excavation, PaleoBOND adhesive was applied to some of the spikes and scaly integument renderings and spikes.

The tail of this early adult is one of the most completely preserved for any hadrosaur, with vertebrae and skin renderings continuing to its distal tip. Additional preparation of the basal and distal portions of the tail and feet were undertaken by T. Keillor and R. Masek at the Fossil Lab at the University of Chicago. Basal and distal portions of the tail were prepared on the right side except for a concretion that surrounds the distalmost vertebrae. The left (down) side also has scaly skin renderings, but they are less complete than on the right (upper) side of the tail. Most of the

right side of the tail and the upper surface of both pedes were exposed in the field, resulting in the loss of the lateral edges of exposed hooves. Further exposure of the hooves of digits III and IV and section of pedal scale renderings was undertaken prior to CT scanning. No adhesives or hardener were applied during laboratory preparation so as not to add any extraneous chemicals.

General features: The specimen preserves the posterior one-half of an articulated skeleton preserved in lateral view resting on its left side. Given the exceptional preservation and articulation of the preserved portion of the skeleton, it is likely that the estimated anterior 40% of the skeleton including the skull was originally preserved but slowly eroded away over decades by the encroaching arc of a cutbank. The pose of the proximal portion of the carcass cannot be determined. Nonetheless, it is entirely possible the torso would have twisted somewhat to one side with ribcage oriented upward like the other three carcasses from the mummy zone, given the degree of desiccation visible in the tail and its slightly dorsiflexed resting position. Very little transport would have been possible to preserve the tail in such pristine condition, with all vertebrae, chevrons and fleshy spikes in place.

The posterior portion of the skeleton is resting on its left side with partially flexed right and left hind limbs extending from the pelvic girdle. The right hind limb is rotated more posteriorly at the hip socket, exposing the left hind limb underneath. The hind limbs are in a semi-flexed pose, with the toes of each pes extended. The preserved skeleton measures 5.58 m in length from the posterior dorsal vertebrae to the tail tip, which would comprise about 55–60% of the length of a complete skeleton. A rough estimate of the total length of the early adult skeleton is approximately 10-11 m (table S6).

Integument renderings: Portions of the skeleton with exposed integument include a slab of desiccated skin found between the hind limbs, the left side of the mid and distal tail including the midline spike row, and portions of the right pes (Figs. 2, 3). The slab between the legs preserves areas of scale clusters exactly as shown in AMNH FARB 5060 (*1*).

The lateral aspect of the tail shows scalation largely consistent with those in other hadrosaurs. Polygonal scales are smallest near the spike row (~3 mm), somewhat larger in the upper one-third of the tail (~5–8 mm), and largest over the ventral two-thirds of the tail (~6–9 mm). There are no feature scales or scale clusters. The desiccated skin on each side of the tail is closely appressed to the contours of underlying bone and ossified tendon.

Low elongate spikes first appear over sacral neural spines (sacral vertebrae 3 and 4) directly above the hip socket. The spikes increase in height to a maximum of about 5 cm in the anterior portion of the tail (around caudal vertebra 20) before gradually decreasing in height and length toward the distal end of the tail, as preserved in situ on a block preserving the last 53 caudal vertebrae of the tail (~caudal vertebrae 11–64; Fig. 2B). The best-preserved spikes have a smooth perimeter fringe about 5 mm in width and only 1 mm in thickness (Fig. 4A). Below the fringe, transverse thickness of the spike increases to 1.3 cm at its base, with each side covered by posterodorsally inclined, irregularly beaded striations (Fig. 4B).

The posterior end of each spike bifurcates to receive the anterior end of the next spike, their subtriangular area of interdigitation slightly raised (Figs. 3E, 4B). A basal groove separates the spike row from polygonal scales covering each side of the tail. The tip of each caudal neural spine projects into the posterior end of the base of each spike, terminating just dorsal to the basal groove.

Table S9. Measurements of a mid-caudal dermal spike. The mid-caudal spike (CA33; Fig 4B) measured here are among the largest atop the tail of an early adult mummy of *E. annectens* (UCRC PV30).

Structure	Measurement	Length (cm)
Spike	Basal length (including inserted end into the preceding spike)	9.0
	Maximum height	4.5
	Basal transverse width	2.8
	Length of inserted proximal portion of spine	3.5
	Length of split distal portion of spine	3.5

Hoof renderings: The right pes is partially exposed on its lateral side (Fig. 3A). Pedal digit IV preserves some small polygonal scales just proximal to the hoof rendering and over more proximal phalanges (Fig. 3A, left), suggesting that the scalation remains small diameter over the anterior (dorsal) aspect of the pes (Fig. 3F). The hoof of digit III is the best exposed, which we were able to continue to outline using CT scans. The hoof is considerably longer than the encased ungual, roughly twice as long (table S10). The wedge-shaped hoof has an arcuate leading edge that reflects the leading edge of the spade-shaped ungual. The perimeter of the bottom surface is flat, which gives way to a central depression, as seen in cross section (Fig. 3A, right). The surface of the hoof has a low linear texture. The hoof blends into a subcircular digital pad as visualized from the CT scan (Fig. 3D). The partially exposed ventral surface of the pad and the heel are covered by very fine scalation.

Table S10. Measurements of the right pedal phalanges and hooves (*E. annectens*, UCRC PV30). The phalanges and hooves of pedal digits III and IV were measured as exposed, whereas the phalanges of pedal digit II were measured from a CT scan.

Right Pes	Measurement	Length (cm)
Digit II	Metatarsal 2, length	25.9
	Phalanx 1, length	12.4
	Phalanx 2, length	7.7
	Ungual, length	8.2
Digit III	Metatarsal 3, length	35.2
	Phalanx 1, length	11.8
	Phalanx 2, length	4.8
	Phalanx 3, length	2.9
	Ungual, length	7.4
	Hoof, length	15.2
	Hoof, proximal width	11.4
	Hoof, proximal depth	6.7
Digit IV	Metatarsal 4, length	25.2
	Phalanx 1, length	9.3
	Phalanx 2, length	3.3
	Phalanx 3, length	2.2
	Phalanx 4, length	2.0
	Ungual, length	8.2

	Hoof, length	12.7
	Hoof, proximal width	8.9

6. Discovering hadrosaurid integument

6.1 Midline crest discovered in *E. annectens*

Osborn (*1*) observed approximately 25 cm of a scaly midline crest at least 7 to 8 cm deep over the mid cervical vertebrae (C8–11) (fig. S6). Although no other midline structures were preserved in AMNH FARB 5060 or known in any other hadrosaurid at that time, Osborn (*1*) extrapolated posteriorly from the cervical region in his reconstruction and positioned the preserved cervical crest over the anterior dorsal vertebrae above the scapula, rather than over the neck (fig. S7). Later the crest was extended farther along the length of the body, from the neck to at least the base of the tail, as shown in a well-known reconstruction by early paleoartist Charles Knight (fig. S8).

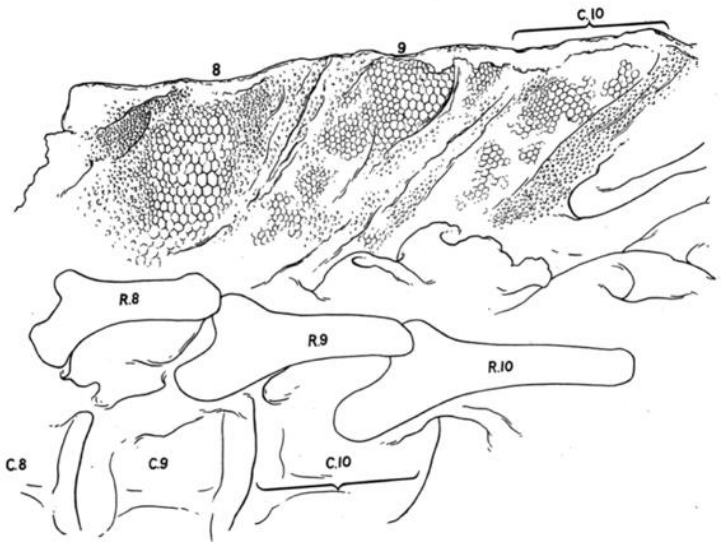

Fig. S6. Drawing of the neck crest. Neck crest in left lateral view from an early adult mummy of *Edmontosaurus annectens* (AMNH FARB 5060; from Osborn, 1912: fig. 5a) (*1*).

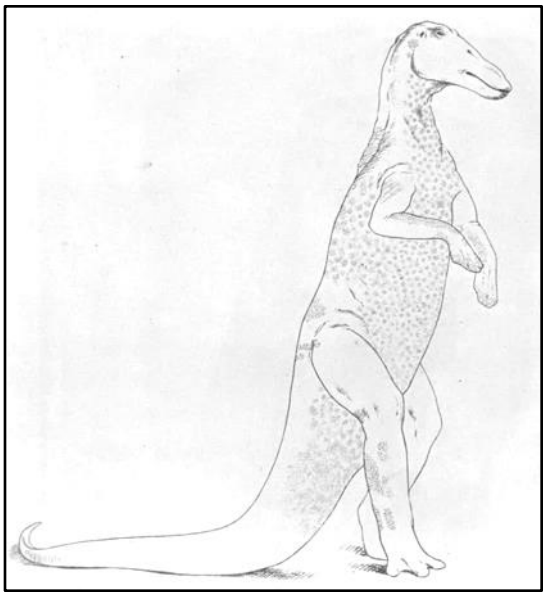

Fig. S7. Preserved skin areas. Drawing showing the preserved areas of integument renderings in an early adult mummy of *Edmontosaurus annectens* (AMNH FARB 5060; from Osborn, 1912: fig. 3) (*1*).

Fig. S8. First restoration based on a dinosaur mummy. Life restoration by early paleoartist Charles R. Knight of *Edmontosaurus annectens* (AMNH FARB 5060) showing a midline crest over the neck, trunk and hips (from Osborn, 1912: fig. 13) (*1*).

A few years later, Brown (*91*) reported on the integument renderings of a well-preserved skeleton of *Corythosaurus casuarius* (AMNH FARB 5240), observing a "median fold of skin" extending over the trunk, hips and tail and "presumably above the neck and skull" as well (Brown,

1916: 713). Lull and Wright (*9*) remarked that the crest is deepest over the hips and anterior tail (~12 cm; Lull and Wright, 1942: 115), although the deepest part of the crest is shown by Brown over the trunk (fig. S9). Because the crest was poorly preserved, Brown did not document details of scalation or its margin. Thus, some scaly skin is present immediately above some the neural spines of *C. casuarius,* but the form of a median crest in *C. casuarius* remains speculative.

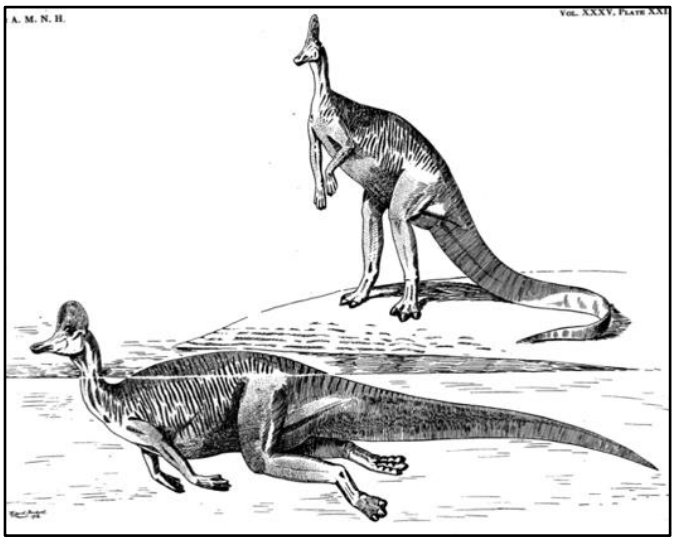

Fig. S9. Flesh rendering of lambeosaurine hadrosaurid. Life restoration of *Corythosaurus casuarius* based on an adult skeleton (AMNH FARB 5240) showing a continuous midline crest over the neck, trunk, hips and tail (from Brown, 1916: pl. 21) (*91*).

Lull and Wright (*9*) followed Osborn (*1*) and Brown (*91*) (fig. S6). They mentioned the neck crest section in AMNH FARB 5060 but also positioned it over the anterior trunk above the scapula (fig. S10). They mapped as preserved more posterior sections of a midline crest over the trunk, hips and tail, citing specimens that do not preserve a midline crest (*Gryposaurus notabilis* [*Kritosaurus incurvimanus*] and "*Claosaurus*" unnumbered). The identify the taxon showing a crest as *Gryposaurus notabilis* (ROM 764), which preserves only a pair of spikes over the hips (*10*, *17*) (fig. 34.3B). These spikes, in fact, document the first median spike-shaped fleshy ornamentation discovered in any hadrosaurid. Lull and Wright (*9*) noted this fact and figured the best-preserved spike, but then depicted a solid crest over the neck, trunk, hips and tail in their composite hadrosaur figure (fig. S10).

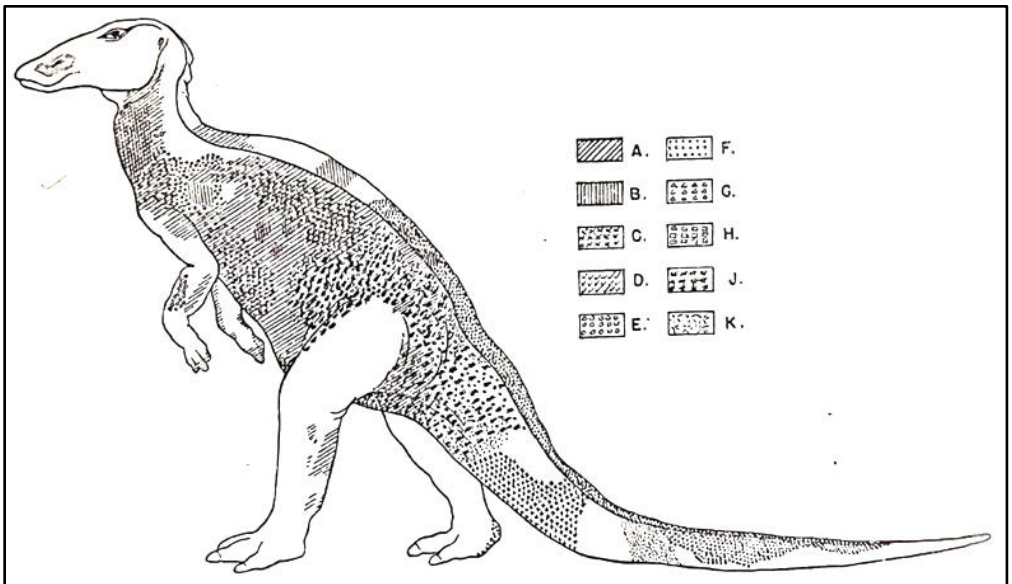

FIGURE 26. *Areas of integument preserved*

Restoration after Knight. (A) *Anatosaurus annectens* No. 5060 A.M.N.H.; (B) *Kritosaurus incurvimanus* No. 4514 R.O.M.P.; (C) "*Trachodon*" sp. No. 5894 A.M.N.H.; (D) *Anatosaurus edmontoni* No. 8399 G.S.C.; (E) *Corythosaurus casuarius* No. 5240 A.M.N.H.; (F) "*Claosaurus*" C.M.; (G) *Kritosaurus notabilis* No. 2278 G.S.C.; (H) *Corythosaurus excavatus* No. 8676 G.S.C.; (J) *Lambeosaurus clavinitialis* No. 8703 G.S.C.; (K) *Kritosaurus marginatus* No. 419 G.S.C.

Fig. S10. Integument composite. Map of preserved hadrosaurid integument and midline crest over neck, trunk, hips and tail on a flesh rendering of *Edmontosaurus* (*Anatosaurus*) *annectens* (from Lull and Wright, 1942: fig. 6) (*9*).

6.2 Midline spikes discovered in *E. annectens*

Some 70 years after discovery of the cervical crest, Horner (*11*) described a meter-long section from the middle of the tail of *Edmontosaurus annectens* showing a series of midline spikes (fig. S11). The specimen was collected by others who may have inadvertently prepared away some of the margins of the integumental structures. The spikes are shown as subrectangular in shape and separated by gaps, although in some places they seen to abut or overlap. The spikes appear to be in natural position proximally, with each neural spine projecting into the posterior end of an associated spike. More distally, the spike row appears to have drifted away from their respective neural spines (fig. S11).

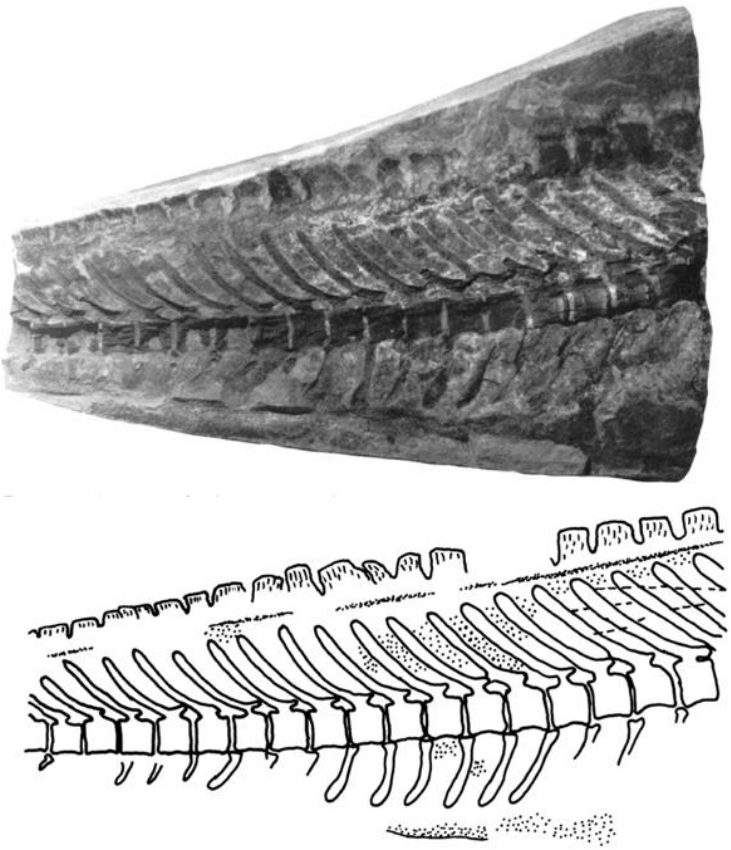

Fig. S11. Mid tail section. Photo and drawing (from Horner, 1984: figs. 1, 2) (*11*) of an articulated section from the middle of the tail of *Edmontosaurus annectens* (originally catalogued as MOR V 007 but now with the rest of the skeleton in the Naturmuseum St. Gallen in eastern Switzerland (NMSG P 0001), except for the negative counterpart of the mid tail section, which is in The Dinosaur Museum in Blanding, Utah. See section 2.1 for museum collection acronyms.

Nonetheless, the segmental arrangement of spikes was apparent to Horner (*11*), who also described a surface texture of vertical striations. He speculated in conclusion that the "segmented frill" likely extended to "the base of the tail, up over the sacral region and possibly to the cervical region" (Horner, 1984: 271). Horner, thus, transformed Osborn's median crest into a segmented row of spikes extending from the neck to the tip of the tail. Campione (*8*) reconstructed *E. regalis* in this fashion with spaced, subrectangular spikes in segmental relationship with underlying vertebrae throughout the length of the vertebral column (Campione, 1915: fig. 13.1).

A recently discovered mummy of *E.* cf. *annectens* from North Dakota (*12*) preserves approximately two dozen spikes in the mid caudal region that touch each other, some appearing to interdigitate (Fig. S12). The relationship of the spikes to underlying vertebrae, however, is not documented, and we have not personally examined this specimen. The apex of several of the spikes may have been truncated to give the appearance of a more subrectangular, as opposed to an arcuate or subtriangular, shape. The spikes have posterodorsally inclined lineations and seem very close in form and position to those in the new early adult mummy from Wyoming (Figs. 2, 3; UCRC PV30).

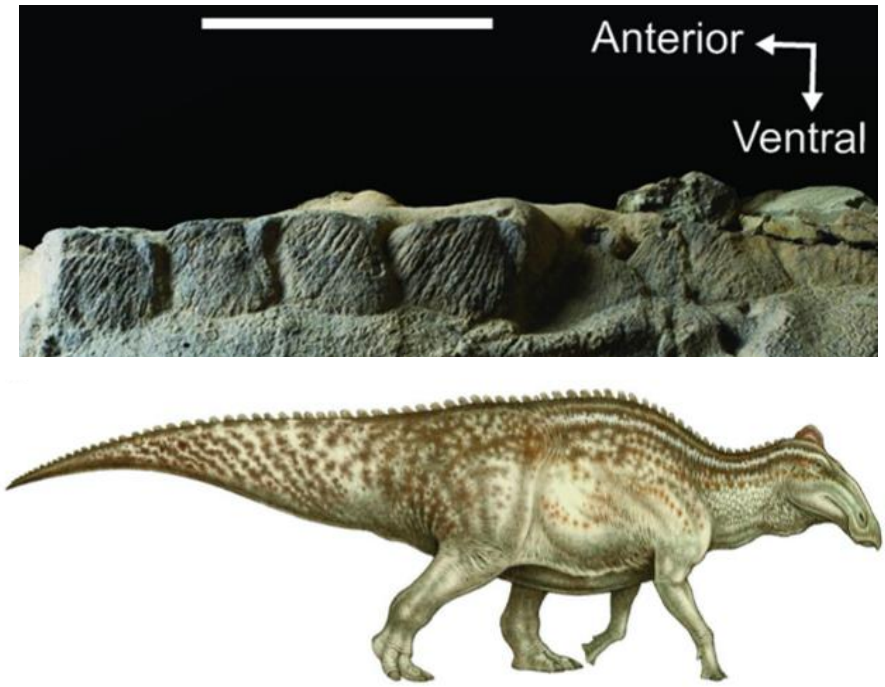

Fig. S12. Tail spikes. Mid-caudal spike row (top) from an adult mummy of *Edmontosaurus* cf. *annectens* (NDGS 2000) and life restoration showing a midline row of spikes over the neck, trunk, hips and tail (from Drumheller et al., 2022: figs. 2A, 8B) (*12*). See section 2.1 for museum collection acronyms.

Their reconstruction (*12*) shows separate, subrectangular or trapezoidal spikes that are fewer in number than the underlying vertebrae and that extend over the entire vertebral column (fig. S12). We have not found clear evidence for spikes anterior to the hips. For the middle one-half of the tail, which is preserved in NDGS 2000, their restoration shows 16 spaced spikes over approximately 30 to 45 caudal vertebrae, or about one spike for every 2 or 3 vertebrae. This restoration does not appear to reflect the best preserved tail sections for this species, which show interdigitating spikes positioned in one-to-one relationship dorsal to caudal neural spines.

6.3 Midline spikes discovered in other hadrosaurines

Bell (*14*) described spikes in three specimens of *Saurolophus angustirostris* from Mongolia, showing separate subrectangular structures bearing vertical striations (fig. S13). He noted the relationship between some neural spines and spikes but remarked that "individual scales do not correspond perfectly with the tip of each neural spine" (*14*). Their segmental relationship, nonetheless, is clear, given the same number of spikes and vertebrae below (Bell, 2012: fig. 3C, D). Preservation also may have damaged the shape and interrelationships of the spikes. One tail section shows the broken bases of spikes with intervening space; another tail section with matrix backing the spikes shows them in contact with each other (although drawn as separate) (Bell, 2012: fig. 3C, D). Bell (2014: fig. 34.6; UALVP 52824) provided a field photograph of an additional tail section, in which a poorly preserved spike row is displaced at some distance from the ends of the neural spines. They are drawn as spaced, subrectangular spikes, although this is less clearly shown in the accompanying photograph (*17*).

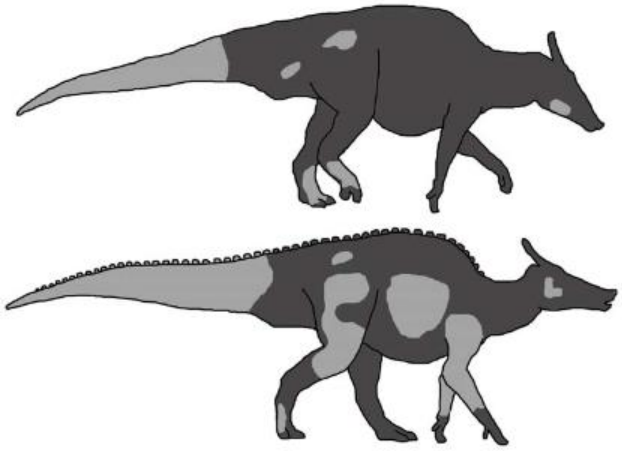

Fig. S13. Midline spikes in the hadrosaurid *Saurolophus*. Life restoration of *Saurolophis osborni* (top) and *Saurolophus angustirostris* from specimens preserving skin renderings (from Bell, 2012: fig. 12) (*14*).

In restorations of *Saurolophus*, Bell (*14*) depicted one species (*S. osborni*) with a smooth body profile, although the integument in the midline of this species was not preserved, and another species (*S. angustirostris*) with separate spikes of relatively uniform height over the trunk and tail (fig. S13). Again, there is no evidence of spikes in any hadrosaurid over the trunk. Over the tail approximately 30 spikes are reconstructed over more than twice that many vertebrae below. In sum, the spike row as it is known in *S. angustirostris,* may be similar to that in *E. annectens* in having a segmental relationship with underlying caudal vertebrae. Whether the spikes are separate or interdigitating is less clear.

Bell (*14*) and Bertozzo et al. (*16*) commented on the well-preserved spike discovered *in situ* over the hips (possibly over the third sacral vertebra) in *Gryposaurus notabilis* (*10*) (fig. S14). A gap separates a second spike of lower proportions located more anteriorly (possibly over the first sacral vertebra). Their precise position relative to neural spines below is uncertain. These spikes are trapezoidal, low in profile (height ~40% length), and have their apex displaced posteriorly (*10*, *14*). Unlike the spikes in *E. annectens*, those in *G. notabilis* do not appear to have a thin perimeter flange. On an inset diagram, Bell (*14*) indicated the preservation of midline spikes over the mid trunk as well, but no spikes have ever been described over presacral vertebrae in any hadrosaurid. The small-sized feature scales Bell highlighted were described by Parks (*10*) in a patch of integument on the side of the trunk.

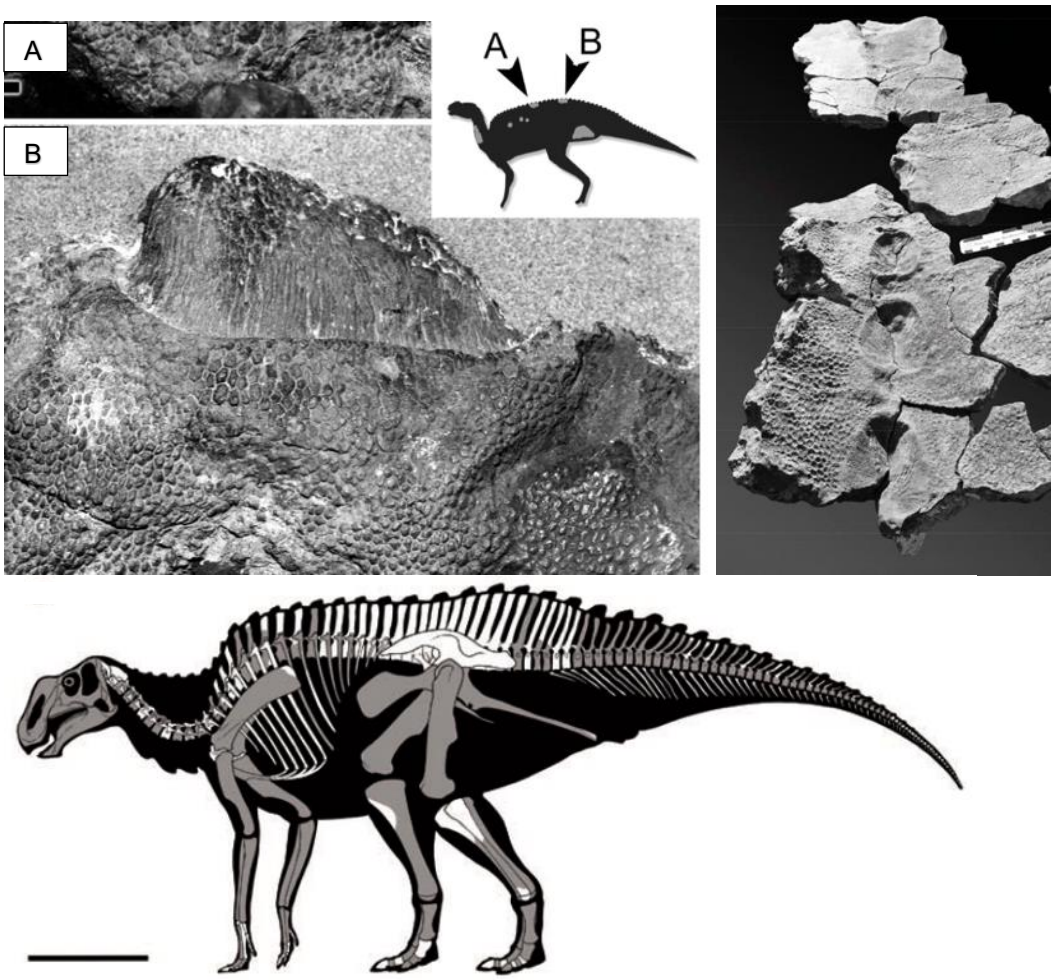

Fig. S14. Midline spikes in *Gryposaurus*. Mid sacral spike (top left; from Bell, 2014: fig. 34.3), and silhouette life restoration (bottom; from Bertozzo et al., 2017: fig. 6) (*16*) based on *Gryposaurus notabilis* (ROM 764). Molds of tail integument for *Gryposaurus* sp. (top right; from Clayton et al., 2011: fig. 2; UMNH VP12265) (*13*). See section 2.1 for museum collection acronyms.

Bertozzo et al. (*16*) reconstructed *G. notabilis* with a spaced spike row, with one spike over every two or three vertebrae. The spike row was shown extending from the head to the tip of the tail, although again, no presacral spikes have been discovered. Another specimen referred to *Gryposaurus* (*13*) preserves an integument mold from the base of the tail that shows a line of separate, wedge-shaped spikes with oval bases that appear to ornament the midline of the tail (fig. S14, upper right). This specimen seems to confirm unequivocally that some hadrosaurs do not have a segmental relationship between spikes and underlying vertebrae. In sum, the midline tail spikes in *Gryposaurus* are spaced and number fewer than underlying vertebrae, based on integument evidence from two specimens.

6.4 Cranial comb discovered in *E. regalis*

In 2014 Bell et al. (*17*) described a fleshy cranial comb over the posterior skull table and occiput in a late adult of *Edmontosaurus regalis*. The large arcuate display crest was apparently composed of soft tissues that left no internal structure. Scaly skin rather than keratin appears to have covered

its surface (*18*) (fig. S15). The comb is longer (~33 cm) than tall (~20 cm) and swells to a width of approximately 7 cm. The adjacent skin area shows excellent three-dimensionality, preserving raised areas of larger scales separated by finely scaled grooves.

Fig. S15. Cranial comb in *Edmontosaurus*. Flesh reconstruction of the head and neck of a late adult *Edmontosaurus regalis* based on UALVP 53722 (from Bell et al., 2014: fig. 4) (*17*). See section 2.1 for museum collection acronyms.

Given the position of the centra of the articulated cervical column on the block, the neck of *E. regalis* could not have borne the narrow, tall, banded midline crest present in *E. annectens* (*1*). The authors remarked that there are no midline feature scales present. This is true, but none have been found either in the presacral midline of other hadrosaurids. The significance of the neck skin is that it demonstrates dramatic variation from that observed in *E. annectens*. Not only does *E. annectens* have a thin neck crest immediately above the cervical neural arches, the finer scaled integument on the side of the neck is extremely thin, as shown by shape-edged wrinkling. There are no raised areas of scales as seen in *E. regalis*. Adding a similar soft comb to a flesh reconstruction of *E. annectens* is uncertain. The comb is positioned so far posteriorly over the occiput in *E. regalis* that it likely would join the neck crest if present in *E. annectens* (Fig. 3E).

6.5 Forefoot hoof in *E. annectens*

Osborn (*1*) described the digitigrade manus of *E. annectens* as covered in scaly skin with manual digits III and IV incorporated into a single mitten-like structure (fig. S16). A recently discovered mummy of *E. annectens* (*12*) with excellent preservation of the manus suggests that there was a keratinous sheath encasing the spade-shaped ungual on digit III (fig. S16). Both specimens suggest that that the sheath turned onto the ventral side of the phalanx, creating a flattened ventral surface for contact with the substrate. Although more study and evaluation of CT scans are needed, the evidence suggests that the ungual phalanx of manual digit III alone was capped by a hoof with a crescentic ventral surface. The digitigrade manus was held vertically, with its distal end leaving crescentic footprints in soft sediment.

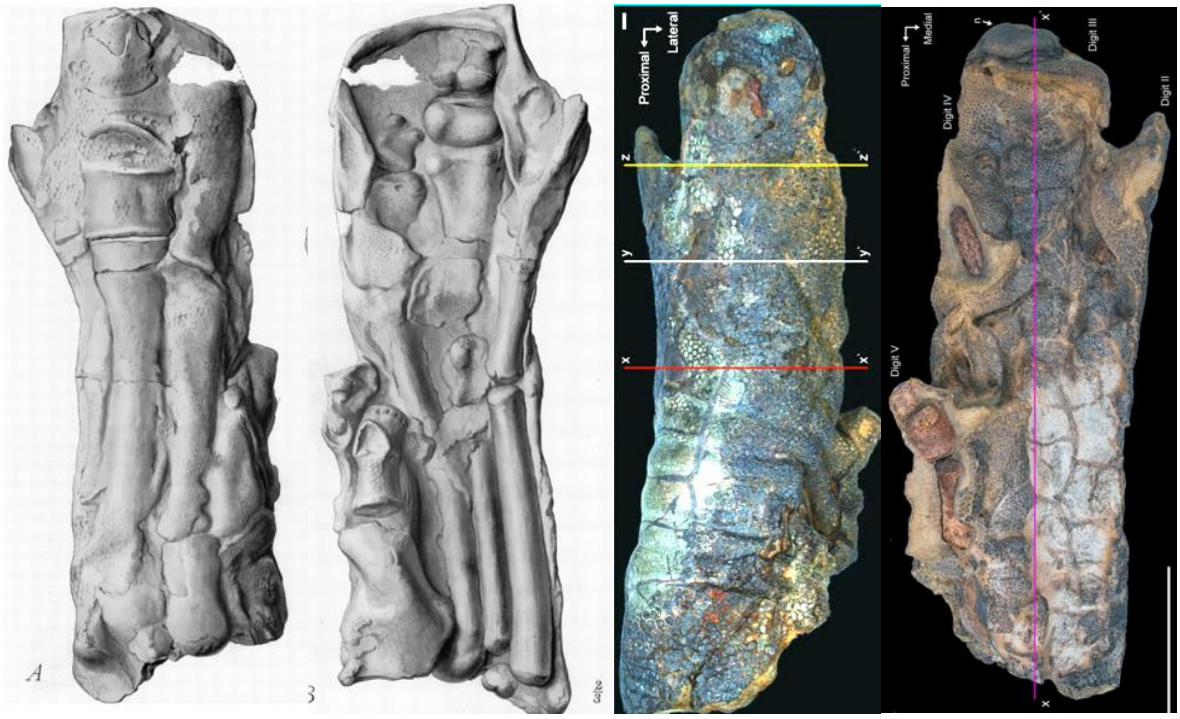

Fig. S16. The manus of *E. annectens*. Right manus (left pair) in dorsal and ventral views (from Osborn, 1912: pl. 8; AMNH FARB 5060) (*1*). Right manus (right pair) in dorsal and ventral views (from Drumheller et al., 2022: figs. 3E, 4B; NDGS 2000) (*12*). See section 2.1 for museum collection acronyms.

6.6 Hindfoot hooves in *E. annectens* and mammalian analogs

We define "hoof" as a "wedge-shaped, flat-bottomed, keratinous sheath surrounding the terminal ungual of a terrestrial non-carnivore" (table S2). The sheath and underlying ungual have a blunt or arcuate distal margin (half-arc if paraxonic), and the foot has a subunguligrade or unguligrade posture that enhances ungual ground support. Hooves, so defined, have evolved multiple times in mammals outside of the two traditional ungulate clades, Perissodactyla and Artiodactyla, including extant elephants[32,33] and the singular case among marsupials in the recently extinct pig-footed bandicoot.

The most appropriate modern analogs to the hooved condition of the hindfoot observed in *E. annectens* are among mesaxonic perissodactyls (*25*, *26*), especially among ceratomorphs (rhinos and tapirs) (fig. S17). Tapirs have three-toed, subunguligrade hindfeet with hooves, digital pads and a heel of similar form. Tapir footprints, consequently, bear a remarkable resemblance to high-fidelity footprints attributed to an end-Cretaceous duck-billed (*21*) (Fig. 3B).

Fig. S17. The hind feet of hooved mammals. Hindfoot (upper left) of a horse (*Equus equus*; from Parks, 2017, fig. 3.17) (*25*). Forefoot of an African elephant (*Loxodonta africanus*). Hindfoot (bottom row) skeleton, hooves, footpads and footprint of tapirs (feet, *Tapirus indicus* feet; footprint, *Tapirus terrestris*).

Mesonychids (*92*, *93*) and early whales (*94*) are transitional forms evolving toward or away from a hooved condition, respectively. Hooved taxa among mammals and nonavian dinosaurs, in contrast, are exclusively herbivores at moderate to large body size with subunguligrade or unguligrade foot posture.

Mesonychids are an extinct clade of mammals of moderate to large body size that are thought to be omnivores, scavengers or bone-crushers, rather than carnivores, because their dentition did not have the carnassials of carnivorans, their spreading metapodials and limb proportions do not suggest great speed, and their feet lacked claws (fig. S18, left). Some have called the unguals of mesonychid hooves, but they are not wedge-shaped, and their external margin is not arcuate (fig. S18, second from left). Thus, mesonychids cannot be considered pursuit carnivores nor did they evolve hooves as here defined, even though some have characterized them as "wolves on hooves." One of the best-known genera, *Pachyaena*, has spreading metapodials and a digitigrade pes. In contrast, hooves have flat bottoms to accommodate the transfer of mass in a subunguligrade or unguligrade foot.

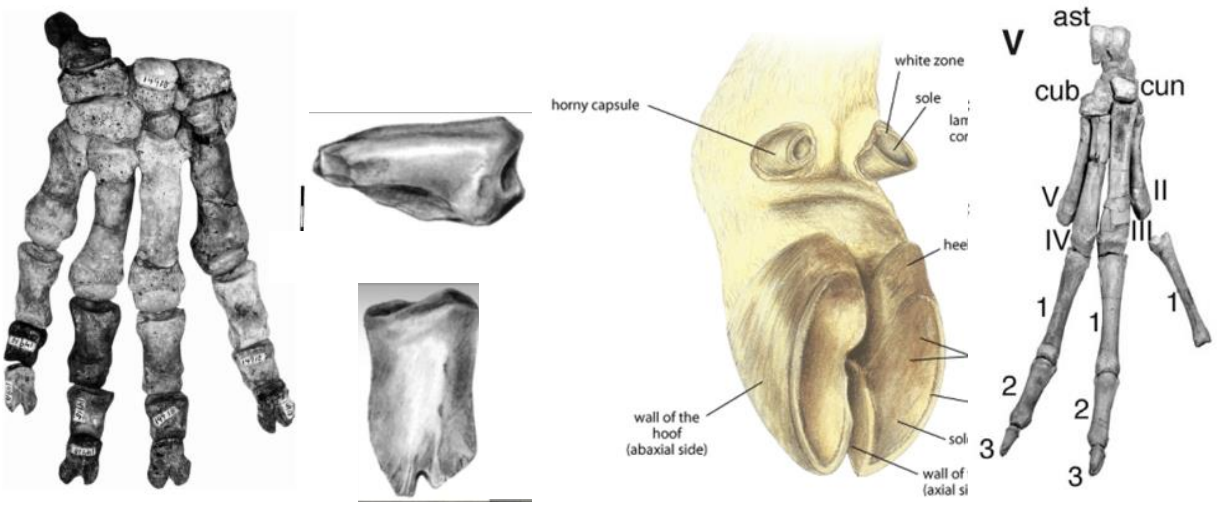

Fig. S18. Evolution and reduction of hooves in therian mammals. Right manus (upper left, dorsal view) and manual ungual (second from left, lateral and dorsal views) of the mesonychid *Pachyaena gigantea* (from Rose and O'Leary, 1995, fig. 1) (*92*). Typical artiodactyl pes (second from right, ventrolateral view) and the right hindfoot (right, dorsal view) of the basal cetacean *Peregocetus pacificus* (from Lambert et al., 2019) (*95*).

Typical artiodactyl fore and hindfeet are paraxonic, unguligrade in posture, and characterized by a par of opposed, crescentic hooves (Fig. S18, second from right). Cetaceans are now widely understood as having originated within the artiodactyl radiation and are usually positioned near hippos or suids (*32*). Some early whales, such as *Peregocetus* (*95*), retain the bound metapodials of their artiodactyl forebears, although the pes appears to have reverted to a digitigrade posture with short, claw-shaped terminal phalanges (fig. S18, right). In the transition to a carnivorous semiaquatic lifestyle, thus, early whales evolved a carnivorous dentition and abandoned the upright, hooved form of the manus and pes common to early artiodactyls.

7. Midline spikes in squamates

7.1 Common non-segmental condition

The location of midline spikes in squamates is most commonly over the posterior portion of the skull and trunk. Midline spikes in only a few squamate species continue to the distal end of the tail, which often has less or muted ornamentation to accommodate flexibility. Squamate spikes are narrow, vertical structures that are positioned in sequence usually without mutual contact. Relative to the underlying vertebral column, squamate spikes tend to be elevated above the neural spines by fleshy axial tissue, and they are typically more numerous in number than underlying vertebrae (Fig. 2C). The common squamate condition for epidermal midline spikes, thus, seems to entail no relation to patterning of the underlying axial column.

7.2 Rare segmental condition

Rarely among squamates, a one-to-one relationship occurs between epidermal midline spikes and the neural spines of the underlying axial column. We show this condition in the trunk of a specimen of Jackson's chameleon *Trioceros*, in which a single neural spine inserts into the base of a single epidermal spike (fig. S19, above). A one-to-one relationship between neural spines and spikes also

appears to obtain in the tail of the basal lepidosaurian, the tuatara *Sphenodon* (*96*) (fig. S19 below). The more proximal midline spikes extending from the cranium to the tail show the more common elevated pattern and greater number than underlying vertebrae.

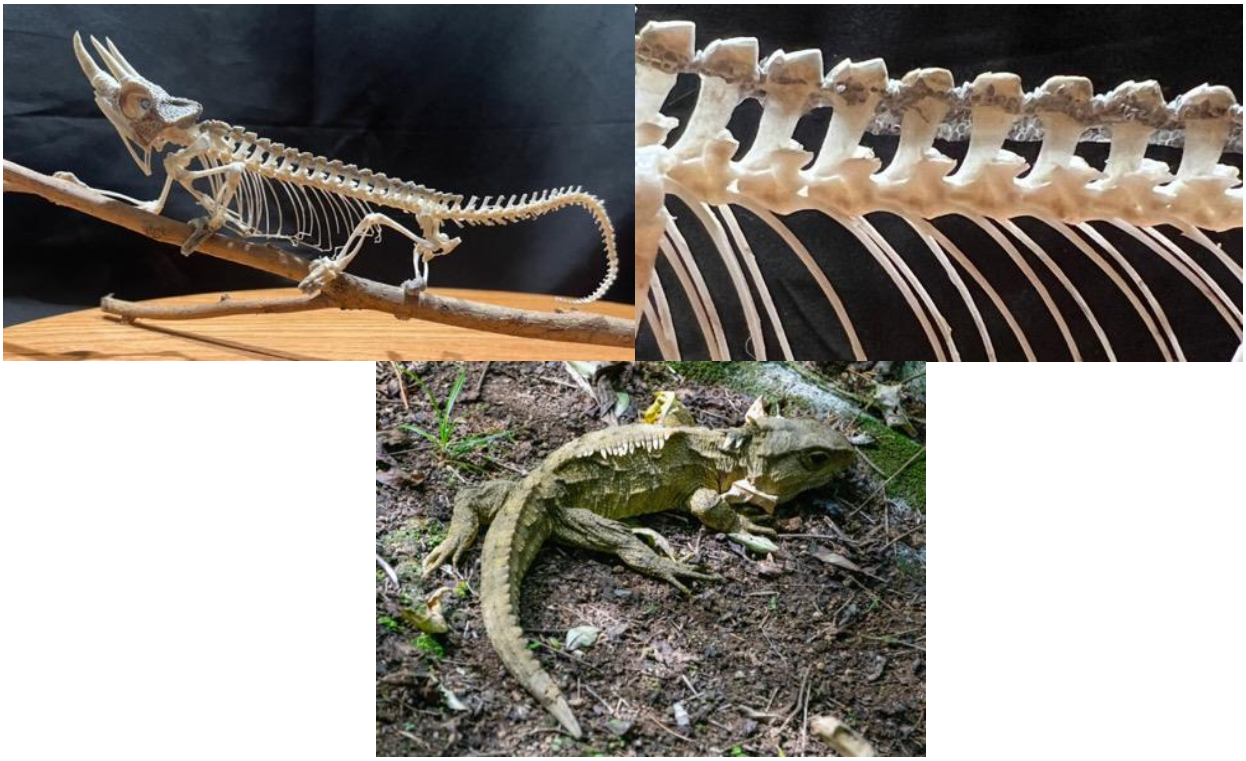

Fig. S19. Segmental midline spikes in chameleons and tuatara. Prepared specimen of *Trioceros jacksonii* (male, UCRC RV78) showing the midline spikes in contact with the neural spines of underlying trunk vertebrae (upper right and left). *Sphenodon punctatus* showing the correspondence of tail spikes with underlying vertebrae (lower).

These examples suggest that in some cases *Hox* gene patterning of the axial column (*97*, *98*) can couple with epidermal patterning of the overlying integument, which in reptiles may be governed by gene clusters (*99*). In *Edmontosaurus annectens* segmental patterning of the midline integument can be seen in the scalation of neck and trunk crest and the positioning of tail spikes. We have observed midline spike interdigitation only in one squamate genus (*Gonocephalus,* angle-headed lizard). These patterns may be species specific. Other hadrosaurines do not appear to have segmental, interdigitating tail spikes. Heightened midline integument structures are not present in the ceratopsians *Psittacosaurus* (*100*) or *Triceratops* (*5*), nor are the ossified scutes or spikes of thyreophorans arranged in correspondence with the axial column (*101*).

8. Sediment analysis

8.1 Spike template composition

Energy dispersive X-ray spectroscopy (EDS) allows spatial mapping of elemental composition of samples at microscopic and ultrascopic scales, when obtained in conjunction with structural information from backscatter electron microscopy (BSE) (Fig. 4C, figs, S20, S21). We obtained data using both methods from a thin section (30 microns thick) of the tail spike from the early adult

mummy (UCRC PV30) (table S10). The section analyzed comes from the posterior end of the section series that includes the median insertion of the anterior end of the posteriormost spike sampled. The clay template renders the surface of the integument is thin, measuring less than 1 mm in thickness (Fig. 4).

Table S11. Laboratory techniques used in visualization and sediment analysis. Summary of methods, laboratories, information sought, and dinosaur mummy specimens examined in the analysis of integument renderings in late juvenile and early adult mummies of *E. annectens*. Abbreviations: UC, University of Chicago; UCRC, University of Chicago Research Collection; UIUC, University of Illinois Urbana-Champaign.

No.	Method	Lab Location	Information Sought	Specimen Involved
1	Stereophotogrammetry (SPG)	UC	Macrostructure, coloration	UCRC PV30 UCRC PV31
2	Light microscopy (LM) (digital, optical, & polarized)	UC	Microstructure, birefringence	UCRC PV30 UCRC PV31
3	Clinical & micro-computed tomography (CT)	UC	Internal structure, electron density	UCRC PV30
4	Back-scattered electron microscopy (BSE)	UC	Ultrastructure, elemental composition, localization	UCRC PV30 UCRC PV31
5	Energy-dispersive X-ray spectroscopy (EDS)	UC	Ultrastructure, elemental composition, localization	UCRC PV30 UCRC PV31
6	X-ray diffraction (XRD)	UIUC	Phase composition	UCRC PV30

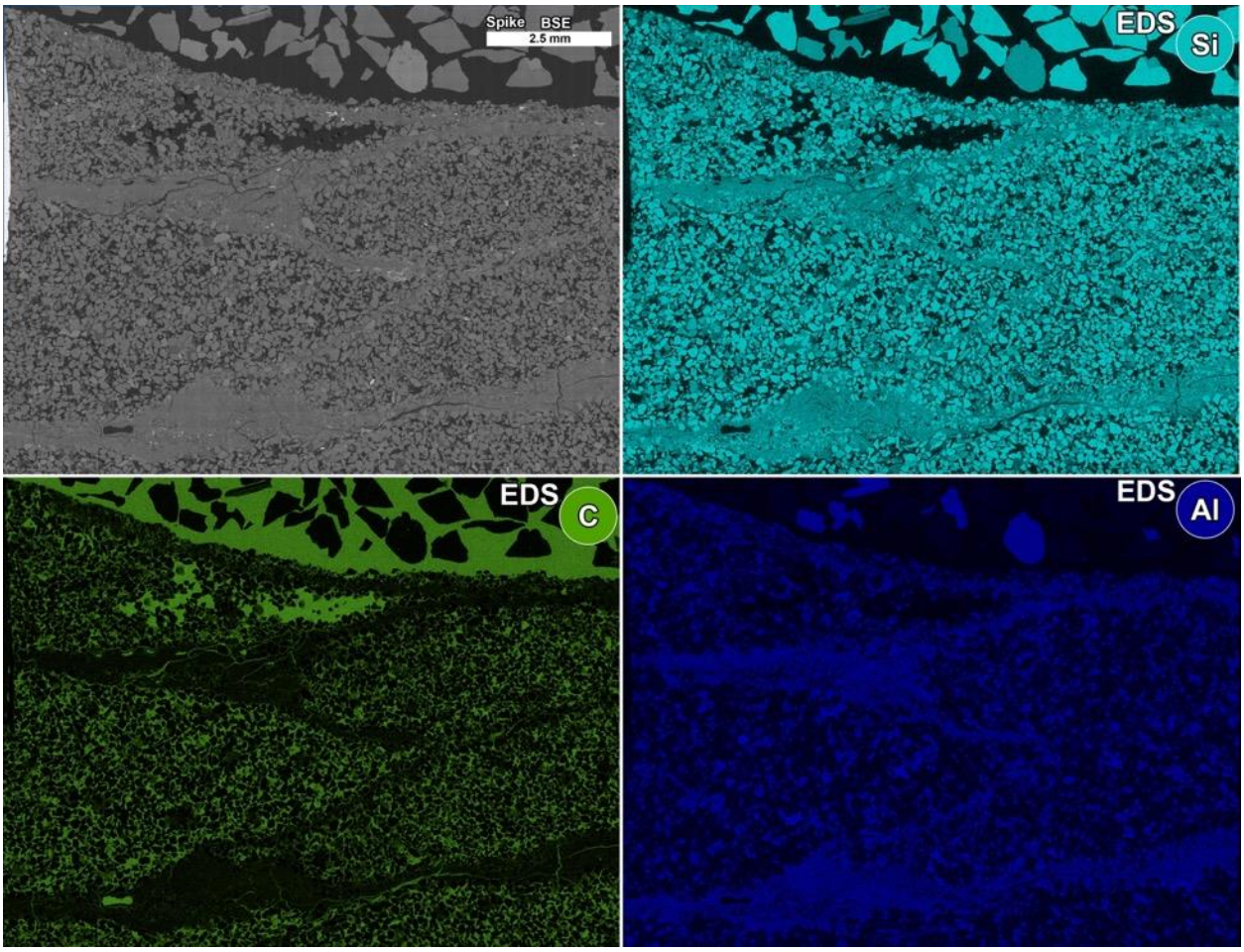

Fig. S20. Enlarged view of BSE and key EDS maps from the thin section of the tail spike from the early adult mummy (UCRC PV30). BSE shows that the material comprising the fossil skin is an extremely thin, external template, while the matrix consists of porous, uncemented sand (top left). Al and Si are present in both the template clay layer (top right, bottom right) and most of the internal and external sand grains in the matrix (e.g., Si is present in quartz; Al and Si are present in feldspars; Al and Si are absent in carbonates). C is present in void spaces and between sediment grains from embedding material. Al and Si are present in both the template layer, which constitutes the fossil skin, and most of the surrounding sand grains in the matrix (e.g., Si present in quartz, Al and Si present in feldspars, and neither Al nor Si present in carbonates). C localizes to the void spaces between sediment grains. Images oriented with dorsal to the right, ventral to the left, and lateral at the top (the prepared surface).

Organics: The clay template is clearly depleted in C (fig. S20), the C signal derived mainly comes from the embedding epoxy in the UCRC PV30 spike thin section. The clay is less porous than the sand (smaller grain size) with less epoxy resin infiltration, except for cracks crossing the clay template. Low C content suggests that organics from the original tissues are not preserved. The lack of elemental evidence for C in the new mummies contrasts with two previous reports on hadrosaurid specimens with preserved integument renderings.

Manning et al. (*39*) and Fabbri et al. (*41*) concluded from other duck-billed specimens with integument renderings that some original or highly altered proteinaceous material, respectively, were preserved, along with evidence of original histological structure. Manning et al. (*39*) reported

on a duck-billed mummy [NDGS 2000; (*12*)] from the laterally equivalent Hell Creek Formation in North Dakota (table S4, number 6) pertaining to the same genus (*Edmontosaurus*) and quite possibly the same species (*E. annectens*) as our two Lancian mummies (UCRC PV30, 31). They inferred from their array of tests that proteinaceous material was potentially present (*39*), which if verified would constitute direct preservation of soft tissue components (*12*).

The sediment within NDGS 2000 and the composition of the external layer preserving the integument renderings have yet to be specifically characterized to enable directly comparison to our results. The available CT scan of the manus (*12*) looks similar to scans of the UCRC PV30 and UCRC PV31, showing areas of apparent tissue deflation, where wrinkled, scaly integument renderings lie immediately adjacent to underlying fossilized bone, as well as a thin radiopaque external layer preserving the rendered integument surface. We look forward to additional information to be able to more fully compare our results with this particular duck-billed mummy regarding its taphonomy, internal versus external sediment composition, and the thickness and composition of the external layer preserving the integument renderings.

Fabbri et al. (*41*) used petrographic thin sectioning, followed by SEM, EDS, and Raman spectroscopy to report the preservation of melanosomes as well as blood vessels and dermal cells in a small patch (~6 cm^2) of integument rendering associated with several hadrosaurid bones (cf. Saurolophinae) found in an older (Campanian) finer-grained marine sediment (Bearpaw Shale Formation). This specimen is not comparable in skeletal or integument integrity, area of integument renderings preserved, or in the terrestrial setting of other duck-billed mummies (table S4), but its taphonomy is worthy of further comparison in future work.

Silicates: The Si and O in the clay template is similar to that in the surrounding sand matrix in the UCRC PV30 spike thin section, suggesting that the clay template also has a silicate composition (fig. S20). Al is also present in the clay template (fig. S20), confirming its aluminosilicate composition. Unlike the larger sand grains, the clay grains are not discernable at this scale. Further evidence consistent with clay identification for the template is provided by enriched Na, Mg, K, and Ca (fig. S21), cations commonly associated with aluminosilicate clay.

Dark stains on the integument renderings of UCRC PV30: With no evidence of organics other than the embedding epoxy resin, dark-staining substances are likely inorganic. The presence of Fe in some regions of the template (fig. S21) possibly explains the sporadic dark staining present on some regions of the skin of the adult mummy (UCRC PV30) (e.g., decay-associated iron sulfides and/or weathering-derived iron oxides). Additionally, the entirety of the observed UCRC PV30 spike thin section in EDS, including the skin template, is low in S (fig. S21). Firstly, the absence of S in combination with the absence of C is further evidence against the hypothesis that this fossil skin is preserved organic “keratin” (corneous beta-proteins), which would be rich in the S-bearing amino acid cysteine or other organosulfur compounds. This tail spike did not show much dark surficial staining from ironstones compared to that present at the tip of the tail (fig. S22A) or to specimens such as the Hell Creek duck-billed mummy (NDGS 2000) (*12*). Pyrite can readily oxidize in curatorial conditions, and the Fe detected in this thin section is more likely to derive from iron oxides than from iron sulfides.

Lack of phosphatization/calcification: The entire UCRC PV30 spike thin section, including the template, is also largely lacking in P (fig. S21), except for a few larger grains (e.g., likely P-feldspar sand grains in the matrix). The paucity of P is inconsistent with the fossil skin preserving

predominantly via authigenic and/or endogenous calcium phosphate, as is many times the case for fossil skin in Konservat-Lagerstätten such the Jehol Biota (*102*). Ca is present in the template layer (fig. S21). Rather than the fossil skin being a direct replacement of a thick histological layer, it appears to be an externally deposited template in that it is a thin layer, which collapsed at internal void spaces where sand is lacking but contains excess material at external void spaces. As such, this detected Ca more likely represents cations associated with clays, rather than Ca associated with calcified "keratin" (corneous beta-proteins) (*103*, *104*).

Clay mineral composition of the template: X-ray diffraction (XRD) semi-quantitative results were obtained from a flake (~15 mm major axis) from the posterior end of a different tail spike on the adult mummy (UCRC PV30), with minimal amounts of adhering matrix due to manual sampling. This spike fragment was fractionated to select clay-sized grains (< 2 micron) at the University of Illinois Urbana-Champaign Illinois State Geological Survey XRD Laboratory. By suspending this clay powder fraction in ethylene glycol, the clay particles can be consistently oriented to give much improved XRD results. The clay species detected, in decreasing semi-quantitative percent weight, were: 54% kaolinite, 37% illite, 6% chlorite, and 3% smectite. As such the clay template of this tail spike can be said to be predominantly kaolinite, with secondary amounts of illite, using our most reliable method of clay identification.

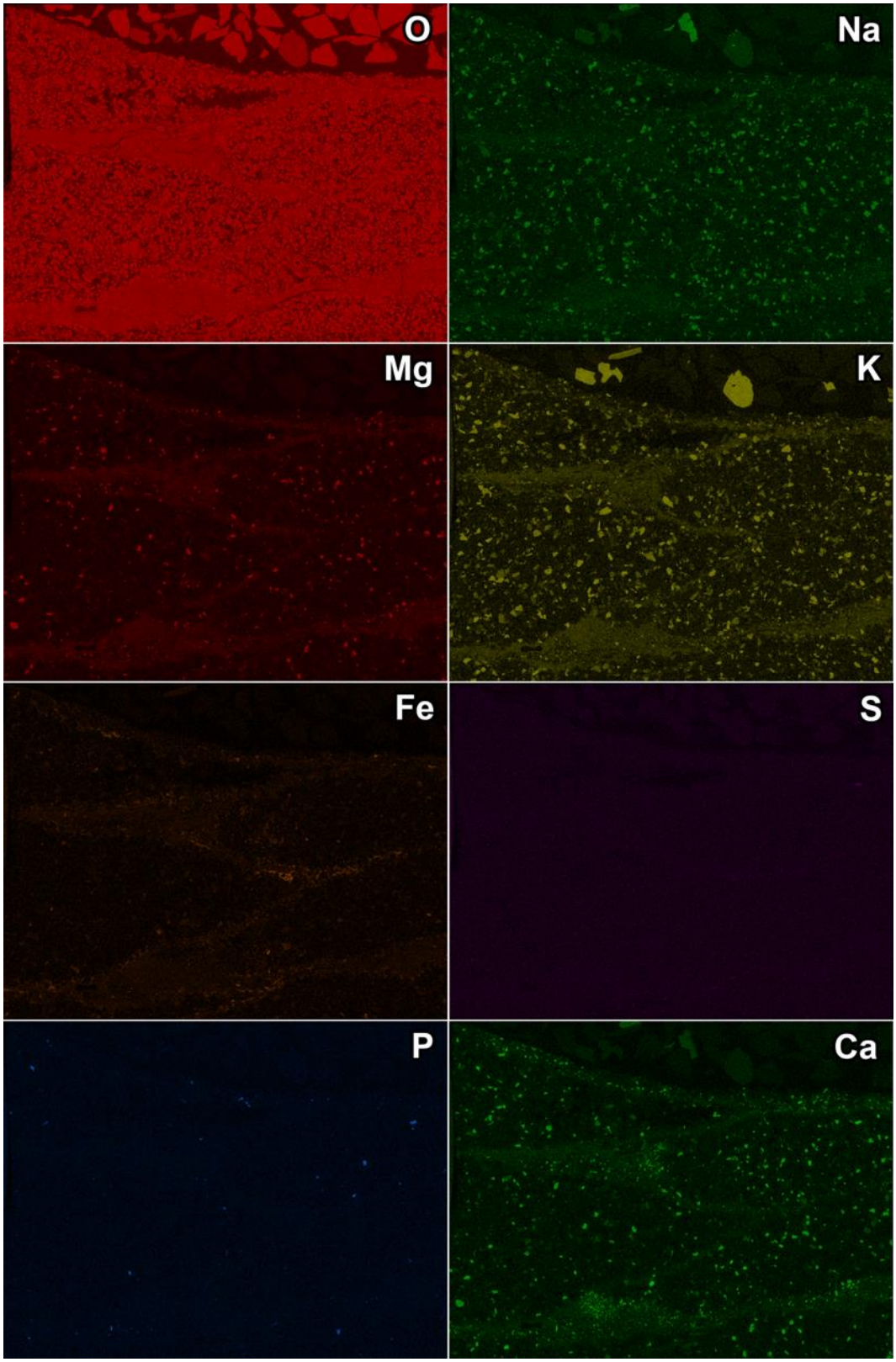

Fig. S21. EDS maps for O, Na, Mg, K, Fe, S, P, Ca of the tail spike thin section from the early adult mummy (UCRC PV30). Images oriented as they are in the specimen: dorsal orientation is to the right, ventral to the left, and the lateral surface at the top is the prepared surface. Large

silicate grains in the external epoxy were added during the embedding process to improve thin sectioning (cropped out in Fig. 4C). Scale as in figs. 4C, fig. S20.

8.2 Sediment matrix characterization

As seen in the BSE and EDS images above (figs. S20, S21), the internal and external sand grains are very similar size, shape, and composition, and both are lacking in cementation. Additionally, a thin section (150-microns thick) from the anterior quarter of the sectioned tail spike of the adult mummy (UCRC PV30) was analyzed with XRD by aiming the X-ray beam at the center of the slide. In decreasing order by semi-quantitative percent weight, the 2.54 cm diameter circular region of sediment immediately external to the fossil layer on this thin section contains: 88% quartz, 4% P-feldspar, 3% illite, 2% K-feldspar, 2% kaolinite, 1% dolomite, 1% chlorite, and 0% smectite.

This data confirms that most of the matrix immediately external to the skin template is larger than clay-sized minerals, namely quartz with a lesser amount of feldspar (~6%) and dolomite, as also suggested by EDS (figs. S20, S21). Si-only grains are quartz, Si- and Al-bearing grains are feldspars (sometimes showing P or K in addition), and Ca- and Mg-bearing grains are dolomites. Secondly, illite and kaolinite are clay species in highest abundance, consistent with the results from the oriented-clay fraction XRD analysis for the tail spike. Although the thin section XRD analysis indicates more illite than kaolinite, external matrix rather than clay template is being analyzed by the X-ray beam. XRD of the thin section, in addition, is not as reliable as the oriented-clay fraction XRD. There is only a small percentage of illite and kaolinite in thin-section, which matrix differ only by 1%.

8.3 Accessory sedimentary features

The presence of heavier elements, such as Fe, precipitated alongside and atop the clay template of the skin is supported by the sporadic dark staining and especially the large ironstone concretion (fig. S22A) seen in the adult *E. annectens* mummy (UCRC PV30). Precipitation of pyrite, for example, is indeed common in other 'death mask' fossils whose soft tissues are preserved as templates (*105*, *106*), and this pyrite can later oxidize through weathering. A sample taken from the tail tip concretion supports such processes when examined with BSE and EDS, showing silicate sand grains suspended in a Fe-rich cement that contains detectable S (i.e., consistent with pyrite). The sand grains are not always in close contact, possibly suggesting that the cement formed prior to sediment compaction during early decay. S does not always co-localize with Fe, suggesting that some Fe is in the form of oxides, possibly weathered from the iron sulfides that formed during decay.

The sediments in which the carcass was buried were likely not organic-limited during decay, as evidenced by thin laminae of black fossil plant material found in close association to the early adult *E. annectens* mummy (UCRC PV30) (fig. S22B), such as beneath the foot and tail. BSE and EDS reveal that this material is indeed organic, demonstrating a strong C signal. Decaying microbes would not have been limited by a lack of organic material to metabolize. Given the sporadic nature of the dark staining and ironstone concretions, the environment was instead more likely to be sulfate limited. Plant fossils are also found in close association with the Senckenberg mummy (*4*) from the Wyoming "mummy zone.". Plant fossils not only give insight into the pore water chemistry during burial, they also are consistent with rapid burial that deposited debris alongside the carcass.

Finally, possible trace fossil burrows (fig. S22C), appearing as a caliche-like material containing sand grains, are observed close to the exterior side of the skin on the late juvenile

mummy (UCRC PV31). If these are indeed burrows formed soon after burial, they indicate a biologically active sediment or possibly even attraction of scavengers to the carcass. Other trace fossils have been proposed to be in close association with mummy hadrosaurs (*107*), but all of these can be difficult to distinguish from fossil root casts, known as rhizoliths, whose age could be either ancient (i.e., indicative of a paleosol) or very recent (i.e., indicative of late-stage weathering).

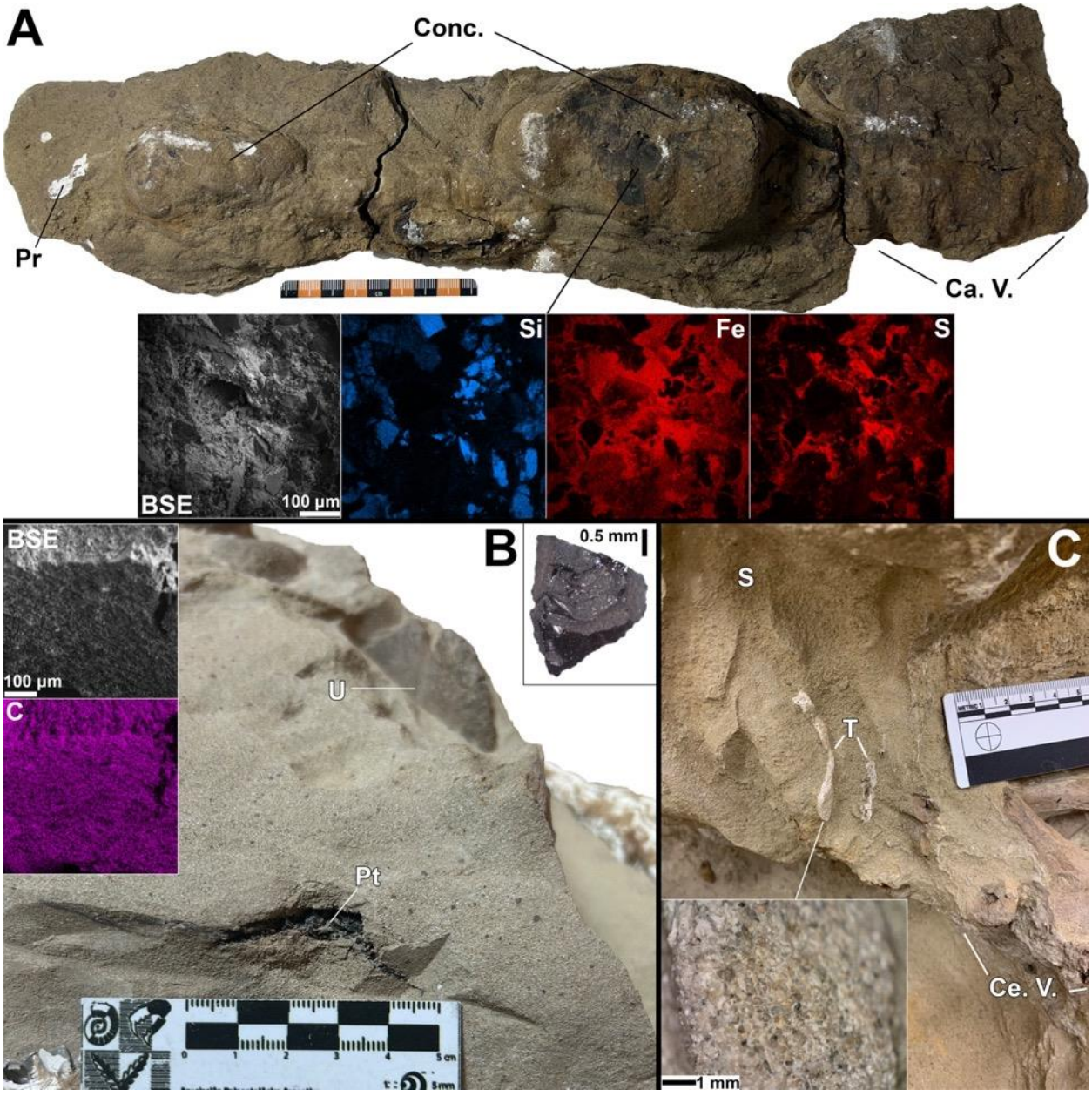

Fig. S22. Sedimentary features in close association with the *E. annectens* mummies. (A) Ironstone concretion (top) at the tip of the tail of the adult (UCRC PV30), showing concretionary material obscuring caudal vertebrae that are enriched in Fe and, to a lesser extent, S under EDS (bottom; 30 kV beam), with some silicate sand grains trapped within. (B) Fossil plant material from the adult (UCRC PV30) found in a laminar layer in close association with the foot (in background), with a sample of plant material from beneath the tail of the adult (UCRC PV30) sampled and

imaged with digital microscopy (top right). The plant material is clearly enriched in C under EDS (top left; 20 kV beam). (C) Putative trace fossil burrows or fossil root casts on the late juvenile (UCRC PV31) that appear as a caliche-like material containing sand grains (bottom left), distinct from spilt plaster (e.g., in A) near the skin at the shoulder girdle and base of the neck. Abbreviations: Conc., concretion; Ca. V., unobscured caudal vertebrae; Pr, plaster; U, ungual; Pt, plant material; S, skin; T, putative trace fossils; Ce. V., cervical vertebrae; UCRC, University of Chicago Research Collection. Photographs were taken with an iPhone 14.

References and notes

1. H. F. Osborn, Integument of the iguanodont dinosaur *Trachodon*. *Am. Mus. Nat. Hist. Mem.* **1**, 33–54 (1912).

2. C. H. Sternberg, Still in the Laramie Country, Converse County, Wyoming. *Trans. Kans. Acad. Sci.* **23**, 219–223 (1911). doi:10.2307/3624588

3. J. Versluys, Der Schadel des Skelettes von *Trachodon annectens* im Senckenberg-Museum. *Abh. Senckenberg. Naturfors. Gesell.* **38**, 1–19 (1923).

4. D. Uhl, A reappraisal of the" stomach" contents of the *Edmontosaurus annectens* mummy at the Senckenberg Naturmuseum in Frankfurt/Main (Germany). *Z. Dtsch. Ges. Geowiss.* **171**, 71–85 (2020). doi:10.1127/zdgg/2020/0224

5. P. Larson, M. Larson, C. Ott, R. Bakker, Skinning a *Triceratops*. *J. Vertebr. Paleontol.* **27**, 104A (2007).

6. C. Lipkin, P. C. Sereno, J. R. Horner, The furcula in *Suchomimus tenerensis* and *Tyrannosaurus rex* (Dinosauria: Theropoda: Tetanurae). *J. Paleontol.* **81**, 1523–1527 (2007). doi:10.1666/06-024.1

7. M. Wosik, D. C. Evans, Osteohistological and taphonomic life-history assessment of *Edmontosaurus annectens* (Ornithischia: Hadrosauridae) from the Late Cretaceous (Maastrichtian) Ruth Mason dinosaur quarry, South Dakota, United States, with implication for ontogenetic segregation between juvenile and adult hadrosaurids. *J. Anat.* **241**, 272–296 (2022). doi:10.1111/joa.13679 Medline

8. N. E. Campione, "Postcranial anatomy of *Edmontosaurus regalis* (Hadrosauridae) from the Horseshoe Canyon Formation, Alberta, Canada" in *Hadrosaurs*, D. A. Eberth, D. C. Evans, Eds. (Indiana Univ. Press, 2015), pp. 208–244.

9. R. S. Lull, N. E. Wright, Hadrosaurian dinosaurs of North America. *Spec. Pap. Geol. Soc. Am.* **40**, 1–242 (1942).

10. W. A. Parks, The osteology of the trachodont dinosaur *Kritosaurus incurvimanus*. *Univ. Toronto Stud. Geol. Ser.* **11**, 1–74 (1920).

11. J. R. Horner, A "segmented" epidermal tail frill in a species of hadrosaurian dinosaur. *J. Paleontol.* **58**, 270–271 (1984).

12. S. K. Drumheller, C. A. Boyd, B. M. S. Barnes, M. L. Householder, Biostratinomic alterations of an *Edmontosaurus* "mummy" reveal a pathway for soft tissue preservation without invoking "exceptional conditions". *PLOS ONE* **17**, e0275240 (2022). doi:10.1371/journal.pone.0275240 Medline

13. C. E. Clayton, R. B. Irmis, M. A. Getty, E. K. Lund, W. J. Nicholls, M. A. Loewen, "Non–osseous dermal scutes and integument impressions from an exceptionally preserved hadrosaurid dinosaur skeleton, Upper Cretaceous Kaiparowits Formation of Utah" in *A Review of Hadrosaurid Skin Impressions. Hadrosaur Symposium 2011 Abstract Volume*, D. R. Braman, D. C. Eberth, D. C. Evans, W. Taylor, Eds. (Royal Tyrrell Museum of Palaeontology, 2011), vol. 589, pp. 23–27.

14. P. R. Bell, Standardized terminology and potential taxonomic utility for hadrosaurid skin impressions: A case study for *Saurolophus* from Canada and Mongolia. *PLOS ONE* **7**, e31295 (2012). doi:10.1371/journal.pone.0031295 Medline

15. N. L. Murphy, D. Trexler, M. Thompson, "'Leonardo,' a mummified *Brachylophosaurus* (Ornithischia: Hadrosauridae) from the Judith River Formation of Montana" in *Horns and Beaks: Ceratopsian and Ornithopod Dinosaurs*, K. Carpenter, Ed. (Indiana University Press, 2007), pp. 117–133.

16. F. Bertozzo, C. D. Sasso, M. Fabbri, F. Manucci, S. Maganuco, Redescription of a remarkably large *Gryposaurus notabilis* (Dinosauria: Hadrosauridae) from Alberta, Canada. *Mem. Soc. Ital. Sci. Nat. Mus. Civ. Storia Nat. Milano* **43**, 1–56 (2017).

17. P. R. Bell, "A review of hadrosaurid skin impressions" in *Hadrosaurs*, D. A. Eberth, D. C. Evans, Eds. (Indiana Univ. Press, 2014), pp. 572–590.

18. P. R. Bell, F. Fanti, P. J. Currie, V. M. Arbour, A mummified duck-billed dinosaur with a soft-tissue cock's comb. *Curr. Biol.* **24**, 70–75 (2014). doi:10.1016/j.cub.2013.11.008 Medline

19. F. D. Ross, G. C. Mayer, "On the dorsal armor of the Crocodilia" in *Advances in Herpetology and Evolutionary Biology*, K. Miyata, A. Rhodin, Eds. (Harvard Univ. Press, 1983), pp. 305–331.

20. P. Wu, Y.-C. Lai, R. Widelitz, C.-M. Chuong, Comprehensive molecular and cellular studies suggest avian scutate scales are secondarily derived from feathers, and more distant from reptilian scales. *Sci. Rep.* **8**, 16766 (2018). doi:10.1038/s41598-018-35176-y Medline

21. P. J. Currie, G. C. Nadon, M. G. Lockley, Dinosaur footprints with skin impressions from the Cretaceous of Alberta and Colorado. *Can. J. Earth Sci.* **28**, 102–115 (1991). doi:10.1139/e91-009

22. R. Zheng, A. A. Farke, G.-S. Kim, A photographic atlas of the pes from a hadrosaurine hadrosaurid dinosaur. *PalArch J. Vertebr. Palaeontol.* **8**, 1–12 (2011).

23. K. Moreno, M. T. Carrano, R. Snyder, Morphological changes in pedal phalanges through ornithopod dinosaur evolution: A biomechanical approach. *J. Morphol.* **268**, 50–63 (2007). doi:10.1002/jmor.10498 Medline

24. T. Thulborn, *Dinosaur Tracks* (Chapman and Hall, 1990).

25. A. H. Parks, "Anatomy and function of the equine digit" in *Equine Laminitis*, J. K. Belknap, R. J. Geor, Eds. (Wiley, 2017), pp. 13–21; https://onlinelibrary.wiley.com/doi/10.1002/9781119169239.ch3.

26. C. C. Pollitt, The anatomy and physiology of the suspensory apparatus of the distal phalanx. *Vet. Clin. North Am. Equine Pract.* **26**, 29–49 (2010). doi:10.1016/j.cveq.2010.01.005 Medline

27. A. Benz, "The elephant's hoof: Macroscopic and microscopic morphology of defined locations under consideration of pathological changes," thesis, Vetsuisse-Fakultät Universität Zürich, Zürich, Switzerland (2005).

28. J. R. Hutchinson, C. Delmer, C. E. Miller, T. Hildebrandt, A. A. Pitsillides, A. Boyde, From flat foot to fat foot: Structure, ontogeny, function, and evolution of elephant "sixth toes". *Science* **334**, 1699–1703 (2011). doi:10.1126/science.1211437 Medline

29. D. A. Croft, J. N. Gelfo, G. M. López, Splendid innovation: The extinct South American native ungulates. *Annu. Rev. Earth Planet. Sci.* **48**, 259–290 (2020). doi:10.1146/annurev-earth-072619-060126

30. N. R. Chimento, F. L. Agnolin, Phylogenetic tree of Litopterna and Perissodactyla indicates a complex early history of hoofed mammals. *Sci. Rep.* **10**, 13280 (2020). doi:10.1038/s41598-020-70287-5 Medline

31. S. Jackson, C. Groves, *Taxonomy of Australian Mammals* (Csiro Publishing, 2015).

32. M. Spaulding, M. A. O'Leary, J. Gatesy, Relationships of Cetacea (Artiodactyla) among mammals: Increased taxon sampling alters interpretations of key fossils and character evolution. *PLOS ONE* **4**, e7062 (2009). doi:10.1371/journal.pone.0007062 Medline

33. W. J. Murphy, N. M. Foley, K. R. Bredemeyer, J. Gatesy, M. S. Springer, Phylogenomics and the genetic architecture of the placental mammal radiation. *Annu. Rev. Anim. Biosci.* **9**, 29–53 (2021). doi:10.1146/annurev-animal-061220-023149 Medline

34. N. M. Foley, V. C. Mason, A. J. Harris, K. R. Bredemeyer, J. Damas, H. A. Lewin, E. Eizirik, J. Gatesy, E. K. Karlsson, K. Lindblad-Toh, M. S. Springer, W. J. Murphy; Zoonomia Consortium‡, A genomic timescale for placental mammal evolution. *Science* **380**, eabl8189 (2023). doi:10.1126/science.abl8189 Medline

35. P. M. Velazco, A. J. Buczek, E. Hoffman, D. K. Hoffman, M. A. O'Leary, M. J. Novacek, Combined data analysis of fossil and living mammals: A Paleogene sister taxon of Placentalia and the antiquity of Marsupialia. *Cladistics* **38**, 359–373 (2022). doi:10.1111/cla.12499 Medline

36. P. Senter, Evidence for a sauropod-like metacarpal configuration in stegosaurian dinosaurs. *Acta Palaeontol. Pol.* **55**, 427–432 (2010). doi:10.4202/app.2009.1105

37. P. J. Currie, D. Badamgarav, E. B. Koppelhus, R. Sissons, M. K. Vickaryous, Hands, feet, and behaviour in *Pinacosaurus* (Dinosauria: Ankylosauridae). *Acta Palaeontol. Pol.* **56**, 489–504 (2011). doi:10.4202/app.2010.0055

38. F. M. Petti, S. D'Orazi Porchetti, E. Sacchi, U. Nicosia, A new purported ankylosaur trackway in the Lower Cretaceous (lower Aptian) shallow-marine carbonate deposits of Puglia, southern Italy. *Cretac. Res.* **31**, 546–552 (2010). doi:10.1016/j.cretres.2010.07.004

39. P. L. Manning, P. M. Morris, A. McMahon, E. Jones, A. Gize, J. H. S. Macquaker, G. Wolff, A. Thompson, J. Marshall, K. G. Taylor, T. Lyson, S. Gaskell, O. Reamtong, W. I. Sellers, B. E. van Dongen, M. Buckley, R. A. Wogelius, Mineralized soft-tissue structure and chemistry in a mummified hadrosaur from the Hell Creek Formation, North Dakota (USA). *Proc. Biol. Sci.* **276**, 3429–3437 (2009). doi:10.1098/rspb.2009.0812 Medline

40. M. Barbi, P. R. Bell, F. Fanti, J. J. Dynes, A. Kolaceke, J. Buttigieg, I. M. Coulson, P. J. Currie, Integumentary structure and composition in an exceptionally well-preserved hadrosaur (Dinosauria: Ornithischia). *PeerJ* **7**, e7875 (2019). doi:10.7717/peerj.7875 Medline

41. M. Fabbri, J. Wiemann, F. Manucci, D. E. G. Briggs, Three-dimensional soft tissue preservation revealed in the skin of a non-avian dinosaur. *Palaeontology* **63**, 185–193 (2020). doi:10.1111/pala.12470

42. L. A. Parry, F. Smithwick, K. K. Nordén, E. T. Saitta, J. Lozano-Fernandez, A. R. Tanner, J. B. Caron, G. D. Edgecombe, D. E. G. Briggs, J. Vinther, Soft-bodied fossils are not simply rotten carcasses – Toward a holistic understanding of exceptional fossil preservation: Exceptional fossil preservation is complex and involves the interplay of numerous biological and geological processes. *BioEssays* **40**, 1700167 (2018). doi:10.1002/bies.201700167 Medline

43. K. M. Towe, Fossil preservation in the Burgess Shale. *Lethaia* **29**, 107–108 (1996). doi:10.1111/j.1502-3931.1996.tb01844.x

44. A. Page, S. E. Gabbott, P. R. Wilby, J. A. Zalasiewicz, Ubiquitous Burgess Shale–style "clay templates" in low-grade metamorphic mudrocks. *Geology* **36**, 855–858 (2008). doi:10.1130/G24991A.1

45. E. Naimark, M. Kalinina, A. Shokurov, N. Boeva, A. Markov, L. Zaytseva, Decaying in different clays: Implications for soft-tissue preservation. *Palaeontology* **59**, 583–595 (2016). doi:10.1111/pala.12246

46. B. Becker-Kerber, A. A. Elmola, A. Zhuravlev, C. Gaucher, M. G. Simões, G. M. E. M. Prado, J. A. G. Vintaned, C. Fontaine, L. M. Lino, D. F. Sanchez, D. Galante, P. S. G. Paim, F. Callefo, G. Kerber, A. Meunier, A. El Albani, Clay templates in Ediacaran vendotaeniaceans: Implications for the taphonomy of carbonaceous fossils. *Geol. Soc. Am. Bull.* **134**, 1334–1346 (2022). doi:10.1130/B36033.1

47. R. P. Anderson, N. J. Tosca, E. E. Saupe, J. Wade, D. E. G. Briggs, Early formation and taphonomic significance of kaolinite associated with Burgess Shale fossils. *Geology* **49**, 355–359 (2021). doi:10.1130/G48067.1

48. J. Reitner, "Biofilms and fossilization" in *Encyclopedia of Geobiology*, J. Reitner, V. Thiel, Eds. (Springer, 2011), pp. 136–137.

49. R. A. Raff, E. C. Raff, The role of biology in the fossilization of embryos and other soft-bodied organisms: Microbial biofilms and Lagerstätten. *Paleontol. Soc. Pap.* **20**, 83–100 (2014). doi:10.1017/S1089332600002813

50. T. Tolker-Nielsen, Biofilm Development. *Microbiol. Spectr.* **3**, MB-0001-2014 (2015). doi:10.1128/microbiolspec.MB-0001-2014 Medline

51. M. A. Norell, X. Xu, Feathered dinosaurs. *Annu. Rev. Earth Planet. Sci.* **33**, 277–299 (2005). doi:10.1146/annurev.earth.33.092203.122511

52. G. Mayr, M. Pittman, E. Saitta, T. G. Kaye, J. Vinther, Structure and homology of *Psittacosaurus* tail bristles. *Palaeontology* **59**, 793–802 (2016). doi:10.1111/pala.12257

53. C. H. Sternberg, Expedition to the Laramie Beds of Converse County, Wyoming. *Trans. Kans. Acad. Sci.* **22**, 113–116 (1908). doi:10.2307/3624729

54. K. Carpenter, How to make a fossil: Part 2 – Dinosaur mummies and other soft tissue. *J Paleontol. Sci.* **7**, 1–23 (2007).

55. K. Carpenter, “Paleoecological significance of droughts during the Late Cretaceous of the Western Interior” in *Fourth Symposium on Mesozoic Terrestrial Ecosystems, Short Papers*, P. M. Currie, E. H. Koster, Eds. (Tyrrell Museum of Palaeontology, 1987), pp. 42–47.

56. R. R. Rogers, Taphonomy of three dinosaur bone beds in the Upper Cretaceous Two Medicine Formation of northwestern Montana: Evidence for drought-related mortality. *Palaios* **5**, 394–413 (1990). doi:10.2307/3514834

57. G. Haynes, *Mammoths, Mastodonts, and Elephants: Biology, Behavior and the Fossil Record* (Cambridge Univ. Press, 1991).

58. P. A. White, C. G. Diedrich, Taphonomy story of a modern African elephant *Loxodonta africana* carcass on a lakeshore in Zambia (Africa). *Quat. Int.* **276–277**, 287–296 (2012). doi:10.1016/j.quaint.2012.07.025

59. A. Galloway, W. H. Birkby, A. M. Jones, T. E. Henry, B. O. Parks, Decay rates of human remains in an arid environment. *J. Forensic Sci.* **34**, 607–616 (1989). doi:10.1520/JFS12680J Medline

60. C. L. Parks, A study of the human decomposition sequence in central Texas. *J. Forensic Sci.* **56**, 19–22 (2011). doi:10.1111/j.1556-4029.2010.01544.x Medline

61. H. C. Fricke, B. Z. Foreman, J. O. Sewall, Integrated climate model-oxygen isotope evidence for a North American monsoon during the Late Cretaceous. *Earth Planet. Sci. Lett.* **289**, 11–21 (2010). doi:10.1016/j.epsl.2009.10.018

62. M. Davis, Census of dinosaur skin reveals lithology may not be the most important factor in increased preservation of hadrosaurid skin. *Acta Palaeontol. Pol.* **59**, 601–605 (2014).

63. T. R. Lyson, N. R. Longrich, Spatial niche partitioning in dinosaurs from the latest cretaceous (Maastrichtian) of North America. *Proc. Biol. Sci.* **278**, 1158–1164 (2011). doi:10.1098/rspb.2010.1444 Medline

64. J. de Rooij, J. H. J. L. Van Der Lubbe, S. Verdegaal, M. Hulscher, D. Tooms, P. Kaskes, O. Verhage, L. Portanger, A. S. Schulp, Stable isotope record of <i>Triceratops<i> from a mass accumulation (Lance Formation, Wyoming, USA) provides insights into Triceratops behaviour and ecology. *Palaeogeogr. Palaeoclimatol. Palaeoecol.* **607**, 111274 (2022). doi:10.1016/j.palaeo.2022.111274

65. S. W. Keenan, J. B. Scannella, “Paleobiological implications of a Triceratops bonebed from the Hell Creek Formation, Garfield County, northeastern Montana” in *Through the End of the Cretaceous in the Type Locality of the Hell Creek Formation in Montana and Adjacent Areas*, G. P. Wilson, W. A. Clemens, J. R. Horner, J. H. Hartman, Eds. (Geological Society of America, 2014), Special Paper 503, pp. 349–364; https://doi.org/10.1130/2014.2503(14).

66. K. Snyder, M. McLain, J. Wood, A. Chadwick, Over 13,000 elements from a single bonebed help elucidate disarticulation and transport of an *Edmontosaurus* thanatocoenosis. *PLOS ONE* **15**, e0233182 (2020). doi:10.1371/journal.pone.0233182 Medline

67. K. R. Johnson, D. J. Nichols, J. H. Hartman, “Hell Creek Formation: A 2001 synthesis” in *The Hell Creek Formation and the Cretaceous-Tertiary Boundary in the Northern Great Plains: An Integrated Continental Record of the End of the Cretaceous*, J. H. Hartman,

K. R. Johnson, D. J. Nichols, Eds. (US Geological Survey, 2002), vol. 361, pp. 503–510; https://doi.org/10.1130/0-8137-2361-2.503.

68. J. R. Gill, W. A. Cobban, Stratigraphy and geologic history of the Montana Group and equivalent rocks, Montana, Wyoming, and North and South Dakota. *Geol. Surv. Profess. Pap.* **776**, 1–37 (1973). doi:10.3133/pp776

69. C. W. Connor, "The Lance Formation: Petrography and stratigraphy, Powder River Basin and nearby basins, Wyoming and Montana" in *Evolution of Sedimentary Basins—Powder River Basin*, V. F. Nuccio, P. L. Hansley, W. A. Cobban, C. G. Whitney, Eds. (US Geological Survey, Bulletin 1917-1, 1992); https://pubs.usgs.gov/bul/1917i/report.pdf.

70. M. H. Schweitzer, Soft tissue preservation in terrestrial Mesozoic vertebrates. *Annu. Rev. Earth Planet. Sci.* **39**, 187–216 (2011). doi:10.1146/annurev-earth-040610-133502

71. E. Saitta, J. Vinther, A perspective on the evidence for keratin protein preservation in fossils: An issue of replication versus validation. *Palaeontol. Electronica* **22.3.2E**, 1–30 (2019). doi:10.26879/1017E

72. J. Vinther, Reconstructing vertebrate paleocolor. *Annu. Rev. Earth Planet. Sci.* **48**, 345–375 (2020). doi:10.1146/annurev-earth-073019-045641

73. V. E. McCoy, R. T. Young, D. E. G. Briggs, Factors controlling exceptional preservation in concretions. *Palaios* **30**, 272–280 (2015). doi:10.2110/palo.2014.081

74. A. W. A. Kellner, Fossilized theropod soft tissue. *Nature* **379**, 32 (1996). doi:10.1038/379032a0

75. P. L. Falkingham, S. M. Gatesy, The birth of a dinosaur footprint: Subsurface 3D motion reconstruction and discrete element simulation reveal track ontogeny. *Proc. Natl. Acad. Sci. U.S.A.* **111**, 18279–18284 (2014). doi:10.1073/pnas.1416252111 Medline

76. K. D'Août, L. Meert, B. Van Gheluwe, D. De Clercq, P. Aerts, Experimentally generated footprints in sand: Analysis and consequences for the interpretation of fossil and forensic footprints. *Am. J. Phys. Anthropol.* **141**, 515–525 (2010). doi:10.1002/ajpa.21169 Medline

77. L. Marchetti, M. Belvedere, S. Voigt, H. Klein, D. Castanera, I. Díaz-Martínez, D. Marty, L. Xing, S. Feola, R. N. Melchor, J. O. Farlow, Defining the morphological quality of fossil footprints. Problems and principles of preservation in tetrapod ichnology with examples from the Palaeozoic to the present. *Earth Sci. Rev.* **193**, 109–145 (2019). doi:10.1016/j.earscirev.2019.04.008

78. R. I. C. Spearman, *The Integument* (CUP Archive, 1973).

79. R. E. Chapman, "Hair, wool, quill, nail, claw, hoof, and horn" in *Biology of the Integument: The Skin of Mammals*, J. Bereiter-Hahn, Ed. (Springer, 1986), pp. 293–317.

80. M. W. Hamrick, Development and evolution of the mammalian limb: Adaptive diversification of nails, hooves, and claws. *Evol. Dev.* **3**, 355–363 (2001). doi:10.1046/j.1525-142X.2001.01032.x Medline

81. C. Hendrickx, P. R. Bell, M. Pittman, A. R. C. Milner, E. Cuesta, J. O'Connor, M. Loewen, P. J. Currie, O. Mateus, T. G. Kaye, R. Delcourt, Morphology and distribution of scales, dermal ossifications, and other non-feather integumentary structures in non-avialan

theropod dinosaurs. *Biol. Rev. Camb. Philos. Soc.* **97**, 960–1004 (2022). doi:10.1111/brv.12829 Medline

82. C. H. Sternberg, An armored dinosaur from the Kansas Chalk. *Trans. Kans. Acad. Sci.* **22**, 257–261 (1909). doi:10.2307/3624735

83. C. H. Sternberg, *The Life of a Fossil Hunter* (Henry Holt & Company, 1909).

84. C. M. Sternberg, Comments on dinosaurian preservation in the Cretaceous of Alberta and Wyoming. *Publ. Palaeontol.* **4**, 1–9 (1970).

85. N. E. Campione, D. C. Evans, Cranial growth and variation in Edmontosauruss (Dinosauria: Hadrosauridae): Implications for latest Cretaceous megaherbivore diversity in North America. *PLOS ONE* **6**, e25186 (2011). doi:10.1371/journal.pone.0025186 Medline

86. H. Xing, J. C. Mallon, M. L. Currie, Supplementary cranial description of the types of *Edmontosaurus regalis* (Ornithischia: Hadrosauridae), with comments on the phylogenetics and biogeography of Hadrosaurinae. *PLOS ONE* **12**, e0175253 (2017). doi:10.1371/journal.pone.0175253 Medline

87. J. C. Mallon, D. C. Evans, Y. Zhang, H. Xing, Rare juvenile material constrains estimation of skeletal allometry in *Gryposaurus notabilis* (Dinosauria: Hadrosauridae). *Anat. Rec. (Hoboken)* **306**, 1646–1668 (2023). doi:10.1002/ar.25021 Medline

88. M. Wosik, M. B. Goodwin, D. C. Evans, A nestling-sized skeleton of *Edmontosaurus* (Ornithischia, Hadrosauridae) from the Hell Creek Formation of northeastern Montana, U.S.A., with an analysis of ontogenetic limb allometry. *J. Vertebr. Paleontol.* **37**, e1398168 (2017)raphy of Hadrosaurinae. *PLOS ONE* **12**, e0175253 (2017).

89. A. G. Reisdorf, M. Wuttke, Re-evaluating Moodie's opisthotonic-posture hypothesis in Fossil Vertebrates Part I: Reptiles—the taphonomy of the bipedal dinosaurs Compsognathus longipes and Juravenator starki from the Solnhofen Archipelago (Jurassic, Germany). *Palaeobio. Palaeobiodivers. Palaeoenviron.* **92**, 119–168 (2012). doi:10.1007/s12549-011-0068-y

90. A. P. Russell, A. D. Bentley, Opisthotonic head displacement in the domestic chicken and its bearing on the 'dead bird' posture of non-avialan dinosaurs. *J. Zool.* **298**, 20–29 (2016). doi:10.1111/jzo.12287

91. B. Brown, *Corythosaurus*: Skeleton, musculature and epidermis. *Bull. Am. Mus. Nat. Hist.* **35**, 709–716 (1916).

92. K. D. Rose, M. A. O'Leary, The manus of *Pachyaena gigantea* (Mammalia: Mesonychia). *J. Vertebr. Paleontol.* **15**, 855–859 (1995). doi:10.1080/02724634.1995.10011269

93. M. A. O'Leary, K. D. Rose, Postcranial skeleton of the Early Eocene mesonychid *Pachyaena* (Mammalia: Mesonychia). *J. Vertebr. Paleontol.* **15**, 401–430 (1995). doi:10.1080/02724634.1995.10011238

94. M. D. Uhen, The origin(s) of whales. *Annu. Rev. Earth Planet. Sci.* **38**, 189–219 (2010). doi:10.1146/annurev-earth-040809-152453

95. O. Lambert, G. Bianucci, R. Salas-Gismondi, C. Di Celma, E. Steurbaut, M. Urbina, C. de Muizon, An amphibious whale from the Middle Eocene of Peru reveals early South

Pacific dispersal of quadrupedal cetaceans. *Curr. Biol.* **29**, 1352–1359.e3 (2019). doi:10.1016/j.cub.2019.02.050 Medline

96. L. Alibardi, V. B. Meyer-Rochow, General and specific microscopic characteristics of the dorsal tail scales and the spines of the crest in the tuatara *Sphenodon pucntatus* (Reptilia; Rhynchocephalia; Sphenodontidae). *Micron* **137**, 102909 (2020). doi:10.1016/j.micron.2020.102909 Medline

97. D. M. Wellik, *Hox* patterning of the vertebrate axial skeleton. *Dev. Dyn.* **236**, 2454–2463 (2007). doi:10.1002/dvdy.21286 Medline

98. D. M. Wellik, *Hox* genes and vertebrate axial pattern. *Curr. Top. Dev. Biol.* **88**, 257–278 (2009). doi:10.1016/S0070-2153(09)88009-5 Medline

99. K. B. Holthaus, L. Alibardi, E. Tschachler, L. Eckhart, Identification of epidermal differentiation genes of the tuatara provides insights into the early evolution of lepidosaurian skin. *Sci. Rep.* **10**, 12844 (2020). doi:10.1038/s41598-020-69885-0 Medline

100. P. R. Bell, C. Hendrickx, M. Pittman, T. G. Kaye, G. Mayr, The exquisitely preserved integument of *Psittacosaurus* and the scaly skin of ceratopsian dinosaurs. *Commun. Biol.* **5**, 809 (2022). doi:10.1038/s42003-022-03749-3 Medline

101. D. B. Norman, *Scelidosaurus harrisonii* from the Early Jurassic of Dorset, England: The dermal skeleton. *Zool. J. Linn. Soc.* **190**, 1–53 (2020). doi:10.1093/zoolinnean/zlz085

102. S. Cai, G. Wei, L. Lo, J. Hu, Z. Sun, T. Zeng, Y. Wei, Z. Zhou, Y.-G. Xu, Volcanism-driven lacustrine redox fluctuations were responsible for the formation of the Jehol Lagerstätte: Evidence from a high-resolution Aptian sedimentary core, Northeast China. *Palaeogeogr. Palaeoclimatol. Palaeoecol.* **631**, 111833 (2023). doi:10.1016/j.palaeo.2023.111833

103. P. R. Blakey, P. Lockwood, The environment of calcified components in keratins. *Calcif. Tissue Res.* **2**, 361–369 (1968). doi:10.1007/BF02279224 Medline

104. F. G. E. Pautard, Calcification of keratin. *Progr. Biol. Sci.Rel. Dermatol.* **2**, 227–315 (1964).

105. A. G. Liu, Framboidal pyrite shroud confirms the “death mask” model for moldic preservation of Ediacaran soft-bodied organisms. *Palaios* **31**, 259–274 (2016). doi:10.2110/palo.2015.095

106. C. Guan, W. Wang, C. Zhou, A. D. Muscente, B. Wan, X. Chen, X. Yuan, Z. Chen, Q. Ouyang, Controls on fossil pyritization: Redox conditions, sedimentary organic matter content, and *Chuaria* preservation in the Ediacaran Lantian Biota. *Palaeogeogr. Palaeoclimatol. Palaeoecol.* **474**, 26–35 (2017). doi:10.1016/j.palaeo.2016.05.013

107. J. Tweet, K. Chin, A. A. Ekdale, Trace fossils of possible parasites inside the gut contents of a hadrosaurid dinosaur, Upper Cretaceous Judith River Formation, Montana. *J. Paleontol.* **90**, 279–287 (2016). doi:10.1017/jpa.2016.43

108. D. E. G. Briggs, A. J. Kear, D. M. Martill, P. R. Wilby, Phosphatization of soft-tissue in experiments and fossils. *J. Geol. Soc. London* **150**, 1035–1038 (1993). doi:10.1144/gsjgs.150.6.1035

109. D. E. Briggs, P. R. Wilby, B. P. Perez-Moreno, J. L. Sanz, M. Fregenal-Martínez, The mineralization of dinosaur soft tissue in the Lower Cretaceous of Las Hoyas, Spain. *J. Geol. Soc. London* **154**, 587–588 (1997). doi:10.1144/gsjgs.154.4.0587

110. S. Q. Dornbos, "Phosphatization through the Phanerozoic" in *Taphonomy*, P. A. Allison, D. J. Bottjer, Eds. (Springer, 2010), vol. 32 of *Topics in Geobiology*, pp. 435–456; http://link.springer.com/10.1007/978-90-481-8643-3_12.

111. T. Clements, M. A. Purnell, S. Gabbott, Experimental analysis of organ decay and pH gradients within a carcass and the implications for phosphatization of soft tissues. *Palaeontology* **65**, e12617 (2022). doi:10.1111/pala.12617

112. A. Roy, M. Pittman, T. G. Kaye, E. T. Saitta, Sediment-encased pressure–temperature maturation experiments elucidate the impact of diagenesis on melanin-based fossil color and its paleobiological implications. *Paleobiology* **49**, 712–732 (2023). doi:10.1017/pab.2023.11

113. T. S. Slater, S. Ito, K. Wakamatsu, F. Zhang, P. Sjövall, M. Jarenmark, J. Lindgren, M. E. McNamara, Taphonomic experiments reveal authentic molecular signals for fossil melanins and verify preservation of phaeomelanin in fossils. *Nat. Commun.* **14**, 5651 (2023). doi:10.1038/s41467-023-40570-w Medline

114. C. E. Brett, J. R. Thomka, "Fossils and fossilisation" in *Encyclopedia of Life Sciences* (Wiley, 2013); https://onlinelibrary.wiley.com/doi/10.1002/9780470015902.a0001621.pub2.

115. W. A. S. Sarjeant, "Fossil tracks and impressions of vertebrates" in *The Study of Trace Fossils: A Synthesis of Principles, Problems, and Procedures in Ichnology*, R. W. Frey, Ed. (Springer, 1975), pp. 283–324.

116. J. S. Benner, R. J. Knecht, Full-body impressions: A category of trace fossils unique to exceptionally preserved bedding planes and indicators of true substrates. *Geol. Soc. Lond. Spec. Publ.* **556**, SP556-2024–87 (2025). doi:10.1144/SP556-2024-87